IN VIVO SUCCESS OF *TRYPANOSOMA CRUZI* IS REGULATED BY HOST CELL TYPE AND PARASITE SENSING OF HOST CELL HEALTH

by

WEIBO ZHANG

(Under the Direction of RICK L. TARLETON)

ABSTRACT

The protozoan parasite *Trypanosoma cruzi* establishes persistent infections in mammals and causes Chagas disease in humans. In mammals, *T. cruzi* trypomastigotes invade host cells and proliferate within as amastigotes. In order to reduce progression and improve control of *T. cruzi* infection, I aim to firstly understand and manipulate host macrophage invasion by *T. cruzi*, and secondly block amastigote-to-trypomastigote differentiation (trypomastigogenesis). One of the molecules that impacts the interaction of *T. cruzi* and macrophages is *T. cruzi* calreticulin (CalR). Here I show that the over-expression of CalR increased *T. cruzi*: macrophage interactions, impacting both the host and immune effector roles of macrophages by enhancing the initial infection and parasite expansion followed by accelerated reduction of parasite burden. The increased invasion in phagocytes upon CalR overexpression was mediated largely via recognition of surface and secreted *T. cruzi* CalR by low-density lipoprotein receptor-related protein 1 (LRP1), an endocytic receptor primarily expressed on phagocytes. Thus enhancing the interaction of *T. cruzi* with macrophages may exert a complex effect on the infection, initially potentiating parasite growth in permissive, non-activated macrophages but decreasing parasite

success once IFNγ production activates these phagocytes. Following the proliferation of *T. cruzi* within host cells, the amastigotes must convert back into trypomastigotes in order to exit the host cell. A previously uncharacterized, kinetoplastid-specific protein (Hyp1) which localizes to the flagellar membrane was shown to be essential for trypomastigogenesis. Disruption of Hyp1 expression completely blocked trypomastigogenesis *in vitro* and prevented the persistence of *T. cruzi in vivo*. Hyp1 overexpression in *T. cruzi* also impaired host cell invasion, further demonstrating the necessity of tightly regulating Hyp1 levels. These findings demonstrate that *T. cruzi* infection progression *in vivo* is regulated by the host cell type and conversion of the parasites before exiting the host cell.

INDEX WORDS: *Trypanosoma cruzi*, Calreticulin, Phagocytes, Low-density lipoprotein-receptor-related protein 1, Trypomastigogenesis, Flagellum

IN VIVO SUCCESS OF *TRYPANOSOMA CRUZI* IS REGULATED BY HOST CELL TYPE AND PARASITE SENSING OF HOST CELL HEALTH

by

WEIBO ZHANG

B.S., Beijing Institute of Technology, China, 2009

A Dissertation Submitted to the Graduate Faculty of The University of Georgia in Partial Fulfillment of the Requirements for the Degree

DOCTOR OF PHILOSOPHY

ATHENS, GEORGIA

2015

IN VIVO SUCCESS OF *TRYPANOSOMA CRUZI* IS REGULATED BY HOST CELL TYPE AND PARASITE SENSING OF HOST CELL HEALTH

by

WEIBO ZHANG

Major Professor:	Rick L. Tarleton
Committee:	Daniel G. Colley
	Robert J. Maier
	Boris Striepen

Electronic Version Approved:

Suzanne Barbour
Dean of the Graduate School
The University of Georgia
December 2015

DEDICATION

This dissertation is dedicated to my parents, Yuan Li and Heng Zhang, and my husband Lei Qu, for their encouragement, patience, understanding and unconditional love during this process.

ACKNOWLEDGEMENTS

I wish to express my deep appreciation to many people. Without their guidance and support, I would have never accomplished this work. First I want to thank my advisor, Dr. Rick Tarleton. Although the journey has not been easy, I have always been grateful for his strict scientific training. His insist on critical thinking, keeping sharp insights and open mindedness has benefited me countless on not only scientific, but life topics as well. I would also like to thank my committee members, Dr. Daniel Colley, Dr. Boris Striepen, and Dr. Robert Maier for their questions, suggestions and discussions on my work.

I want to thank all the past and current TRG members. Dr. Angel Padilla, Dr. Juan Bustamante and Dr. Todd Minning, Dr. Charles Rosenberg, thank you for sharing me knowledge, skills and guidance. For the TRG lunch crew, Angela Pack, Duo Peng and Phil Yao, thank you for the friendship and strong support in and outside the lab. I am very lucky to have you all. I want to give special thanks to Gretchen Cooley, for her help and being such a wonderful friend. Timothy Minning and Karthik Bhat helped me with different projects. I wish the two young men all the best in their future careers. To the rest of TRG, especially Wei, Britton, Donna, Arlene and Fernando, thank you for being supportive during my last year in lab. For the past members, Ashley, Donna, Bharath, thank you for all the help.

To my friends in the graduate program of Microbiology, Jennifer, Teresa, Brandon and Nick, thank you for the good times together. Julie Nelson of the Flow cytometry core facility, Dr. Muthugapatti Kandasamy of the Biomedical Microscopy Core, Sophia in the Microbiology

office, and the staffs at the Coverdell center animal facility have also been very supportive throughout.

Last but not least, I want to thank my family, for the endless love, support and patience during my study overseas. My parents, my husband Lei and parents-in-law, aunt Xi Chen and uncle Hui Li, aunt Jining Zhang and uncle Desuo Wang, thank you for the strong support and faith in me. It means everything.

TABLE OF CONTENTS

Page

LIST OF FIGURES

Page

CHAPTER 1

INTRODUCTION AND LITERATURE REVIEW

1.1 Introduction

Chagas disease, caused by the protozoan parasite *Trypanosoma cruzi*, is a neglected infectious disease mostly endemic in Latin America. Understanding the mechanism of *T. cruzi*-mammalian host interaction is essential for the discovery of new drugs and design of effective and safe vaccines. In the first part of this review, I briefly introduce the disease, current medical challenges and the parasite itself. Next I discuss how interactions between *T. cruzi* and its mammalian host influence progression of the infection, with an initial focus on strategies utilized by *T. cruzi* to establish and maintain infection, including aspects of infectivity, proliferation and differentiation. A second emphasis is on the potent but insufficient defense strategies used by mammalian hosts, including both innate and adaptive immunity. The final part of the review covers some major questions, research directions and suggestions for enhancing parasitic clearance, which leads into the specific goal of this project and the experimental plan.

1.2 Chagas disease and *Trypanosoma cruzi*

1.2.1 *Disease: presentations, epidemiology and transmission*

According to the World Health Organization, about 6 million to 7 million people in the world are estimated to be infected with *Trypanosoma cruzi*, the etiologic agent for Chagas disease (http://www.who.int/mediacentre/factsheets, March 2015). Chagas disease is endemic in certain underdeveloped, rural regions of Latin America. However, due to increased global migration, it is estimated that between 50,000 and 70,000 people in Spain, 300,000 in United

States and 4,500 in Japan are infected, mostly in immigrant populations from endemic regions, highlighting Chagas disease as a growing global public health concern [1-3].

In the endemic rural areas of Latin America, the most common transmission route for human infection is via infected triatomine bugs present in poor housing conditions. Dogs and other companion animals that ingest infected bugs are also at high risk of being infected, aiding in potential transmission to humans [4]. Food or drink contaminated with infected bug feces was also recently reported to be the cause of large outbreaks in endemic areas [5]. In non-endemic areas, records indicate the major transmission routes to be blood transfusion, organ transplantation and congenital infection [6-8].

T. cruzi infection has both acute and chronic phases. During the acute phase, no or very mild symptoms appear. Clinical manifestations may develop in the chronic phase. Cardiomyopathy develops in up to 30% of the chronically infected patients; while up to 10% of the chronically infected patients develop neurological, digestive damage or a combination of the two [9, 10]. The economic burden caused by Chagas disease is significant from individual, regional, national and global perspectives. For individuals, in addition to the loss in productivity, disability-adjusted life-years are predicted to be 3.57 and the economic burden of Chagas disease for an infected individual is estimated to be $3,456 per lifetime based on the computational simulation model by Lee *et al* [11]. Based on the work by Lee *et al*, the global healthcare cost for Chagas patients is estimated to be $627.46 million annually. Due to the large repertoire of host animal species in Americas, *T. cruzi* is impossible to be eliminated. However, blocking transmission is the main target of parasite control. Particularly, vector control is the most effective and cost-effective disease-prevention method in Latin America, despite potential public health concern on insecticide resistance[12].

1.2.2 *Diagnosis, drug treatment and vaccines*

Diagnosis for Chagas disease is complex and questionable. While no agreed 'gold-standard' for diagnosis is available, widely used diagnostic strategies are based on positive results from a combination of multiple serological tests for identification of anti-*T. cruzi* antibodies, such as enzyme-linked immunosorbent assay (ELISA), indirect haemagglutination assay (IHA) and indirect immunofluorescence (IIF) [13], with the addition of examining clinical symptoms and history of living in an endemic area. Based on WHO recommendation, positive results in two serological tests are considered positive. But this leaves caveat for confirmation about the health status for patients with only one positive result. Other diagnostic issues include cross-reactivity of the antibodies produced by other pathogens and poor standardization of reagents causing variation in the reproducibility and reliability of the tests [13, 14].

Two anti-trypanosomal drugs are used in treating acutely infected humans, nifurtimox and benznidazole, but have unsatisfactory performance because of the toxic side effects and the failure to consistently achieve complete cure in chronically infected patients [15]. No vaccines are available for humans or animals. The slow development of vaccines for Chagas disease is partly due to the still prevalent controversy over whether Chagas disease is caused by autoimmune responses or parasite persistence, as well as the little economic interest predicted by pharmaceutical and vaccine companies and thus little incentives to put in resources for Chagas vaccine research [16-19].

1.2.3 *T. cruzi taxonomy*

T. cruzi is a single cell protozoa belonging to the order of Trypanosomatida in the class of Kinetoplastida which is under the phylum Euglenozoa. Similar to other kinetoplastids, *T. cruzi* contains a DNA-dense granule called the kinetoplast located within the parasite's single

mitochondrion associated with the basal body at the base of its single flagella. *Trypanosoma brucei* spp. causing African trypanosomiasis and *Leishmania* spp. causing leishmaniasis are phylogenetically related pathogens for humans and mammals.

1.2.4 *T. cruzi life cycle*

T. cruzi has four life forms cycling between insect and mammalian hosts. In the insect vector, *T. cruzi* multiplies as epimastigotes in the midgut before moving to the hindgut where epimastigotes transform to infective metacyclic trypomastigotes. To infect a mammalian host, metacyclic trypomastigotes are passed out in bug feces during a blood meal and the parasites enter the host through mucosal membranes or the bite wound. The insect-stage metacyclic trypomastigotes or the blood-form trypomastigotes released from infected cells are able to infect a variety of nucleated cells. After being internalized in a membrane-bound acidic compartment known as the parasitophorous vacuole (PV) for 1-2 hours after infection, *T. cruzi* enters the host cytoplasm where the flagellum is lost and the parasites transform to proliferative amastigotes, at least partially via asymmetric division [20, 21]. Extracellular amastigotes are able to infect host cells, although the efficiency is low compared to trypomastigotes. After multiple rounds of replication, amastigotes differentiate into infective but non-proliferative trypomastigotes with an extended flagellum. Trypomastigotes released from the destroyed host cell enter the bloodstream to infect other cells within which another infection cycle begins.

Proteome analysis in the four life forms of *T. cruzi* CL Brener strain revealed distinct stage-specific energy sources, suggesting the flow of metabolism changes in response to changes of nutrition sources in different environments [22]. The steady-state transcriptome analysis comparing four life stages of CL Brener strain demonstrates that transcription of over 50% of *T. cruzi* genes are stage-regulated [23]. The results of the *T. cruzi* stage-specific proteome and

transcriptome collectively suggest that parasites undergo massive changes in both transcription and expression levels during transformation in response to environment changes. Potential mechanisms for conversion between life stages will be discussed in more details in 1.3.2.

1.3 *T. cruzi* pathogenesis in mammalian infection

1.3.1 *Invasion*

T. cruzi blood-form trypomastigotes, insect-form metacyclic trypomastigotes and extracellular amastigotes are all able to invade various host cell populations but with different efficiencies and strategies depending on strains, life forms and host cell types. Nonetheless, the parasitophorous vacuole (PV) is the key organelle to retain invading parasites under all conditions. The PV during *T. cruzi* invasion is formed in a lysosome-dependent [24] or lysosome-independent, plasma membrane-mediated fashion [25]. However, lysosomal fusion is necessary for irreversibly retaining parasites in PV, a prerequisite to ensure subsequent parasite escape to the host cytoplasm [26]. Parasites also seem to exploit the plasma membrane lesion repair pathway by inducing Ca^{2+}-triggered lysosomal exocytosis for invasion [27].

Trypomastigotes are the dominant life cycle stage to invade host cells. Differential invasion abilities between insect-stage and blood-form trypomastigotes are at least partially attributed to their stage-specific composition of surface molecules [28]. Infectivity variation across strains is believed to result from differences in their genomic, transcriptomic and proteomic profiles in triggering different signaling cascades for invasion [29]. Amastigotes of highly virulent strains are able to infect both phagocytic and non-phagocytic cells by inducing phagocytosis, while amastigotes from less virulent strains are only able to infect phagocytic cells and occasionally non-phagocytic cells [30].

T. cruzi surface adhesion molecules contributing to invasion of trypomastigotes into non-professional phagocytes have been studied extensively. *T. cruzi* surface proteins are primarily members encoded by large gene families, including *trans*-sialidase, mucin, gp63, and mucin-associated surface protein. These large repertoires of variant surface proteins are major contributors mediating invasion. Recognitions between surface protein members of glycoprotein superfamily gp85/*trans*-sialidase (Tc85) and the receptors, laminin and fibronectin, trigger dephosphorylation of α-actin and paraflagellar rod proteins and trypomastigote adhesion to extracellular matrix (ECM) [31]. Other macromolecules in ECM, such as thrombospondin and heparin sulfate, also interact with gp85 for parasite invasion in non-phagocytic cells [32]. Another member of the *trans*-sialidase family, gp82, enables macropinocytosis of microparticles in non-phagocytic cells via acting on a G protein-coupled receptor at the parasite synapse upon *T. cruzi* attachment [33]. GPI-anchored mucin is derived from *T. cruzi* mucin superfamily with abundant expression on the parasite surface. It also induces trypomastigote invasion in non-phagocytic cells [34].

T. cruzi surface calreticulin (CalR) is one of the few conserved and invariant molecules currently known to participate in invasion. *T. cruzi* surface CalR interacts with the N-terminus of thrombospondin-1 in ECM, which enhances trypomastigote invasion in mouse embryo fibroblasts [35]. *T. cruzi* CalR also binds to complement components C1q deposited on the surface of host cells [36, 37]. Interaction between *T. cruzi* calreticulin and C1q facilitates invasion not only by deactivating complement-mediated killing, but also via C1q's bridging of parasite and host surface calR [37-39].

Mammalian CalR shares 47% of protein sequence identity with *T. cruzi* CalR and normally resides in the ER, serving as a calcium-binding chaperone to ensure correct folding of

glycoproteins and assembly of class I MHC molecules. However, under ER stress, mammalian CalR is re-translocated from the lumen of ER to the cellular surface membrane, providing an 'eat-me' signal referred to as a danger-associated molecular pattern (DAMP) for phagocytes to recognize and engulf. Surface-exposed CalR is recognized by low-density lipoprotein receptor-related protein 1 (LRP1). As a 500-kDa macromolecule with high affinities for about 60 ligands, LRP1 is mostly expressed on professional phagocytes such as monocytes, macrophages and dendritic cells. Low-level LRP1 expression is also found in a few non-phagocytic cells, e.g., endothelial cells and fibroblasts. Ecto CalR-LRP1-mediated phagocytosis of apoptotic cells, tumor cells and stressed cells enhances immunogenicity of those cells for their more efficient innate and adaptive immune control.

Because of the high similarity shared between *T. cruzi* and mouse calR, it was of interest to investigate whether *T. cruzi* CalR may also function as an 'eat-me' signal during invasion in professional phagocytes, and whether CalR-mediated parasite entry and expansion in professional phagocytes will backfire, leading to more parasite killing elicited by host immunity. In addition, due to the low copy number (2) of calR in the genome, enhanced expression of *T. cruzi* CalR could be achieved in parasites transfected with *T. cruzi*-adapted expression plasmid containing full-length CalR gene.

1.3.2 *Differentiation*

In mammalian hosts, *T. cruzi* cycles between trypomastigotes and amastigotes. The mechanism for differentiation in either direction remains unknown. In particular it is unclear how *T. cruzi* senses environmental changes and initiates downstream signaling for massive metabolic and morphological changes. It is believed that sensor molecules are likely to be surface proteins directly monitoring environmental changes.

Differentiation from infective trypomastigotes to replicative amastigotes (amastigogenesis) occurs within host cells after being retained within acidic PV. *In vitro*, trypomastigotes incubated in acidic media transform to extracellular amastigotes, indicating low pH as one critical environmental cue for amastigogenesis. Yet it is unclear how *T. cruzi* senses the pH drop. Very few surface membrane molecules have been linked to amastigogenesis. One of them is phosphatidylinositol-phospholipase C (TcPI-PLC) [40]. TcPI-PLC is a lipid-modified surface membrane protein induced and activated during amastigogenesis. It is involved in releasing secondary messengers in signaling cascades, including diacylglycerol that controls cellular protein phosphorylation states and IP3 that triggers Ca^{2+} releasing from intracellular stores [41]. The proteomic analysis of the plasma membrane extracted from tissue-culture-derived trypomastigotes and axenic amastigotes indicated that regulation of PI-PLC was consistent with massive changes in lipid profiles between the two life stages [42]. However, whether and how TcPI-PLC is involved in the pH-triggered signaling cascade is unknown. Quantitative proteomic and phosphoproteomic analysis of *in vitro* amastigogenesis have demonstrated that a significant proportion of protein regulation takes place in membrane proteins and that phosphorylation of protein kinases and phosphatases is largely modulated [43].

One regulated kinase that may be involved in *T. cruzi* amastigogenesis is mitogen-activated protein kinase (TcMAPK2) located to the flagella surface in trypomastigotes and plasma membrane in amastigotes [44]. TcMAPK2 phosphorylation is drastically different between amastigote and trypomastigote stages, suggesting differential regulation of *T. cruzi* MAPK signaling pathways in the two life stages in the mammalian host [44]. Although MAPK signaling pathways have been well characterized in many prokaryotic and eukaryotic systems for transforming environmental cues to various signal transduction cascades controlling

proliferation, differentiation, growth and apoptosis [45], it is unclear whether *T. cruzi* MAPK signaling pathways have similar regulatory functions in parasite differentiation.

Like in many other organisms, MAPK signaling pathways in *T. cruzi* may be also regulated by and cross-communicates with cyclic adenosine monophosphate (cAMP)-dependent pathways. This is suggested by the fact that TcMAPK2 recombinant protein can phosphorylate cAMP-specific phosphodiesterase, an important regulator of cAMP intracellular level [44, 46]. Cyclic AMP is a common secondary messenger that transfers the effects of extracellular signals into the cell. In *T. cruzi*, exogenous cAMP has been identified in triggering the differentiation from epimastigotes to metacyclic trypomastigotes (metacyclogenesis) in the insect stage [47]. It is worthwhile to investigate whether change in cAMP transient triggers differentiation in the mammalian host. In conclusion, complex signaling networks may occur on the surface membrane to tightly regulate amastigogenesis.

Differentiation from amastigotes to trypomastigotes occurs after extensive intracellular proliferation, when amastigotes fully occupy the host cytoplasm – and provides the means for *T. cruzi* to exit one host cell and infect others. How *T. cruzi* determines the checkpoint for reprogramming from replicating amastigotes to flagellated trypomastigotes is poorly understood. Unlike metacyclogenesis and amastigogenesis, amastigote-to-trypomastigote differentiation has yet to be mimicked in a cell-free environment, thus generating additional obstacles to understanding the fine mechanism of this process.

Several factors have been suggested to be relevant during the decision making process, including poly (ADP-ribose) polymerase (pADPRT), certain amino acids, optimal temperature for specific strains, and host quorum sensing effects of an amastigote-derived eicosanoid molecule [48-50]. Early research conducted by Williams indicated that 5-methylnicotinamide and

3-methoxybenzamide, two pADPRT inhibitors targeting NAD^+ synthesis specifically blocked amastigote-to-trypomastigote differentiation in infected mammalian cells and extracellular amastigote differentiation to flagellated forms including both epimastigotes and trypomastigotes in cell-free media with no impact on proliferation, suggesting *T. cruzi* pADPRT as a critical regulator in this differentiation process [51, 52]. However, later work conducted by Larrea *et al* showed different results. Treatment with another potent pADPRT inhibitor Olaparib reduced the number of intracellular amastigotes with no loss of initial invasion and the final release of trypomastigotes, suggesting that Olaparib may affect amastigote proliferation, but not amastigote-to-trypomastigote differentiation [53]. Nonetheless, knockdown of host pADPRT gene by siRNA in human A549 cancer cells reduced the number of intracellular amastigotes per infected cell and the released trypomastigotes, suggesting a potential role of host pADPRT in *T. cruzi* amastigote proliferation and amastigote-to-trypomastigote differentiation [53]. Because Olaparib only targets the catalytic domain of pADPRT while siRNA knockdown affects expression of all three domains including an N-terminal zinc-dependent DNA-binding domain, a central auto-modification domain and a C-terminal NAD-binding domain, it is likely that the DNA-binding and/or auto-modification domain may be required for amastigote-to-trypomastigote differentiation. Specifically, single-stranded DNAs, which initiate pADPRT activity by binding to its DNA-binding domain, are released from the nucleus and accumulate in the cytoplasm in an infected and damaged cell to activate the host STING pathway for robust anti-microbial responses [54]. It may be worthwhile to further explore whether/how host and *T. cruzi* pADPRT affects amastigote-to-trypomastigote transition.

L-proline, an essential amino acid required in the epimastigote stage and metacyclogenesis, may also be required for amastigote-to-trypomastigote differentiation, as such

differentiation in ι-proline-auxotrophic *T. cruzi* amastigotes is dose-dependent on supply of ι-proline [50]. Amastigote-to-trypomastigote differentiation is also temperature-sensitive for certain *T. cruzi* strains. Compared to infection of CL strain at 33°C, infection of CL strain at 37°C showed inhibited amastigote-to-trypomastigote differentiation while invasion, amastigogenesis and amastigote proliferation were not affected [48, 50]. Another molecule possibly involved in amastigote-to-trypomastigote differentiation is eicosanoid thromboxane A2, a parasite-derived molecule released from infected host cells (TXA_2) [49]. Infection in murine endothelial cells lacking a TXA_2 receptor showed increased intracellular parasitism but impaired amastigote-to-trypomastigote differentiation which could be rescued by restoration of TXA_2 receptor, suggesting that TXA_2-associated host signaling may be involved in parasite intracellular amastigote-to-trypomastigote transformation [49]. A quorum-sensing model proposed by Ashton *et al* suggests TSA_2 as the quorum sensor as accumulation of TSA_2 may correlate with the number of intracellular amastigotes per infected cell, and thus host signaling may be triggered once TSA_2 level reaches the threshold to initiate programming from amastigote proliferation to differentiation [49]. However, information on amastigote-to-trypomastigote differentiation is still limited and disparate, most of which requires more solid experimental validation. Elucidating this process is not only essential to understanding *T. cruzi* life cycles, but also beneficial to understanding of host: *T. cruzi* interaction.

1.3.3 *Replication*

Amastigotes undergo binary fission within the host cytoplasm. Transforming growth factor α (TGF-α) secreted by macrophages binds to amastigotes and induces DNA synthesis and amastigote replication in a cell-free environment and in macrophages, suggesting amastigote proliferation is mediated by TGF-α-dependent signal transduction pathway [55]. *T. cruzi*

replication in mammalian cells requires a sufficient energy supply. Proteomic analysis of *T. cruzi* indicated an up-regulation of enzymes involved in fatty acid β-oxidation in amastigotes compared to other life forms, suggesting fatty acids as the major energy source for amastigote proliferation [22]. Indeed, interference with fatty acid β-oxidation in parasites by knocking-down the fatty acid transporter-like protein gene (*fatp*), transcription of which is highest in amastigotes in *T. cruzi* life cycle [23], selectively ablated amastigote proliferation with no obvious impact during the other life stages in infected Vero culture *in vitro* (Hartley *et al*, unpublished data). In addition, during chronic murine infection *in vivo*, *T. cruzi* preferentially persists in muscle cells and adipocytes, both utilizing fatty acid as a major energy source, highlighting host fatty acid metabolism as a promising target for eliminating chronic infection [19, 56]. Because developing parasites with impaired intracellular proliferation is one promising strategy for making live attenuated vaccines, it is worthwhile to further explore the requirement for amastigote proliferation and how to control the process.

1.4 Host immunity controls *T. cruzi* infection

1.4.1 *Innate immunity*

Innate immune cells, such as infiltrating neutrophils and monocytes, tissue-resident macrophages, and dendritic cells, build up the first host defense line against *T. cruzi* infection. Those phagocytic cells allow efficient parasite invasion soon after parasites enter the body of the host. Intracellular parasites residing within those phagocytic cells are subsequently killed via different mechanisms. Neutrophils rapidly initiate apoptosis at inflamed sites and are phagocytosed by macrophages. Macrophages and dendritic cells clear intracellular parasites upon activation via Toll-like receptor (TLR) signaling, as is demonstrated by the fact that the two phagocyte populations with deficiency in both myeloid differentiation primary-response

(MyD88) and Toll/IL-1R (TIR) domain-containing adaptor protein inducing interferon-β (TRIF), two adaptor proteins involved in TLR signaling, were impaired in infection clearance [57].

Activation of macrophages and dendritic cells (both tissue-resident and monocyte-derived) could be further enhanced by secondary signals such as IFNγ, a critical pro-inflammatory cytokine produced by activated macrophages, natural killer cells and γδ T cells during the first 7 – 10 days of *T. cruzi* infection and then by T- helper 1 (Th1) $CD4^+$ cells and activated $CD8^+$ T cells [58]. In the absence of IFNγ, macrophages were defective in production of nitric oxide (NO), the trypanocidal mediator against *T. cruzi*. It is therefore not surprising to see that selectively desensitizing monocytes, macrophages and dendritic cells to IFNγ in mice resulted in impaired parasite control *in vivo* [59]. In addition to trypanocidal activity, infected macrophages and dendritic cells also sense infected non-haematopoietic cells, and activate adaptive immunity by processing and presenting MHC class I and MHC class II -restricted parasitic antigens to prime cognate antigen-specific T cells and B cells.

Among multiple professional phagocytes, macrophages have a multifaceted role during *T. cruzi* infection. Macrophages may contribute to the initial establishment of *T. cruzi* infection, as evidenced by the fact that macrophage depletion reduced parasite load during the first 8 days in infected mice (Padilla *et al*, unpublished data). Since IFNγ is minimally released before day 10 of infection possibly due to lack of proper endogenous pathogen-associated molecular patterns (PAMPs) in *T. cruzi* [60], the modest levels of IFNγ may not efficiently activate trypanocidal activity of macrophages, thus providing an initial strong support of parasite infection and expansion. However, as mentioned previously, upon IFNγ -mediated activation, macrophages exert potent trypanocidal activity primarily via nitric oxide biosynthesis [61, 62]. During the process, TNFα produced by IFNγ-activated macrophages amplifies NO production

and trypanocidal activity [63]. Taken together, these results suggest a complex role of macrophages in parasite control before and after IFNγ-mediated activation, and it is unclear how *T. cruzi* entry and expansion in macrophages affects infection control throughout the course of infection *in vivo*. In my work I have tested the hypothesis that driving infection towards macrophages will lead to more efficient control despite an initial increase in parasite expansion.

1.4.2 *Adaptive immunity*

Following innate immune responses, *T. cruzi* infection elicits both humoral (B cell) and cellular ($CD4^+$ and $CD8^+$ T cell) adaptive immune responses. Both of these responses mediate infection control and confer some level of protection but unable to be cure infection. Humoral immunity contributes to protection against *T. cruzi* as mice that received anti-*T. cruzi* (CL or Y strain) immune sera displayed reduced parasitemia and mortality upon Y strain challenge than the group that received normal mouse serum. However, in contrast to the antibody-sensitive Y strain which was effectively controlled in infected mice, trypomastigotes from CL strain did not display decreased infectivity upon murine infection, suggesting the protective effect of humoral responses may be strain specific [64].

For cellular immune responses, depletion of either $CD4^+$ or $CD8^+$ or both T-cell subpopulations by antibody treatment prior to *T. cruzi* infection increased infectivity and mortality in a highly susceptible mouse strain, suggesting the critical contribution of both $CD4^+$ and $CD8^+$ T cells to protective immunity in this highly susceptible mouse model [65]. In a *T. cruzi*-resistant mouse model, both $CD4^+$ and $CD8^+$ T cells displayed predominant effector memory phenotype during chronic infection and specifically responded to *T. cruzi* antigens by producing IFNγ and rapid proliferation upon secondary *T. cruzi* antigen exposure. This suggests potent parasite-destructive T cell responses exist during chronic infections in *T. cruzi*-resistant hosts [66].

Specifically, for $CD4^+$ T cell responses, Th1, but not Th2 or regulatory $CD4^+$ T cell response contributes to parasitic control and confers protection against *T. cruzi* infection [67, 68].

The critical role of $CD8^+$ T cells for infection control has been extensively reviewed [69-71]. Upon activation, $CD8^+$ T cells produce a large amount of IFNγ and TNFα and account for the release of cytotoxicity granules. $CD8^+$ T cells exert their function primarily by killing infected cells upon recognition of *T. cruzi*-derived antigens in the context of class I MHC complex on the infected cell surface. β2-microglobulin-deficient mice with disrupted class I MHC antigen presentation produced normal $CD4^+$ T cell responses but no $CD8^+$ T cell responses, and failed to control *T. cruzi* infection [72]. In addition, $CD8^+$ T cell depletion by anti-CD8 antibody treatment in either acute or chronic infection gave rise to increased parasite burden (Pack, unpublished data), indicating an indispensable role of $CD8^+$ T cells throughout the course of infection. However, the persistence of infection after potent immune responses suggests that while some intracellular parasites are killed, some manage to escape from the lysis of infected cells, thus allowing subsequent infection and chronicity.

Multiple potential mechanisms have been proposed to explain why potent *T. cruzi*-specific $CD8^+$ T cell responses may be able to control but not to clear infection. One school of thought views *T. cruzi*-specific $CD8^+$ T cell responses as delayed in onset with the consequence that the time window for optimal infection control is missed as the cause for incomplete infection clearance. Several factors may contribute to this delay of *T. cruzi*-specific $CD8^+$ T cell responses, including slow activation of innate immunity, and late and/or suppressed MHC-I presentation of *T. cruzi* antigens. Innate immune responses with minimal production of pro-inflammatory cytokines and chemokines are retarded likely by lack of appropriate *T. cruzi* endogenous PAMPs [60]. The slow induction of innate immunity also at least partially delays the

onset of adaptive immune responses, which may eventually contribute to the failure of parasitic clearance [73]. Consistent with this hypothesis, heterologous expression of exogenous PAMPs such as TLR1/2 and TLR5 ligands in *T. cruzi* boosted stronger innate immune responses and moderately earlier and stronger $CD8^+$ T cell responses, leading to enhanced parasite control accompanied with occasional complete clearance of the infection in mice [73].

In addition, *T. cruzi* proteins containing antigens for $CD8^+$ T cells may be released from intracellular parasites at a slow rate, which also leads to slow generation of $CD8^+$ T cell responses. This hypothesis is supported by the recent work of Kurup *et al* demonstrating that by over-expressing *T. cruzi* paraflagllar rod protein 4 (PAR4) released early after parasite invasion and containing a $H2^d$-restricted epitope, infection was better controlled due to an earlier induction of PAR4-derived epitope-specific $CD8^+$ T cell responses [20]. Late antigen presentation may also be partially attributed to suppressed surface expression of Class I MHC upon *T. cruzi* infection, as seen in *T. cruzi*-infected Hela cells [74]. Conversely, enhancing Class I MHC expression may improve $CD8^+$ T cell responses, leading to enhanced infection control. This hypothesis was supported by the fact that in class I MHC molecule-overexpressing mice, $CD8^+$ T cell responses became more potent and infection was more rapidly controlled (Pack, unpublished data).

The second set of hypotheses views *T. cruzi* variant surface proteins encoded by large gene families as the cause of the insufficiency of $CD8^+$ T cell response for infection clearance. *T. cruzi* GPI-anchored surface proteins and secreted proteins provide the major epitopes for $CD8^+$ T cell recognition. In the *T. cruzi*-resistant B57BL/6 murine model, two $H2k^b$-restricted antigens TSKB20 (ANYKFTLV) and TSKB18 (ANYDFTLV) derived from GPI-anchored surface proteins *trans*-sialidases, elicit about 20% and 8% of all $CD8^+$ T cells during the peak of

the response, respectively, dominating the response against other antigens documented so far [75]. However, *trans*-sialidase-derived epitopes may not be optimal $CD8^+$ T cell targets for vaccine development, where boosting a protective response to conserved epitopes is desirable. Depletion of TSKB20- and TSKB18-specific $CD8^+$ T cell response either in the short term by peptide tolerization or in the long term by central tolerization made no significant difference in parasitic control, suggesting that $CD8^+$ T cell responses against these *trans*-sialidase-derived dominant epitopes are dispensable for infection control [76] (Rosenberg *et al*, unpublished data).

The *trans*-sialidase gene has experienced massive expansion resulting in an extended family. This gene family is *T. cruzi*'s largest and comprises more than 693 full genes with only less than 20 genes predicted to have retained enzymatic activity, 823 partial genes and 1693 pseudogenes (Weatherly and Peng *et al*, unpublished data). Bioinformatic research conducted in our lab unveiled frequent homologous recombination among the members of the *trans*-sialidase gene family, supporting the idea that *T. cruzi* may utilize the large repertoire of *trans*-sialidases for immune evasion (Weatherly and Peng *et al*, unpublished data). Therefore, identifying $CD8^+$ T cell targets derived from invariant proteins will be crucial for successful vaccine development. Overexpression of those targets may not only elicit more protective $CD8^+$ T cell responses but may also limit $CD8^+$ T cell recognition of *trans*-sialidase-derived epitopes, therefore resulting in better control of infection.

1.5 Summary and major questions

T. cruzi infection causes human Chagas disease, a neglected tropical disease with no or insufficient approaches to diagnosis, treatment and vaccine development. To enhance control of *T. cruzi* infection, strategies could be designed with the goal of boosting host immune responses, or restricting parasite pathogenesis, or a combination of the two. In mammalian infection, *T.*

cruzi cycles between the invasion stage and the proliferation stage connected by differentiation. Disruption in invasion, proliferation or differentiation may lead to impaired establishment, development and persistence of infection. In chapter 2, by using transgenic parasites overexpressing calreticulin, a natural 'eat-me' signal, I study the manipulation of parasite invasion by driving the direction of *T. cruzi* infection towards professional phagocytes to determine whether boosted invasion in macrophages may induce an overall enhanced control of infection. In chapter 3, I attempt to block parasite differentiation from amastigotes to trypomastigotes by disrupting expression of a previously uncharacterized flagellar membrane protein in the parasites and evaluate whether this affects infection establishment, development and persistence. By doing this, I aim to gain new insights into infection control strategies that specifically inhibit parasite differentiation. Lastly, I will discuss the potential mechanism of amastigote-to-trypomastigote differentiation in the light of my experiments.

1.6 References

1. Gascon, J., Bern, C. & Pinazo, M.J. Chagas disease in Spain, the United States and other non-endemic countries. *Acta tropica* **115**, 22-27 (2010).

2. Bern, C., Kjos, S., Yabsley, M.J. & Montgomery, S.P. *Trypanosoma cruzi* and Chagas' Disease in the United States. *Clinical microbiology reviews* **24**, 655-681 (2011).

3. Imai, K. *et al.* Chronic Chagas disease with advanced cardiac complications in Japan: Case report and literature review. *Parasitology international* **64**, 240-242 (2015).

4. Esch, K.J. & Petersen, C.A. Transmission and epidemiology of zoonotic protozoal diseases of companion animals. *Clinical microbiology reviews* **26**, 58-85 (2013).

5. Alarcon de Noya, B. *et al.* Large urban outbreak of orally acquired acute Chagas disease at a school in Caracas, Venezuela. *The Journal of infectious diseases* **201**, 1308-1315 (2010).

6. Fearon, M.A. *et al.* A case of vertical transmission of Chagas disease contracted via blood transfusion in Canada. *The Canadian journal of infectious diseases & medical microbiology = Journal canadien des maladies infectieuses et de la microbiologie medicale / AMMI Canada* **24**, 32-34 (2013).

7. Lattes, R. & Lasala, M.B. Chagas disease in the immunosuppressed patient. *Clinical microbiology and infection : the official publication of the European Society of Clinical Microbiology and Infectious Diseases* **20**, 300-309 (2014).

8. Barona-Vilar, C. *et al.* Prevalence of *Trypanosoma cruzi* infection in pregnant Latin American women and congenital transmission rate in a non-endemic area: the experience of the Valencian Health Programme (Spain). *Epidemiology and infection* **140**, 1896-1903 (2012).

9. Pinazo, M.J. *et al.* Characterization of digestive involvement in patients with chronic *T. cruzi* infection in Barcelona, Spain. *PLoS neglected tropical diseases* **8**, e3105 (2014).

10. Cordova, E., Maiolo, E., Corti, M. & Orduna, T. Neurological manifestations of Chagas' disease. *Neurological research* **32**, 238-244 (2010).

11. Lee, B.Y., Bacon, K.M., Bottazzi, M.E. & Hotez, P.J. Global economic burden of Chagas disease: a computational simulation model. *The Lancet. Infectious diseases* **13**, 342-348 (2013).

12. Mougabure-Cueto, G. & Picollo, M.I. Insecticide resistance in vector Chagas Disease: evolution, mechanisms and management. *Acta tropica* (2015).

13. da Silveira, J.F., Umezawa, E.S. & Luquetti, A.O. Chagas disease: recombinant *Trypanosoma cruzi* antigens for serological diagnosis. *Trends in parasitology* **17**, 286-291 (2001).

14. Camargo, M.E. *et al.* Three years of collaboration on the standardization of Chagas' disease serodiagnosis in the Americas: an appraisal. *Bulletin of the Pan American Health Organization* **20**, 233-244 (1986).

15. Sosa-Estani, S. & Segura, E.L. Etiological treatment in patients infected by *Trypanosoma cruzi*: experiences in Argentina. *Current opinion in infectious diseases* **19**, 583-587 (2006).

16. Bonney, K.M. & Engman, D.M. Autoimmune Pathogenesis of Chagas Heart Disease: Looking Back, Looking Ahead. *The American journal of pathology* **185**, 1537-1547 (2015).

17. Tarleton, R.L. Parasite persistence in the aetiology of Chagas disease. *International journal for parasitology* **31**, 550-554 (2001).

18. Teixeira, A.R., Hecht, M.M., Guimaro, M.C., Sousa, A.O. & Nitz, N. Pathogenesis of chagas' disease: parasite persistence and autoimmunity. *Clinical microbiology reviews* **24**, 592-630 (2011).

19. Zhang, L. & Tarleton, R.L. Parasite persistence correlates with disease severity and localization in chronic Chagas' disease. *The Journal of infectious diseases* **180**, 480-486 (1999).

20. Kurup, S.P. & Tarleton, R.L. The *Trypanosoma cruzi* flagellum is discarded via asymmetric cell division following invasion and provides early targets for protective CD8(+) T cells. *Cell host & microbe* **16**, 439-449 (2014).

21. Burleigh, B.A. & Andrews, N.W. The mechanisms of *Trypanosoma cruzi* invasion of mammalian cells. *Annual review of microbiology* **49**, 175-200 (1995).

22. Atwood, J.A., 3rd *et al.* The *Trypanosoma cruzi* proteome. *Science* **309**, 473-476 (2005).

23. Minning, T.A., Weatherly, D.B., Atwood, J., 3rd, Orlando, R. & Tarleton, R.L. The steady-state transcriptome of the four major life-cycle stages of *Trypanosoma cruzi*. *BMC genomics* **10**, 370 (2009).

24. Tardieux, I. *et al.* Lysosome recruitment and fusion are early events required for trypanosome invasion of mammalian cells. *Cell* **71**, 1117-1130 (1992).

25. Woolsey, A.M. *et al.* Novel PI 3-kinase-dependent mechanisms of trypanosome invasion and vacuole maturation. *Journal of cell science* **116**, 3611-3622 (2003).

26. Andrade, L.O. & Andrews, N.W. Lysosomal fusion is essential for the retention of *Trypanosoma cruzi* inside host cells. *The Journal of experimental medicine* **200**, 1135-1143 (2004).

27. Fernandes, M.C. & Andrews, N.W. Host cell invasion by *Trypanosoma cruzi*: a unique strategy that promotes persistence. *FEMS microbiology reviews* **36**, 734-747 (2012).

28. Burleigh, B.A. & Woolsey, A.M. Cell signalling and *Trypanosoma cruzi* invasion. *Cellular microbiology* **4**, 701-711 (2002).

29. Yoshida, N. & Cortez, M. *Trypanosoma cruzi*: parasite and host cell signaling during the invasion process. *Sub-cellular biochemistry* **47**, 82-91 (2008).

30. Mortara, R.A. *et al.* Mammalian cell invasion and intracellular trafficking by *Trypanosoma cruzi* infective forms. *Anais da Academia Brasileira de Ciencias* **77**, 77-94 (2005).

31. Mattos, E.C., Schumacher, R.I., Colli, W. & Alves, M.J. Adhesion of *Trypanosoma cruzi* trypomastigotes to fibronectin or laminin modifies tubulin and paraflagellar rod protein phosphorylation. *PloS one* **7**, e46767 (2012).

32. Ulrich, H., Magdesian, M.H., Alves, M.J. & Colli, W. In vitro selection of RNA aptamers that bind to cell adhesion receptors of *Trypanosoma cruzi* and inhibit cell invasion. *The Journal of biological chemistry* **277**, 20756-20762 (2002).

33. Butler, C.E., de Carvalho, T.M., Grisard, E.C., Field, R.A. & Tyler, K.M. Trans-sialidase stimulates eat me response from epithelial cells. *Traffic* **14**, 853-869 (2013).

34. Soares, R.P. *et al.* Intraspecies variation in *Trypanosoma cruzi* GPI-mucins: biological activities and differential expression of alpha-galactosyl residues. *The American journal of tropical medicine and hygiene* **87**, 87-96 (2012).

35. Johnson, C.A. *et al.* Thrombospondin-1 interacts with *Trypanosoma cruzi* surface calreticulin to enhance cellular infection. *PloS one* **7**, e40614 (2012).

36. Sosoniuk, E. *et al. Trypanosoma cruzi* calreticulin inhibits the complement lectin pathway activation by direct interaction with L-Ficolin. *Molecular immunology* **60**, 80-85 (2014).

37. Ferreira, V. *et al.* The classical activation pathway of the human complement system is specifically inhibited by calreticulin from *Trypanosoma cruzi*. *Journal of immunology* **172**, 3042-3050 (2004).

38. Cestari, I. & Ramirez, M.I. Inefficient complement system clearance of *Trypanosoma cruzi* metacyclic trypomastigotes enables resistant strains to invade eukaryotic cells. *PloS one* **5**, e9721 (2010).

39. Castillo, C. *et al.* The interaction of classical complement component C1 with parasite and host calreticulin mediates *Trypanosoma cruzi* infection of human placenta. *PLoS neglected tropical diseases* **7**, e2376 (2013).

40. Okura, M. *et al.* A lipid-modified phosphoinositide-specific phospholipase C (TcPI-PLC) is involved in differentiation of trypomastigotes to amastigotes of *Trypanosoma cruzi*. *The Journal of biological chemistry* **280**, 16235-16243 (2005).

41. Furuya, T., Kashuba, C., Docampo, R. & Moreno, S.N. A novel phosphatidylinositol-phospholipase C of *Trypanosoma cruzi* that is lipid modified and activated during trypomastigote to amastigote differentiation. *The Journal of biological chemistry* **275**, 6428-6438 (2000).

42. Queiroz, R.M. *et al.* Cell surface proteome analysis of human-hosted *Trypanosoma cruzi* life stages. *Journal of proteome research* **13**, 3530-3541 (2014).

43. Queiroz, R.M. *et al.* Quantitative proteomic and phosphoproteomic analysis of *Trypanosoma cruzi* amastigogenesis. *Molecular & cellular proteomics : MCP* **13**, 3457-3472 (2014).

44. Bao, Y. *et al.* Molecular cloning and characterization of mitogen-activated protein kinase 2 in *Trypanosoma cruzi*. *Cell Cycle* **9**, 2888-2896 (2010).

45. Zhang, W. & Liu, H.T. MAPK signal pathways in the regulation of cell proliferation in mammalian cells. *Cell research* **12**, 9-18 (2002).

46. Oki, N., Takahashi, S.I., Hidaka, H. & Conti, M. Short term feedback regulation of cAMP in FRTL-5 thyroid cells. Role of PDE4D3 phosphodiesterase activation. *The Journal of biological chemistry* **275**, 10831-10837 (2000).

47. Gonzales-Perdomo, M., Romero, P. & Goldenberg, S. Cyclic AMP and adenylate cyclase activators stimulate *Trypanosoma cruzi* differentiation. *Experimental parasitology* **66**, 205-212 (1988).

48. Brener, Z., Golgher, R., Bertelli, M.S. & Teixeira, J.A. Strain-dependent thermosensitivity influencing intracellular differentiation of *Trypanosoma cruzi* in cell culture. *The Journal of protozoology* **23**, 147-150 (1976).

49. Ashton, A.W. *et al.* Thromboxane A2 is a key regulator of pathogenesis during *Trypanosoma cruzi* infection. *The Journal of experimental medicine* **204**, 929-940 (2007).

50. Tonelli, R.R. *et al.* L-proline is essential for the intracellular differentiation of *Trypanosoma cruzi*. *Cellular microbiology* **6**, 733-741 (2004).

51. Williams, G.T. Specific inhibition of the differentiation of *Trypanosoma cruzi*. *The Journal of cell biology* **99**, 79-82 (1984).

52. Williams, G.T. *Trypanosoma cruzi*: inhibition of intracellular and extracellular differentiation by ADP-ribosyl transferase antagonists. *Experimental parasitology* **56**, 409-415 (1983).

53. Vilchez Larrea, S.C. *et al.* Inhibition of poly(ADP-ribose) polymerase interferes with *Trypanosoma cruzi* infection and proliferation of the parasite. *PloS one* **7**, e46063 (2012).

54. Hartlova, A. *et al.* DNA damage primes the type I interferon system via the cytosolic DNA sensor STING to promote anti-microbial innate immunity. *Immunity* **42**, 332-343 (2015).

55. Alexander, A.D., Villalta, F. & Lima, M.F. Transforming growth factor alpha binds to *Trypanosoma cruzi* amastigotes to induce signaling and cellular proliferation. *Infection and immunity* **71**, 4201-4205 (2003).

56. Combs, T.P. *et al.* The adipocyte as an important target cell for *Trypanosoma cruzi* infection. *The Journal of biological chemistry* **280**, 24085-24094 (2005).

57. Koga, R. *et al.* TLR-dependent induction of IFN-beta mediates host defense against *Trypanosoma cruzi*. *J Immunol* **177**, 7059-7066 (2006).

58. Rodrigues, M.M., Oliveira, A.C. & Bellio, M. The Immune Response to *Trypanosoma cruzi*: Role of Toll-Like Receptors and Perspectives for Vaccine Development. *Journal of parasitology research* **2012**, 507874 (2012).

59. Lykens, J.E. *et al.* Mice with a selective impairment of IFN-gamma signaling in macrophage lineage cells demonstrate the critical role of IFN-gamma-activated macrophages for the control of protozoan parasitic infections in vivo. *J Immunol* **184**, 877-885 (2010).

60. Padilla, A.M., Simpson, L.J. & Tarleton, R.L. Insufficient TLR activation contributes to the slow development of CD8+ T cell responses in *Trypanosoma cruzi* infection. *J Immunol* **183**, 1245-1252 (2009).

61. Munoz-Fernandez, M.A., Fernandez, M.A. & Fresno, M. Synergism between tumor necrosis factor-alpha and interferon-gamma on macrophage activation for the killing of intracellular *Trypanosoma cruzi* through a nitric oxide-dependent mechanism. *European journal of immunology* **22**, 301-307 (1992).

62. Metz, G., Carlier, Y. & Vray, B. *Trypanosoma cruzi* upregulates nitric oxide release by IFN-gamma-preactivated macrophages, limiting cell infection independently of the respiratory burst. *Parasite immunology* **15**, 693-699 (1993).

63. Silva, J.S., Vespa, G.N., Cardoso, M.A., Aliberti, J.C. & Cunha, F.Q. Tumor necrosis factor alpha mediates resistance to *Trypanosoma cruzi* infection in mice by inducing nitric oxide production in infected gamma interferon-activated macrophages. *Infection and immunity* **63**, 4862-4867 (1995).

64. Krettli, A.U. & Brener, Z. Protective effects of specific antibodies in *Trypanosoma cruzi* infections. *J Immunol* **116**, 755-760 (1976).

65. Vasconcelos, J.R. *et al.* Protective immunity against *Trypanosoma cruzi* infection in a highly susceptible mouse strain after vaccination with genes encoding the amastigote surface protein-2 and trans-sialidase. *Human gene therapy* **15**, 878-886 (2004).

66. Martin, D.L. & Tarleton, R.L. Antigen-specific T cells maintain an effector memory phenotype during persistent *Trypanosoma cruzi* infection. *J Immunol* **174**, 1594-1601 (2005).

67. Kotner, J. & Tarleton, R. Endogenous CD4(+) CD25(+) regulatory T cells have a limited role in the control of *Trypanosoma cruzi* infection in mice. *Infection and immunity* **75**, 861-869 (2007).

68. Kumar, S. & Tarleton, R.L. Antigen-specific Th1 but not Th2 cells provide protection from lethal *Trypanosoma cruzi* infection in mice. *J Immunol* **166**, 4596-4603 (2001).

69. Tarleton, R.L. CD8(+) T cells in *Trypanosoma cruzi* infection. *Seminars in immunopathology* **37**, 233-238 (2015).

70. Padilla, A.M., Bustamante, J.M. & Tarleton, R.L. CD8+ T cells in *Trypanosoma cruzi* infection. *Current opinion in immunology* **21**, 385-390 (2009).

71. Martin, D. & Tarleton, R. Generation, specificity, and function of CD8+ T cells in *Trypanosoma cruzi* infection. *Immunological reviews* **201**, 304-317 (2004).

72. Tarleton, R.L., Koller, B.H., Latour, A. & Postan, M. Susceptibility of beta 2-microglobulin-deficient mice to *Trypanosoma cruzi* infection. *Nature* **356**, 338-340 (1992).

73. Kurup, S.P. & Tarleton, R.L. Perpetual expression of PAMPs necessary for optimal immune control and clearance of a persistent pathogen. *Nature communications* **4**, 2616 (2013).

74. Camargo, R. *et al. Trypanosoma cruzi* infection down-modulates the immunoproteasome biosynthesis and the MHC class I cell surface expression in HeLa cells. *PloS one* **9**, e95977 (2014).

75. Martin, D.L. *et al.* CD8+ T-Cell responses to *Trypanosoma cruzi* are highly focused on strain-variant trans-sialidase epitopes. *PLoS pathogens* **2**, e77 (2006).

76. Rosenberg, C.S., Martin, D.L. & Tarleton, R.L. CD8+ T cells specific for immunodominant trans-sialidase epitopes contribute to control of *Trypanosoma cruzi* infection but are not required for resistance. *J Immunol* **185**, 560-568 (2010).

CHAPTER 2

TRYPANOSOMA CRUZI CALRETICULIN PROMOTES INFECTION OF LOW-DENSITY LIPOPROTEIN RECEPTOR-RELATED PROTEIN 1 (LRP1)-EXPRESSING PHAGOCYTES[1]

[1] Zhang, W. and Tarleton, R.L. To be submitted to *PLoS Pathogens*.

2.1 Abstract

Trypanosoma cruzi calreticulin (CalR) is known to increase parasite infection in mammalian cells, but its potential role as a target of innate and adaptive immune responses has not been thoroughly investigated. Here we show that the overexpression of *T. cruzi* CalR (TcCalR) in the parasite markedly increased infection of Vero cells and mouse macrophages *in vitro* and infection efficiency and parasite proliferation in mice. However, after an initial period of increased parasite expansion, infection with TcCalR parasites was controlled more rapidly when compared to infection with wild-type (WT). TcCalR overexpression drove increased infection primarily in infiltrating monocytes, tissue-resident macrophages and neutrophils *in vivo* and was largely dependent on recognition of surface and secreted *T. cruzi* CalR by low-density lipoprotein receptor-related protein 1 (LRP1) on these host cells. The subsequent accelerated parasite clearance was also dependent on LRP1 expression and on the production of IFNγ. Collectively, these results suggest that CalR overexpression enhances parasite invasion, particularly into LRP1-expressing macrophages, providing an initial boost in parasite production. However, as adaptive immune responses are generated, increased activation of TcCalR-infected macrophages allowed more efficient control of the infection via IFNγ-dependent mechanisms.

2.2 Introduction

Infection by the intracellular parasite *Trypanosoma cruzi* in mammalian hosts is largely controlled but rarely eradicated, leading to persistent infection and the development of human Chagas disease, one of the world's most neglected tropical diseases [1]. Mammals become infected with *T. cruzi* when metacyclic trypomastigotes in the feces of the triatomine insect vector cross skin or mucosal barriers, and then infect a variety of host cell types, including macrophages, epithelial cells, myocytes, adipocytes, fibroblasts and smooth muscle cells [2-4]. *T.*

cruzi infection elicits potent innate and adaptive immune responses that are crucial to control of the infection. Among immune effector mechanisms, $CD8^+$ T cells are particularly important for efficient parasitic reduction as the absence of $CD8^+$ T cells in β-2-microglobulin-deficient or following anti-CD8-antibody treatment results in increased parasite burden and loss of infection control [5, 6]. However, $CD8^+$ T cells generated during *T. cruzi* infection are dominated by populations recognizing epitopes encoded by a large and hyper-variant gene family of *trans*-sialidases [7]. However the $CD8^+$ T cells targeting the two most dominant *trans*-sialidase-derived epitopes are dispensable for the control of infection [8], it is likely that other, subdominant antigens possibly derived from conserved *T. cruzi* surface or secreted proteins, may be important targets of protective $CD8^+$ T cells.

Macrophages have long been recognized as the initial points of contact/infection for *T. cruzi*, and thus play an important but complex role in establishing, expanding and subsequently controlling infection [4, 9]. This interaction of macrophages and *T. cruzi* has been studied extensively *in vitro* [10, 11], but less is known about *T. cruzi* :macrophage interactions *in vivo*. One of the parasite molecules that has significant potential to impact the *T. cruzi*:macrophage interaction is calreticulin (CalR). *T. cruzi* CalR is an intracellular, surface, and potentially secreted protein [12-14]. Sharing 47% sequence identity with human and mouse CalR, *T. cruzi* CalR possesses functional conservation with its human and murine homologues. Mammalian CalR is classically defined as a calcium-binding chaperone that among other functions, facilitates folding and assembly of major histocompatibility complex (MHC) class I molecules [15].

Recently mammalian CalR was identified as an ‘eat-me’ signal and danger-associated molecular pattern (DAMP), due to the fact that during immunogenic programmed cell death (ICD), the normally ER-resident CalR is translocated to the surface of stressed, early apoptotic

and cancer cells (ecto-CalR) [16, 17]. The ecto-CalR then triggers phagocytosis of these abnormal cells by macrophages and dendritic cells (DCs) via low-density lipoprotein receptor-related protein 1 (LRP1 or CD91), in the process, enhancing MHC-I-restricted antigen presentation to $CD8^+$ T cells and subsequent killing of abnormal cells by antigen-specific CTLs [17-20]. Markedly enhanced tumor control has been observed in many cases upon ecto-CalR presence on tumor cells (reviewed in [21]).

Extracellular CalR in *T. cruzi* has been reported to promote parasite entry in mammalian cells by inhibiting classical and lectin-dependent complement activation pathways and through interactions with thrombospondin 1 (TSP1) [12, 13, 22]. Based on the potential functional conservation with host CalR, we hypothesized that extracellular *T. cruzi* CalR may act as an 'eat-me' signal similarly as the mammalian ecto-CalR to trigger entry into macrophages via LRP1 recognition. Here, by using engineered *T. cruzi* -overexpressing CalR, we demonstrate that CalR can drive significantly increased LRP1-dependent parasite entry, enhancing invasion into professional phagocytes and resulting in an increased initial parasite burden. Interestingly, this preferential invasion in professional phagocytes ultimately led to a more rapid control of the infection in mice.

2.3 Materials and Methods

2.3.1 *Mice and infections*

C57BL/6J (B6), BALB/cByJ background (National Cancer Institute at Frederick) and B7.129S7-*Ifng*^{tm1Ts}/J (abbreviated as IFN$\gamma^{-/-}$, Jackson Laboratory) were bred in Coverdell Center animal facility (University of Georgia, Athens, GA) under specific pathogen-free conditions. Homozygous LysM^{cre} mice (B6.129P2-*Lyz2*$^{tm1(cre)Ifo}$/J, Jackson Laboratory) were mated with LRP1$^{flox/flox}$ (B6.129S7-*Lrp1*^{tm2Her}/J, Jackson Laboratory) to obtain littermates (mLRP1$^{-/-}$) in

which myeloid cells are LRP1-deficient. In most cases females of 6-8 weeks were used for experiments. *T. cruzi* CL epimastigotes of the wild-type were transfected [23] with pTREX plasmid [24] containing the coding sequence of *T. cruzi* calreticulin (*calR*) with fusion to a downstream influenza haemagglutinin (HA) tag. Parasites used for all infections were prepared by inoculating Vero cell culture passaged-trypomastigote stage *T. cruzi*. Infected animals were inoculated intraperitoneally (10^3 parasites) or subcutaneously in the ear (10^4 parasites or 2.5×10^5 parasites if stained with 1 μM CellTrace-violet, Life Technologies). Animals were euthanized with CO_2 inhalation. All animal protocols were approved by the University of Georgia Institutional Animal Care and Use Committee.

2.3.2 *Anti-T. cruzi CalR antibody production*

Recombinant His-tagged proteins produced as described below were attached to Dynabeads TALON magnetic beads (Invitrogen) by incubating excess protein (300 μg) with pre-equilibrated beads (30 mg) at RT for 10 min followed by washing the protein-bound beads in Binding and Washing buffer (recipe in the product's instruction manual) for 5 times via magnetic separation. The separated beads were resuspended in 700 μl PBS and kept at 4˚C. BALB/cByJ mice were subcutaneously injected with 70-100 μl protein-bound beads and boosted twice using the same regime at two week intervals. Blood was collected into serum separator tubes (BD Microtainer) and mouse sera were isolated following manual instruction and kept at -20 ˚C until use. Antibody specificity and sensitivity was confirmed by ELISA using the recombinant protein as the bait, BSA and ddH_2O as negative control.

2.3.3 *Immunoblotting*

10^8 freshly-cultivated parasites were washed twice in serum-free RPMI and incubated in 10 ml serum-free RPMI for 2 h at 27 ˚C for epimastigotes or 37 ˚C for trypomastigotes. After

centrifugation at 1,600 × g for 10min, the supernatant was collected and passed through 0.22 μm pore size, PVDF membrane filter (Millipore), concentrated to 200 μl using Amicon Ultra 30k centrifugal filters (Millipore). Cell pellets of 10^8 parasites were washed in PBS and subjected to three or more rounds of freeze-thawing supplemented with protease inhibitor cocktail (Sigma) followed by sonication and centrifugation at 13,500 × g, 20 min at 4 ˚C. Pellets were washed twice in PBS to be used as a membrane fraction, while the supernatant was passed through a 0.22 μm pore size, PVDF membrane filter (Millipore) used as the cytosolic fraction. Protein concentration in cytosolic and membrane *T. cruzi* fractions was determined in Bradford assay (Bio-Rad). Twenty microgram of soluble and insoluble lysates or 20 μl culture supernatant were probed with anti-CalR mouse serum (1:500) or rat monoclonal anti-HA antibody (1:20,000; Roche), and mouse monoclonal anti-α-tubulin antibody (1:15,000; Sigma) were used as control.

2.3.4 *Immunofluorescence assay*

The protocol was modified from that previously described [25]. Briefly, parasites and 3 day-infected Vero cells (trypomastigotes: Vero = 10:1) adhered to poly-L-lysine cellware coverslips (BD Biosciences) were fixed in 3.7% paraformaldehyde in PBS. Parasites without permealization were first stained with rabbit polyclonal anti-*T. cruzi* calR antibody (1:250; generously provided by Dr. Sanchez Valdez) followed by goat anti-rabbit IgG Alexfluor 488 (1:200; Life Technologies), stained with propidium iodide (PI, 5μg/ml) and then washed with DAPI (4 μg/ml). Fixed Vero cells were permeabilized using 10% Triton X-100 in PBS before staining. Vero cells were then stained with rat monoclonal anti-HA antibody (1:500) followed by goat-anti-rat IgG Alex fluor488 (1:200; Life Technologies), and washed with PI (5μg/ml). Coverslips were mounted with Fluoro-Gel, with TES buffer (Electron Microscopy Sciences) before microscopy analysis. Images were either acquired with an Applied Precision Delta Vision

microscope and deconvolved and adjusted for contrast using its Softworx software (Applied Precision) or acquired with a Zeiss LSM710 Confocal Microscope and adjusted for contrast using Zen lite 2011 software (Zeiss).

2.3.5 *Phenotyping cells by flow cytometry*

T. cruzi CalR surface expression was determined by staining with anti-*T. cruzi* CalR mouse serum or control mouse serum (1:100) followed by goat-anti-mouse Alexfluor 488 (1:200). To measure T cell memory phenotype, peripheral blood was collected from the tail vein and lysis of red blood cells were performed before staining in staining buffer (2% BSA, 0.02% azide in PBS (PAB)) with tetramer-phycoerythrin (TSKB20-PE; ANYKFTLV peptide on H2Kb; NIH Tetramer Core Facility, Emory University; 1:800) and the followings: anti-CD8 efluor 450 (1:800), anti-CD127 APC (1:100), anti-CD44 FITC (1:400), anti-B220 PE- Cy5 (1:200), anti-CD11b PE-Cy5 (1:200), anti-CD4 PE-Cy5 (1:200). Staining with PE-Cy5-conjugated antibodies was used for a dump channel. T cell activation phenotype was determined by staining with anti-CD8 efluor 450 (1:800), anti-CD4 APC-efluor 780 (1:400), anti-CD69 PerCP-Cy5.5 (1:200). Draining lymph nodes and spleens were collected and single-cell suspension was prepared by gently crushing using thin-tip tweezers or frosted-edged glass slides, followed by lysis of red blood cells for spleen cells.

To determine parasite entry and expansion at the infection site, the tissue (pinna of the ear) was digested in liberase (Roche) and DNase (Roche) at 37°C/5% CO_2 for 1 h followed by gently crushing between the frosted edges of glass slides to dissociate the cells. Cells were stained in the dark on ice as follows: live/dead stain using LIVE/DEAD Fixable Aqua Dead Cell Stain Kit (1:1,000; Invitrogen) for 30 min, washed, incubated with Fcblock (1:50), then anti-CD11b APC-efluor 780 (1:800), anti-CD45.2 FITC (1:200), anti-Ly6G PerCP-Cy5.5 (1:200), anti-CD11c

APC (1:200), F4/80 PE-Cy7 (1:200). HBSS was used to dilute antibodies and to wash cells. All antibodies for tissue cell staining or blocking were purchased from eBioscience.

2.3.6 *Determination of NFκB/AP-1 activity*

RAW-Blue mouse macrophages (Invivogen) (5×10^4) were incubated with 5×10^5 *T. cruzi* trypomastigotes at 37°C/5% CO_2. Nuclear translocation of activated NFκB and AP-1 activity was determined at various time points by colorimetrically quantifying the secreted embryonic alkaline phosphatase using Quanti-Blue media as described in the manufacturer's manual (Invivogen). *E. coli* LPS or media were served as positive or negative controls, respectively.

2.3.7 *In vitro infection assay*

Vero cells or RAW-Blue macrophages or thioglycollate-elicited murine peritoneal exudate macrophages (5×10^4/well) pre-seeded in chamber slides (Thermo Scientific) were exposed to 5×10^5 trypomastigotes for 2 hours with or without 15 min 0.1% H_2O_2 pre-treatment. Cells were washed at least six times to eliminate extracellular parasites. In some cases, cells were incubated with Fcblock (1:200) for 20 min followed by rabbit anti-mouse LRP1 antibody (1:100; Novus BioLogicals) and rabbit IgG antibody (1:100; Invitrogen) in 100 μl serum-free RPMI for 80 min before addition of trypomastigotes diluted in 100 μl 10%s FBS RPMI. Upon removal of supernatant, slides were dried at 37˚C and stained with Hema 3 fixative and solutions (Fisher Diagnostics). Numbers of infected cells per 100 cells and the number of parasite in at least 50 infected cells were counted per well under a compound light microscope (100×).

2.3.8 *Assessment of in vivo infection and clearance of T. cruzi*

Blood (5 μl) from IFN$\gamma^{-/-}$ mice or mice that had received immunosuppression with cyclophosphamide (200 mg kg^{-1}; 6× at 2-day intervals) [27] was collected from the tail vein. The number of parasites was quantified using a compound light microscope (40×) and expressed as

the number of live trypomastigotes per μl. Survival was monitored daily. Hemocultures were generated by adding 1 ml of blood to liver digest-neutralized tryptose (LDNT) media followed by incubation at 27 °C/5% CO_2 and parasites were monitored at 20-50 days. Sections (5 μm) from paraffin-embedded tissues were stained with H&E (Histological laboratory, Dept. of Pathology, University of Georgia) and the number of amastigote nests was counted for 100 fields in each histological sample using a compound light microscope (100×).

2.3.9 *Production of recombinant protein and temporary anchoring onto T. cruzi*

Recombinant *T. cruzi* CalR was generated in *E. coli* BL21(DE3)pLysS strain by transformation of the Gateway-adapted and His-tagged pBAD plasmid containing the coding sequence of *T. cruzi* CalR without KDEL ER-retention sequence. Bacteria were cultured overnight in Luria-Bertani (LB) broth at 37 °C, 280 rpm before transferring to terrific broth. Once bacteria reached the early exponential phase, L-arabinose was added and culture was shaken at 28 °C, 280 rpm until the late stationary phase. His-tagged CalR was harvested as described [28]. Proteins were re-natured in 30K MWCO Slide-A-Lyzer Dialysis Cassettes (Thermo Scientific) in PBS overnight at 4 ˚C following the manufacturer's protocol. Recombinant proteins were anchored with FSL-biotin GPI with a single biotin F-moiety (FSL-CONJ(1 Biotin)-SC2-L1, KODE Biotech Materials Ltd.) as described [29]. The GPI-anchored protein prepared in this method can persist on the parasite surface for up to 12 h [29].

2.3.10 *Peptide stimulation and intracellular cytokine staining*

We stimulated 1 million spleen cells from naïve mice or mice intraperitoneally inoculated with 1,000 TcCalR trypomastigotes 80-120 days previously with 15-mer synthetic peptides derived from *T. cruzi* CalR (China Peptide) for 4-6 hrs at 37 °C in the presence of Golgiplug (eBioscience). These synthetic peptides cover the complete ORF of *T. cruzi* CalR with each

peptide sharing 10-amino-acid overlap with the following one. Peptides were pooled in 13 groups at a final concentration of 1 μM with each group containing 10 peptides. Cells were stained with anti CD8-efluor 450 (1:800), anti CD4-APC efluor780 (1:400), anti CD44-FITC (1:400) in PAB, permeablized with Cytofix/Cytoperm (eBioscience), and stained with anti IFNγ-APC (1:400) in Perm Wash buffer (eBioscience). IFNγ^{+} cells were gated in CD44^{hi} CD8^{+}CD4^{-} cells. TSKB20, SIINFEKL peptides (Genscript) at 1nM served as positive and negative controls, respectively.

2.3.11 *Quantitative real-time PCR*

Parasite load in the skeletal muscle or the pinna of the ear was analyzed by quantitative real-time PCR as previously described [26].

2.3.12 *Statistical analysis*

Data are presented as the mean ±SEM. Comparison of the means was performed using two-tailed Student's *t* test. P-values of $p<0.05$ were considered significant.

2.4 Results

2.4.1 *Increased expression of T. cruzi CalR promotes initial host cell entry and parasite expansion in vitro*

Previous studies have identified *T. cruzi* CalR as both an intracellular and surface protein [12, 13] with the potential to be secreted [30]. We first confirmed the surface localization of *T. cruzi* CalR in wild-type *T. cruzi* (TcWT) amastigotes and trypomastigotes (Fig. 2.1A). As expected, parasites transfected with a pTREX expression plasmid with CalR gene tagged with HA (Supplementary Fig. 2.1A, B) [24] exhibited increased CalR production (Fig. 1B), as well as detectable CalR released extracellularly by both epimastigotes and intracellular amastigotes (Fig. 2.1C, D).

Fig. 2.1D also suggests increased infection or replication by TcCalR in host cells, relative to TcWT, as previously reported [12, 13, 31]. To further explore this, we assayed infection by TcCalR in Vero, RAW-Blue macrophages and mouse primary peritoneal exudate macrophages, measuring the percentage of cells infected and the parasite number per infected cell (Fig. 2.2A, B). Notably, TcCalR numbers were the highest in the two macrophage populations, relative to the Vero cells. Incubation of RAW-Blue macrophages with trypomastigotes killed by hydrogen peroxide treatment also showed increased uptake of TcCalR parasites relative to TcWT (Fig. 2.2C), indicating enhanced phagocytosis as one potential mechanism of increased TcCalR entry into host cells.

Antibody blockade of *T. cruzi* extracellular CalR greatly reduced both TcWT and TcCalR infection to comparable levels of parasite entry in RAW-Blue macrophages (Fig. 2.2D). To further examine the contribution of *T. cruzi* surface and secreted CalR protein in enhancing infection, GPI-anchored CalR protein was inserted into the plasma membrane of WT trypomastigotes (TcWT-GPI-CalR) to simulate surface CalR overexpression while exogenous CalR (exo CalR) was added to WT trypomastigotes pre-incubated with GPI-anchored BSA, an irrelevant control protein, to simulate enhanced CalR secretion. *T. cruzi*- incubated in either GPI-CalR or exogenous non-GPI-anchored CalR (exo CalR) exhibited increased infection of RAW Blue macrophages (Fig. 2.2E). Notably, TcWT trypomastigotes, which should express no less surface CalR than BSA-anchored parasites, displayed boosted CalR surface expression following incubation with exo CalR compared to that in irrelevant protein-treated parasites, and the high surface expression was comparable or even modestly higher than that in parasites with GPI-anchored CalR. A similar ability of CalR protein to efficiently bind to cell surface membranes has been previously documented in mammalian cells [18]. As in the case of TcCalR

parasites, killed trypomastigotes incubated with exogenous non-GPI-anchored CalR also showed increased uptake by macrophages relative to control BSA-sensitized parasites (Fig. 2.2F), indicating that an increased level of surface CalR enhances phagocytosis of *T. cruzi*.

2.4.2 *Increased CalR expression results in an initial intensification in parasite burden in vivo and subsequent rapid parasite control*

We next assessed whether CalR overexpression in *T. cruzi* also leads to greater infection efficiency *in vivo*. For this purpose, we initially used IFN$\gamma^{-/-}$ mice wherein *T. cruzi* growth can be observed largely unimpeded by cellular immune control. In IFN$\gamma^{-/-}$ mice TcCalR infection resulted in increased parasitemia (Fig. 2.3A) and greatly reduced host survival time (Fig. 2.3B) as compared to infection with TcWT. Likewise in immunocompetent WT mice, TcCalR parasites showed an increased early rate of expansion when compared to WT parasites (Fig. 2.3C). However, surprisingly, parasite burden in TcCalR infection was reduced below that in TcWT infection at 30-50 days post infection, as assessed by both quantitative real-time PCR (Fig. 2.3D) and histological examination of infected cells in the skeletal muscle (Fig. 2.3E). Despite this reduced post-acute phase parasite load, the TcCalR-infected mice nevertheless remained persistently infected as demonstrated by the detection of parasites in blood or tissues following immunosuppression. The possibility that the failure to cure may be the result of loss of CalR overexpression over time was ruled out by the observation that parasites recovered from mice with chronic TcCalR infections continued to express elevated levels of CalR (Supplementary Fig. 2.3A) and displayed higher parasitemia and early mortality in IFN$\gamma^{-/-}$ mice as characteristic of TcCalR (Supplementary Fig. 2.3B). Therefore *T. cruzi* CalR also serves as an “eat-me” signal such that over-expression of CalR by *T. cruzi* both in vitro and in vivo results

in better infection of host cells and parasite growth. However this early expansion advantage is quickly lost in vivo via an IFN-gamma-dependent control mechanism.

2.4.3 *T. cruzi overexpressing CalR enhances infection primarily in professional phagocytes in vivo via recognition by the low-density lipoprotein receptor-related protein 1 (LRP1)*

To determine if the enhanced infection and growth characteristics of TcCalR parasites in vivo was related to preferential infection/uptake by monocytes/macrophages, as we observed in vitro, we identified the cell types infected at the site of parasite inoculation. Enhanced infection by TcCalR was observed in infiltrating monocytes ($CD45^{+}Ly6G^{mid}CD11b^{+}$), neutrophils ($CD45^{+}Ly6G^{hi}CD11b^{+}$) and tissue-resident macrophages ($CD45^{+}Ly6G^{lo}CD11b^{+}F4/80^{mid}CD11c^{-}$) relative to that in TcWT infection at 1.5 dpi, as indicated by both increased frequency of infected cells and the enhanced mean fluorescence intensity in infected populations (Fig. 2.4A-C).

In mammals, stressed, dying or neoplastic cells expressing ecto-CalR, are engulfed by professional phagocytes via recognition by its cognate receptor, LRP1. To determine if LRP1 played an integral role in CalR-mediated and -enhanced infection of phagocytic cells by TcCalR, the effect of antibody blockage of the LRP1 receptor on invasion of host cells by *T. cruzi* was measured. Both the percentage of macrophages infected and parasites per infected cell for both TcWT and TcCalR populations were reduced by addition of anti-LRP1 blocking antibodies. In contrast, infection of Vero cells which express no or little LRP1 was unaffected by the presence of anti-LRP1 antibody (Fig. 2.5A, B). The interaction between LRP1 receptor and *T. cruzi* CalR was also examined in vivo using mice lacking LRP1 expression specifically in myeloid cells ($mLRP1^{-/-}$). At 1.5 days post infection, infiltrating monocytes, infiltrating neutrophils and tissue-resident macrophages from $mLRP1^{-/-}$ mice all displayed reduced TcCalR infection/expansion

relative to those in mLRP1$^{+/+}$ mice (Fig. 2.5C). These same phagocyte populations also showed a modest but not statistically significant reduction in TcWT infection in mLRP1$^{-/-}$ vs mLRP1-expressing mice. Infection by TcCalR in non-phagocytic CD45^{+} cells (CD45^{+}Ly6G^{-}CD11b^{-}) was unaffected by LRP1 expression (Fig. 2.5D). By 4 dpi the overall tissue-wide impact of LRP1 expression on parasite load was apparent in the case of both TcCalR and TcWT parasites (Fig. 2.5E). Thus the interaction of *T. cruzi* CalR with host LRP1 likely accounts for the increased infection potential of TcCalR parasites for monocyte/macrophages and for the increase of parasite burden early in infection.

2.4.4 *LRP1 is required for the rapid post-acute phase control of TcCalR*

The increased interaction between host LRP1 in phagocytes and *T. cruzi* CalR accounts for the rapid infection and expansion of the TcCalR parasites in vivo and in vitro. To determine if the accelerated control of TcCalR *in vivo* was also related to LRP1 expression on host cells, parasite load in the post-acute phase (35-40 dpi) in mLRP1$^{-/-}$ mice was measured. TcCalR parasites displayed dramatically higher parasite load relative to TcWT in mLRP1$^{-/-}$ mice (Fig. 2.6A). To explore further the mechanisms of this LRP1-dependent parasite control, we investigated several alternatives. In addition to diverting infection towards professional phagocytes, CalR overexpression may also enhance activation of innate and adaptive immune responses intrinsically for more effective parasite control. To test this possibility, we first measured the activating capacity of TcCalR and TcWT on macrophages *in vitro*. TcCalR and TcWT infection activated transcription factors nuclear factor-κB (NFκB)/activator protein (AP)-1 similarly from 2 – 16 h (Fig. 2.6B). Furthermore, CalR expression did not result in substantially enhanced activation of either *T. cruzi*- responsive CD8^{+} T cells, as assessed via CD69 expression (Fig. 2.6C), nor to the induction of CalR-specific CD8^{+} T cells in TcCalR-

infected mice (Fig. 2.6D). Taken together, these results indicate that the accelerated clearance of the TcCalR infection is likely due to the targeting of TcCalR for professional phagocytes, potent killers of *T. cruzi* in the developing adaptive immune response to this infection.

2.5 Discussion

CalR is a calcium-binding chaperone whose primary role is to ensure correct folding of glycoproteins and assembly of the MHC molecules. Recently CalR has been shown to facilitate the uptake of cancer cells by phagocytes via recognition of surface-exposed CalR by endocytic receptor LRP1 [18, 20, 21]. In light of these recent findings, we have evaluated the potential of CalR to influence the interaction of *T. cruzi* with host cells, in particular macrophages, which can serve as both host cells for parasite replication and effectors of parasite destruction. As in mammalian cells, *T. cruzi* CalR is primarily located in the ER, but is also reported in other cellular compartments, including reservosomes, the cytosol, the flagellar pocket and kinetoplast [14]. Similar to the mammalian CalR, ER-resident CalR in *T. cruzi* appears important for folding of glycoproteins and regulating calcium homeostasis, which may be essential for parasite survival [32-35]. Additionally, cell surface localization of *T. cruzi* CalR has been reported [12, 13] and its potential secretion has been proposed but not documented [30].

Herein we confirmed the localization of CalR on the surface of both amastigotes and trypomastigotes of WT *T. cruzi* and detected secretion of CalR to extracellular space in the epimastigotes and amastigotes overexpressing CalR (Fig. 1). The mechanism of the heterogeneous intra- and extra-celullar localization of *T. cruzi* CalR is largely unknown, although Ca^{2+} depletion is suggested in triggering translocation of *T. cruzi* CalR from ER to the cytosol [36]. Extracellular *T. cruzi* CalR has been indicated in a number of studies for improving parasite success in infectivity and the proposed mechanisms for this activity have revolved around the

interaction between CalR and host complement. Studies by Ferreira *et al.* claimed that surface *T. cruzi* CalR interacts with complement component C1q, mannan-binding lectin and F-ficolin from serum and these interactions not only prevent complement-mediated destruction of *T. cruzi* [12, 37, 38], but also enhance parasite invasion to host cells by binding to certain surface receptors on the host cells [31, 39]. Here we identified that interaction of LRP1 and *T. cruzi* CalR enhances parasite invasion in phagocytes *in vitro* and *in vivo* (Fig. 2.5A-D). However, whether complement components are involved in this process is unclear. Current studies on the interaction of LRP1 and mammalian surface-exposed CalR have opposing opinions on whether the complement molecule C1q is required for this interaction. While some studies have indicated engagement of C1q with the co-complex formed by LRP1 and mammalian surface-exposed CalR [40], other studies suggest C1q being unnecessary and that CalR activates LRP1 via direct binding [18, 41]. Interestingly, the extracellular matrix protein thrombospondin 1 (TSP1) may also have a role in the interplay of *T. cruzi* CalR and LRP1, as TSP1 signals focal adhesion disassembly via binding to the co-complex of mammalian surface-exposed CalR and LRP1 [42]. Further investigation on the molecules involved in the interaction of LRP1 and *T. cruzi* CalR may be worth exploring. In addition to CalR, LRP1 also binds to TGF-β and α-2-macroglobulin [43-45]. As TGF-β and α-2-macroglobulin are both detected on the surface of *T. cruzi* [46, 47], it is interesting to explore whether LRP1 can recognize those two host-derived but parasite surface-bound molecules and whether these potential interactions can trigger phagocytosis of the parasites. In non-phagocytic cells in which CalR over-expressers also displayed increased invasion compared to WT parasites, receptors other than LRP1 may mediate CalR-triggered infection albeit with reduced efficiency. One such receptor candidate may be TSP1, as direct interaction of TSP1 and *T. cruzi* CalR induces infection in murine embryo fibroblasts [13].

Macrophages serve multiple roles during *T. cruzi* infection. In the absence of IFNγ-dependent activation, macrophages support parasite proliferation *in vitro* [4] and *in vivo* by the fact that depletion of macrophage populations results in increased parasite load in the early-acute phase of murine infection (Padilla, *et al.*, unpublished data). Meanwhile, macrophages are also capable of processing and presenting class I and II MHC-restricted antigens for adaptive immune control as well as performing trypanocidal activity with production of nitric oxide and ROS upon IFNγ-dependent activation [9]. Due to the potential of macrophages in both supporting parasite proliferation and parasite destruction, the integral impact of macrophages during the course of infection has been elusive. Here in this study, we observed a steady increase of parasite load and earlier mortality in IFNγ$^{-/-}$ mice infected with *T. cruzi* overexpressing CalR compared to WT parasites. Enhanced infection severity upon CalR overexpression was also observed in immune competent mice during the initial expansion period when IFNγ was not yet largely produced, which was followed by an equally accelerated parasite control during post-acute phase. The exacerbated initial expansion and subsequent control are both due to enhanced infection in phagocytes, primarily in macrophages, likely because the switch from an infection supporter to a parasite destructor is regulated by IFNγ-dependent activation.

In contrast to the accelerated parasitic control upon CalR overexpression in LRP1-expressing immune competent mice, parasite burden in mLRP1$^{-/-}$ mice was increased upon *T. cruzi* CalR overexpression during post-acute phase (Fig. 6A). Unable to be recognized by LRP1, parasite invasion was geared more towards the non-phagocytic cells via recognition by other receptors such as TSP1. Despite an initially less efficient invasion of non-phagocytic cells, parasite expansion was less likely to be impeded during the post-acute infection since non-phagocytic cells lack IFNγ-mediated trypanocidal activity. Given that *T. cruzi* CalR failed to

enhance activation of innate and adaptive immune cells intrinsically (Fig. 6B-D), those results collectively suggest that the interaction of host LRP1 and *T. cruzi* CalR and the resulting increased infection in phagocytes is important for both the initial enhanced infection and the accelerated post-acute control. Not surprisingly, CalR over-expressers developed a chronic infection despite an accelerated post-acute control. One likely cause is that activated macrophages are unable to completely kill intracellular parasites [48], and some *T. cruzi* survivors may therefore invade surrounding or distal cells via circulation, particularly in muscle cells and adipocytes wherein high fatty acid metabolism is favored for amastigote growth and parasite persistence [49].

This study highlights the role of *T. cruzi* CalR in host-parasite interplay and identifies a new host receptor for *T. cruzi* CalR that contributes to parasite invasion. The mechanism and the impact of extracellular *T. cruzi* CalR on invasion, particular on diverting invasion focus towards professional phagocytes and the subsequent influence can be further investigated. Our findings also illustrate a complex role for phagocytes in the control of infection. Manipulation to regulate host cell types in combination with other strategies to enhance innate and immune responses, can be designed to further influence the control of *T. cruzi* infection.

Figure 2.1. *Wild-type and CalR-overexpressing T. cruzi exhibits CalR on plasma membrane and secretes CalR.* (A) CalR expression in amastigote and trypomastigote stages of TcWT determined by indirect immuno-fluorescence microscopy using modified non-permeablizing staining protocol [25]. Rabbit polyclonal anti-*T. cruzi* CalR antibody was used to mark the target protein in trypomastigotes and amastigotes. PI and DAPI were applied sequentially to label DNA in non-permealized cells (PI labeling not shown). Images were acquired with an Applied Precision Delta Vision microscope and were deconvolved and adjusted for contrast using its Softworx software (Applied Precision). Scale bars represent 5 μm. (B) Cytosolic, membrane fractions and culture supernatant of TcWT and TcCalR epimastigotes immuno-blotted with antibodies against HA. (C) Cytosolic and membrane lysates of TcWT and TcCalR extracellular amastigotes immune-blotted with anti-*T. cruzi* CalR mouse serum and mouse monoclonal anti-α-tubulin antibody (Sigma). (D) CalR secretion in TcCalR amastigotes in infected Vero cells determined by indirect immuno-fluorescence microscopy after permeablization. Rat monoclonal anti-HA antibody (Roche) was used to target HA-labeled CalR protein. PI was used to stain DNA. Images were acquired with a Zeiss LSM710 Confocal Microscope and were adjusted for contrast using Zen lite 2011 software (Zeiss). Scale bar represents 5 μm.

Figure 2.1

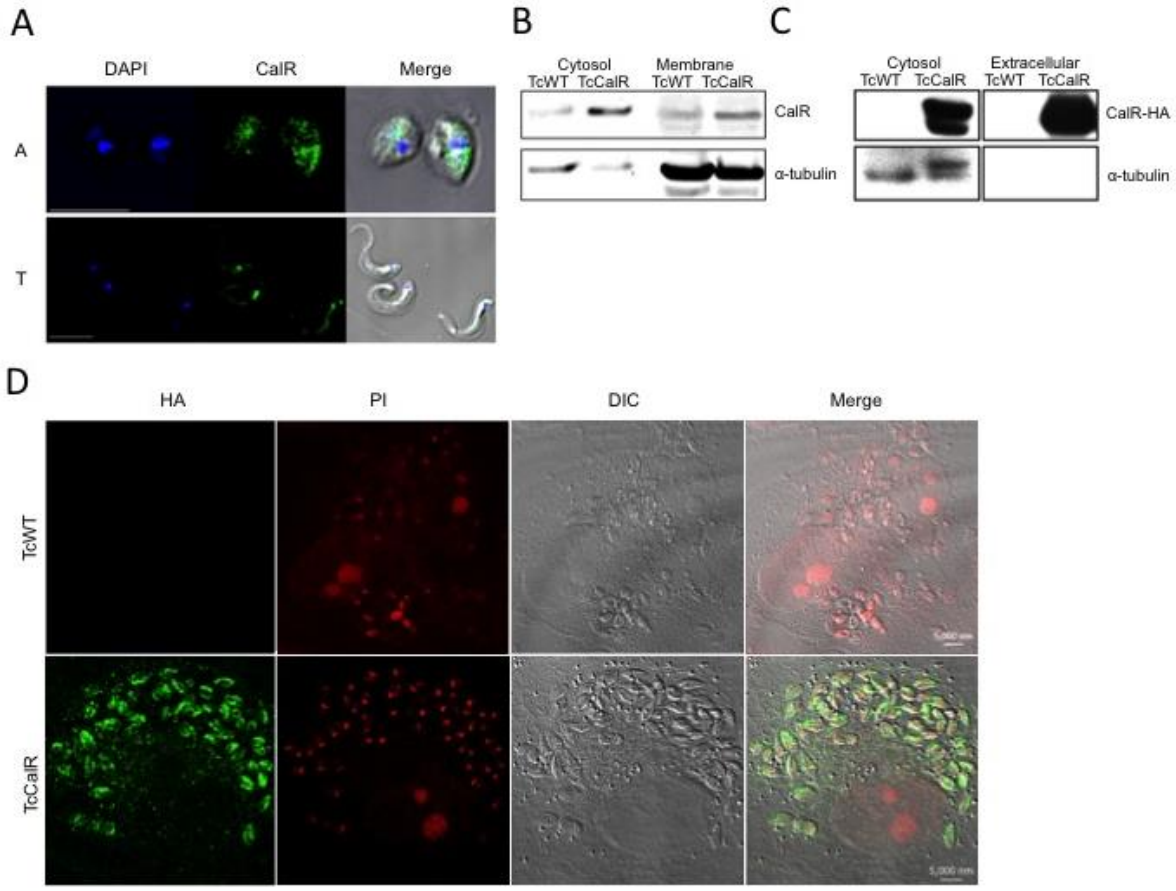
A
DAPI
CalR
Merge
A
T
B
Cytosol
Membrane
TcWT TcCalR TcWT TcCalR
CalR
α-tubulin
C
Cytosol
Extracellular
TcWT TcCalR TcWT TcCalR
CalR-HA
α-tubulin
D
HA
PI
DIC
Merge
TcWT
TcCalR

Figure 2.2. *CalR overexpression results in increased parasite expansion in vitro.* (A-B) *In vitro* parasite entry of TcCalR or TcWT in Vero, Raw-Blue macrophages and peritoneal exudate macrophages (p-MΦs) (parasite: host = 10:1), as determined by the percentage of infected cells in A and number of parasites per infected cell in B. Data represent at least three separate experiments with triplicates/ group in A and at least 50 infected cells/group in B. (C) TcCalR and TcWT parasites with or without 15 min pre-treatment in 0.1% H_2O_2 were incubated with RAW-Blue macrophages in 10:1 ratio for 2 hours and examined for parasite uptake. At least 200 cells were counted in triplicate wells per condition. Data are representative of three separate experiments. (D) RAW-Blue macrophages pre-treated with anti-CalR antibody were assessed for the percentage of infected cells post 2 h infection (parasite: host=5:1). 100 cells were counted per well with triplicate wells per group. Data represent three separate experiments. (E) Entry of TcWT trypomastigotes temporarily surface-anchored with recombinant CalR or BSA (TcWT-GPI-CalR, TcWT-GPI-BSA, respectively) supplemented with exogenous CalR or BSA (exo CalR or exo BSA) in RAW-Blue macrophage line, as determined by the percentage of macrophages infected in 100 cells after 3-4 hours of incubation. Data represented as mean±SEM from one of three separate experiments, with four replicates per group. (F) Phagocytic index in RAW-Blue macrophage line supplemented with exogenous CalR (exo CalR) or BSA (exo BSA) and incubated with TcWT trypomastigotes pretreated with 0.1% of hydrogen peroxide, as determined by the percentage of macrophages with internalized parasites post 3 h incubation. Data represent three separate experiments. Mean ±SEM. * $p \leq 0.05$, ** $p \leq 0.01$ or *** $p \leq 0.001$, as determined by Student's *t*-test.

Figure 2.2

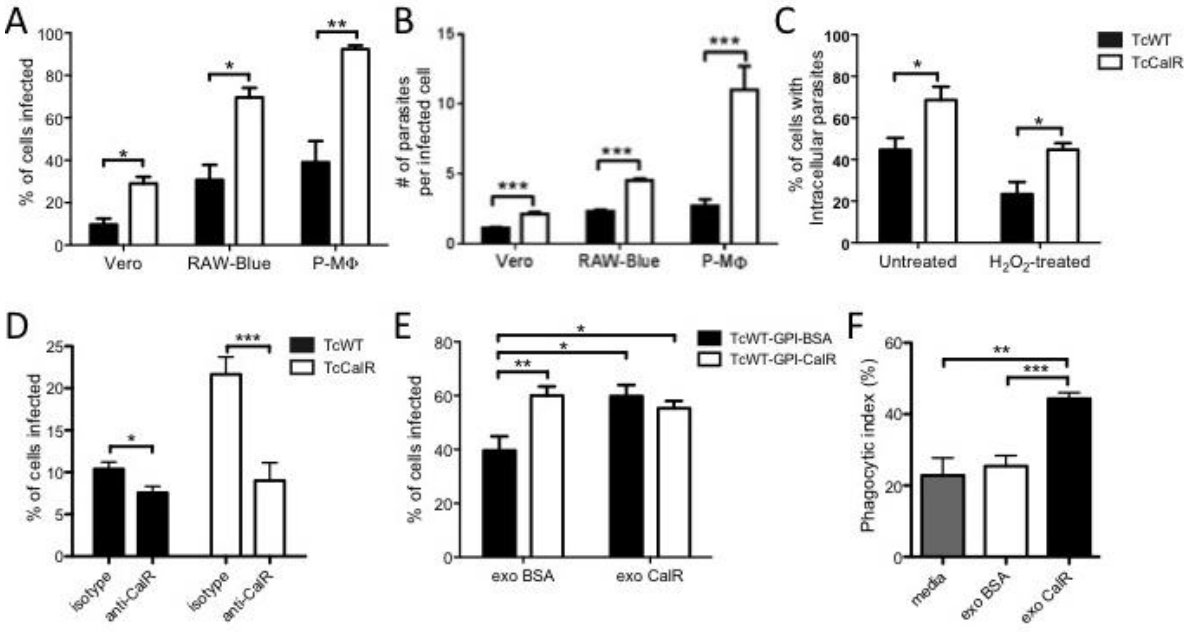
A
% of cells infected
Vero
RAW-Blue
P-MΦ
B
# of parasites per infected cell
Vero
RAW-Blue
P-MΦ
C
% of cells with intracellular parasites
TcWT
TcCalR
Untreated
H2O2-treated
D
% of cells infected
TcWT
TcCalR
isotype
anti-CalR
isotype
anti-CalR
E
% of cells infected
TcWT-GPI-BSA
TcWT-GPI-CalR
exo BSA
exo CalR
F
Phagocytic index (%)
media
exo BSA
exo CalR

Figure 2.3. *Infection with CalR-overexpressing T. cruzi in immune competent mice displayed initial parasite expansion followed by accelerated immune control.* (A) The parasitemia and (B) the survival rate in TcWT or TcCalR-infected IFN$\gamma^{-/-}$ C57BL/6 mice. Data represents three separate experiments with five mice per group. (C) *T. cruzi* DNA in ears of C57BL/6 mice *s.c.* inoculated with 250,000 TcWT or TcCalR trypomastigotes at 12 dpi as determined by quantitative real-time PCR. Data are combined from two separate experiments with 6 ears per group in each experiment. (D-E) *T. cruzi* in skeletal muscle of C57BL/6 mice at 30-50 days p.i., as determined by quantitative real-time PCR (D), and histological examination of amastigote nests (E). Data are combined from two separate experiments with 4-6 mice/group in each experiment. Similar results were obtained in two more separate experiments. Mean ±SEM. * $p \leq 0.05$, ** $p \leq 0.01$ or *** $p \leq 0.001$, as determined by Student's *t*-test.

Figure 2.3

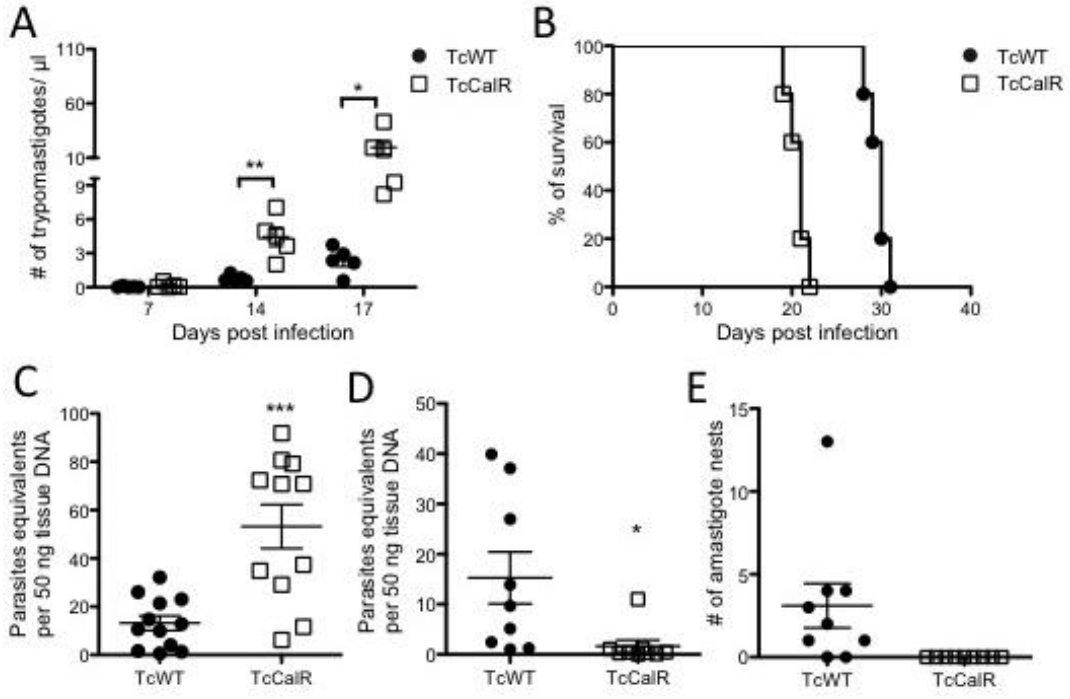
A
# of trypomastigotes/ µl
110
60
10
9
6
3
0
7
14
17
Days post infection
**
*
TcWT
TcCalR
B
% of survival
100
80
60
40
20
0
0
10
20
30
40
Days post infection
TcWT
TcCalR
C
Parasites equivalents per 50 ng tissue DNA
100
80
60
40
20
0
***
TcWT
TcCalR
D
Parasites equivalents per 50 ng tissue DNA
50
40
30
20
10
0
*
TcWT
TcCalR
E
# of amastigote nests
15
10
5
0
TcWT
TcCalR

Figure 2.4. *TcCalR increases infection in phagocytes in vivo.* (A) Representative flow cytometry histograms demonstrating *T. cruzi* infection in distinct cell populations *in vivo* upon 100,000 trypomastigotes *s.c.* inoculation into ears of B57BL/6 mice at 1.5 dpi. TcCalR and TcWT were pre-stained with CellTrace violet (Life Technologies) following the manufacturer's protocol. Gating strategies for different cell types were as follows: $CD45^+$ followed by $Gr1^{mid}CD11b^+$ for infiltrating monocytes, $Gr1^{hi}CD11b^+$ for infiltrating neutrophils and $Gr1^-CD11b^+F4/80^{mid}CD11c^-$ for tissue-resident macrophages. Numbers indicate the percentage of infected ($violet^+$) cells in each cell population (open red). The shaded grey line indicates violet-unstained control. (B) Summary data as in Fig. A. (C) Mean fluorescence intensity in violet channel in infected cells. Data in A-C are representative of three separate experiments (n=6/group). Mean±SEM. * $p \leq 0.05$, ** $p \leq 0.01$, *** $p \leq 0.001$ or **** $p \leq 0.0001$, as determined by student's *t*-test.

Figure 2.4

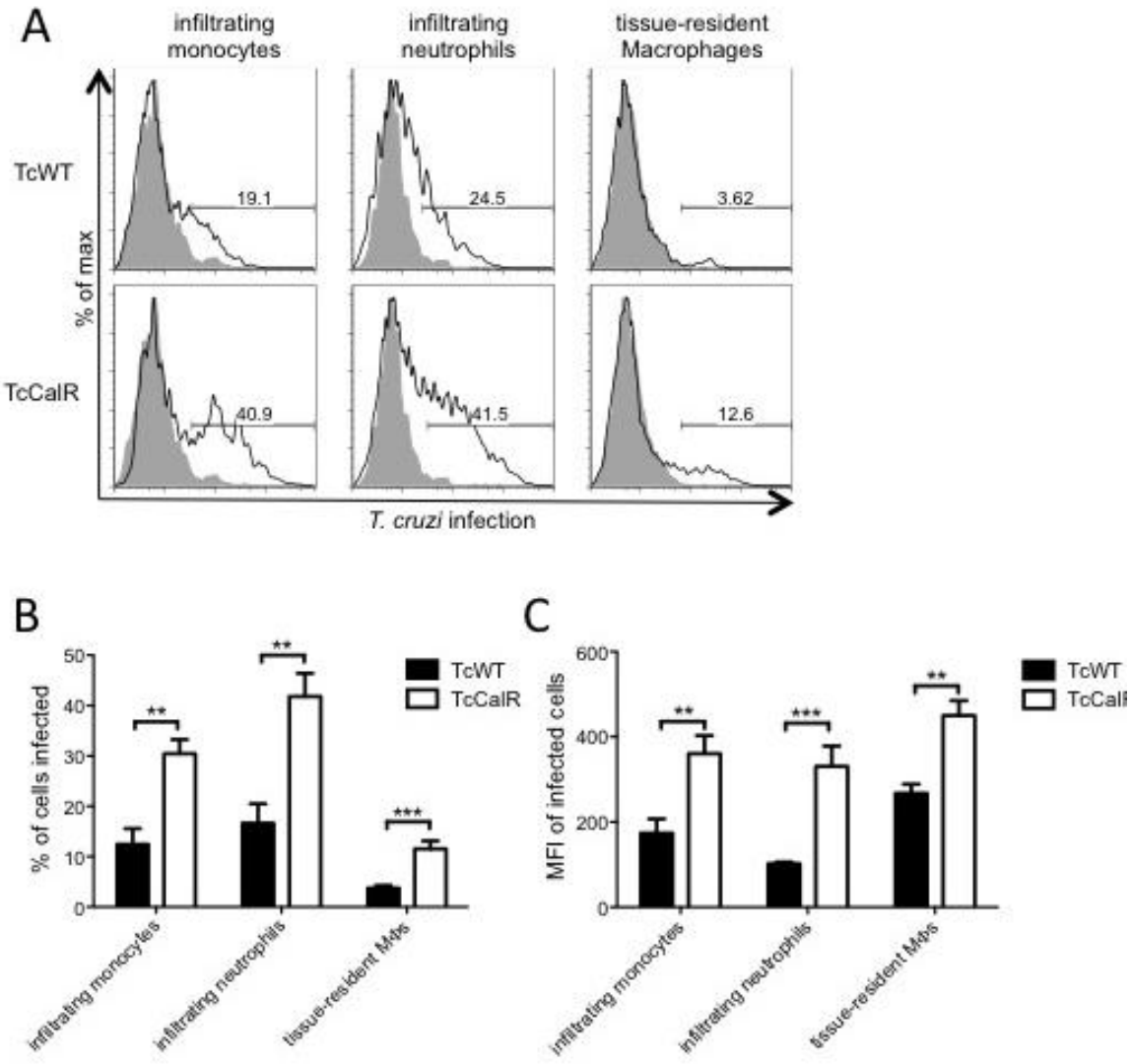
A
infiltrating monocytes
infiltrating neutrophils
tissue-resident Macrophages
TcWT
TcCalR
% of max
19.1
24.5
3.62
40.9
41.5
12.6
T. cruzi infection
B
% of cells infected
TcWT
TcCalR
infiltrating monocytes
infiltrating neutrophils
tissue-resident Mϕs
C
MFI of infected cells
TcWT
infiltrating monocytes
infiltrating neutrophils
tissue-resident Mϕs

Figure 2.5. *The increased infection in professional phagocytes upon CalR overexpression is at least in part mediated through LRP1 in vitro and in vivo.* (A-B) Vero cells, RAW-Blue macrophages and peritoneal exudate macrophages pretreated with Fcblock were incubated with anti-murine LRP1 rabbit monoclonal antibody or rabbit isotype IgG antibody before TcWT or TcCalR infection (parasite: host=10:1). Parasite entry was determined by the percentage of infected cells (A) and the number of parasites per infected cell (B). Data are representative of three separate experiments with at least triplicates per condition. Infection rate in (C) infiltrating monocytes, infiltrating neutrophils, tissue-resident macrophages and (D) in non-phagocytic lymphocytes ($CD45^{+}CD11b^{-}Gr1^{-}$) upon *s.c.* inoculation of 250,000 TcCalR or TcWT trypomastigotes stained with CellTrace violet into ears of $mLRP1^{+/+}$ or $mLRP1^{-/-}$ B57BL/6 mice at 1.5 dpi. See Fig. 3 legend for staining and gating strategies. (E) *T. cruzi* in ears of $mLRP1^{+/+}$ or $mLRP1^{-/-}$ mice *s.c.* inoculated with 32, 000 TcCalR or TcWT trypomastigotes at 4 dpi, as determined by quantitative real-time PCR. Data represent two separate experiments with four to six mice per group. Mean±SEM. * $p \leq 0.05$, ** $p \leq 0.01$ or *** $p \leq 0.001$, as determined by Student's *t*-test.

Figure 2.5

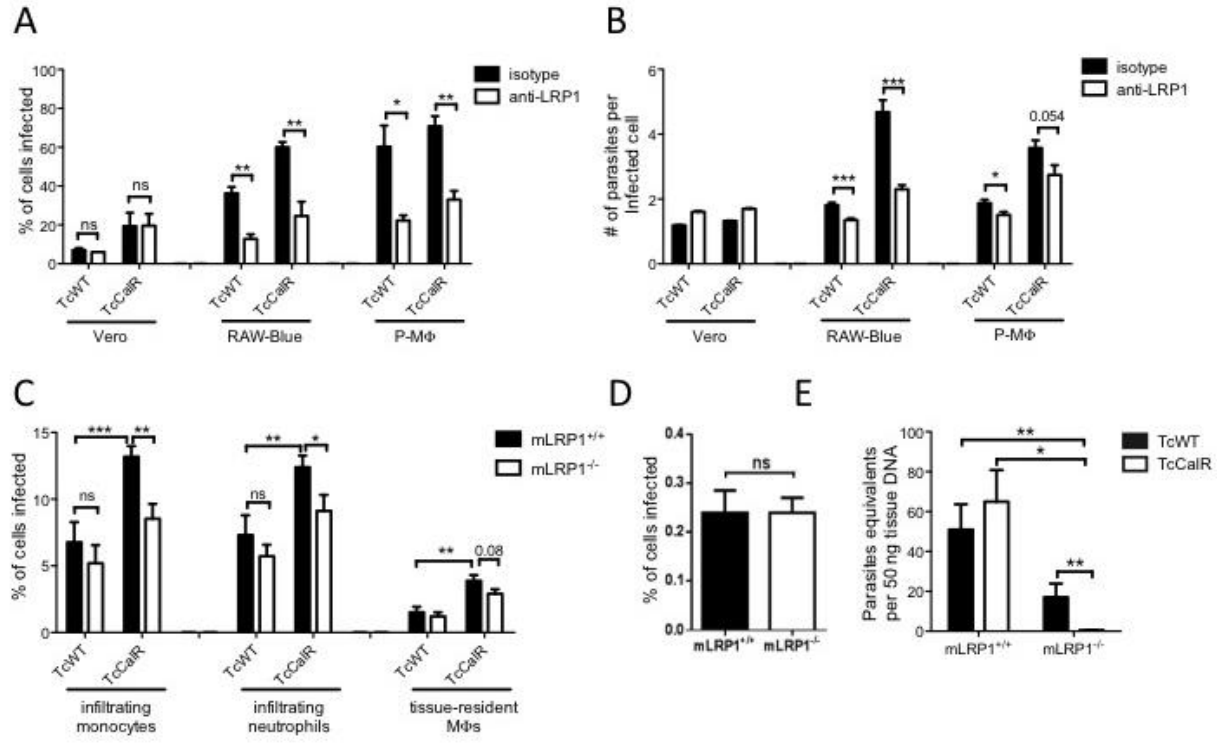
A
% of cells infected
isotype
anti-LRP1
ns
ns
**
**
*
**
TcWT
TcCalR
Vero
RAW-Blue
P-MΦ
B
# of parasites per Infected cell
isotype
anti-LRP1
***
***
*
0.054
TcWT
TcCalR
Vero
RAW-Blue
P-MΦ
C
% of cells infected
mLRP1+/+
mLRP1-/-
***
**
ns
**
*
ns
**
0.08
TcWT
TcCalR
infiltrating monocytes
infiltrating neutrophils
tissue-resident MΦs
D
% of cells infected
ns
mLRP1+/+
mLRP1-/-
E
Parasites equivalents per 50 ng tissue DNA
**
*
**
TcWT
TcCalR
mLRP1+/+
mLRP1-/-

Figure 2.6. *The interaction of LRP1 and CalR in professional phagocytes is crucial for accelerated immune control in vivo.* (A) Parasite load in the skeletal muscle of mLRP1$^{+/+}$ or mLRP1$^{-/-}$ mice *i.p.* inoculated with 1,000 trypomastigotes of TcCalR or TcWT at 35 dpi, as determined by quantitative real-time PCR. Data represent two separate experiments with four to six mice per group. (B) NFκB/AP-1 activation in reporter cells incubated with TcWT, TcCalR trypomastigotes at various time points. Media or *E. coli*-derived LPS were used as negative and positive controls, respectively. (C) Early activation in CD8^{+} T cells indicated by the percentage of CD69^{hi} cells in the spleen and the draining lymph node at 7 and 9 days post *s.c.* inoculation of 10,000 TcWT or TcCalR trypomastigotes into ears of B57BL/c mice. Data represent three separate experiments with 3 mice per group. (D) Percentage of IFNγ-producing cells in CD8^{+} T cells upon peptide stimulation. Splenocytes from TcCalR-infected mice were treated with Golgiplug (BD Biosciences) and incubated with 13 pools of 15-mer peptides with 10 peptides per pool overlapping full-length CalR sequence at a final concentration of 1 μM for 4 -6 hours and surface stained for CD8, CD4, CD44 followed by intracellular staining for IFNγ. Data are representative of three separate experiments with 3 mice per group. Mean±SEM. * $p \leq 0.05$, ** $p \leq 0.01$ or *** $p \leq 0.001$, as determined by Student's *t*-test.

Figure 2.6

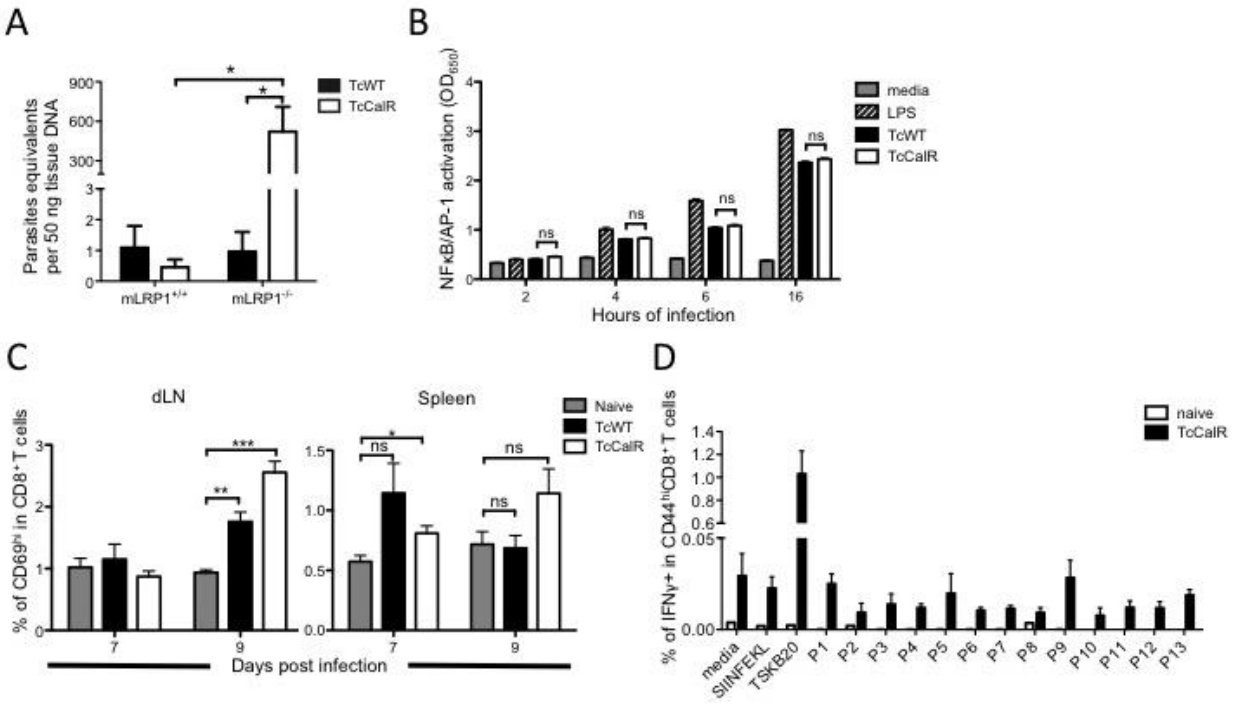
A
Parasites equivalents per 50 ng tissue DNA
TcWT
TcCalR
mLRP1+/+
mLRP1-/-
B
NFκB/AP-1 activation (OD650)
media
LPS
TcWT
TcCalR
ns
Hours of infection
C
dLN
Spleen
% of CD69hi in CD8+ T cells
Naive
TcWT
TcCalR
Days post infection
D
% of IFNγ+ in CD44hiCD8+ T cells
naive
TcCalR
media
SIINFEKL
TSKB20
P1
P2
P3
P4
P5
P6
P7
P8
P9
P10
P11
P12
P13

Supplementary Figure 2.1. *Construction of CalR transgenic T. cruzi.* (A) The *T. cruzi* calreticulin gene (*calR*) was amplified from a *T. cruzi* cosmid library and subsequently cloned into pTREX expression vector with an HA tag at its 3' end to produce transgenic *T. cruzi* overexpressing CalR (TcCalR). (B) TcCalR or TcWT epimastigote stage genomic DNA amplified with primers specific for 5' end of *calR* and 3' end of HA sequence with the expected fragment size as 1.3 kb.

Supplementary Figure 2.1

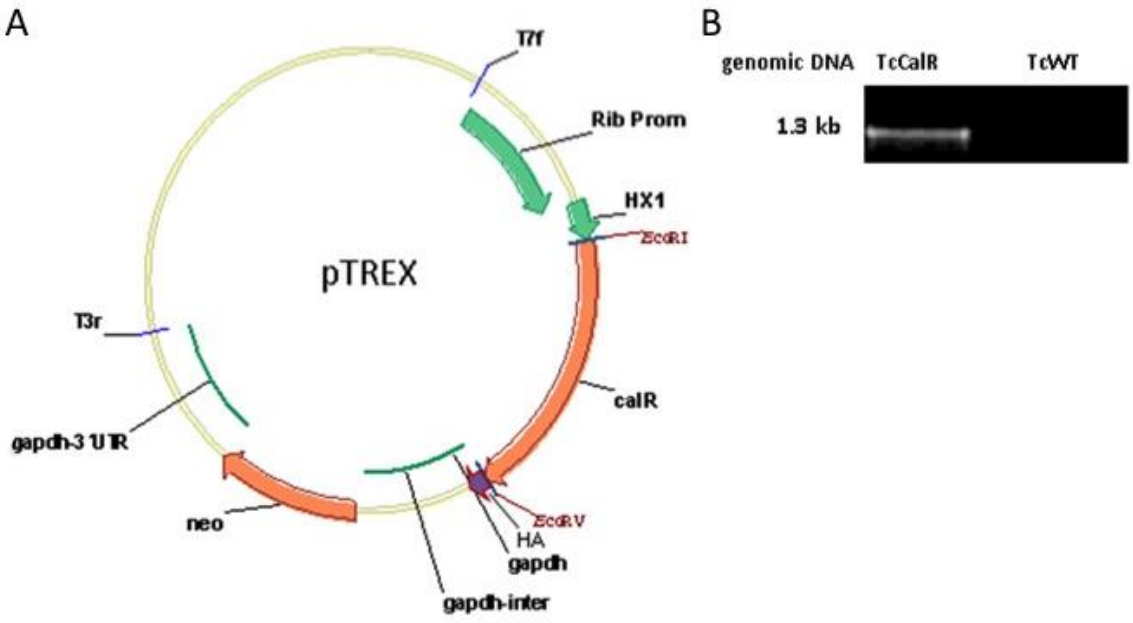

Supplementary Figure 2.2. *Temporarily anchoring to or co-incubating CalR recombinant protein with T. cruzi enhances CalR presence in T. cruzi.* (A) TcWT trypomastigotes GPI-anchored with CalR (TcWT-GPI-CalR) or BSA (TcWT-GPI-BSA), or co-incubated with exogenous, non-GPI-anchored CalR (TcWT-exo CalR) or BSA (TcWT-exoBSA) were surface stained with mouse anti-*T. cruzi* CalR serum (shaded red) or control mouse serum (open grey) followed with goat anti-mouse IgG Alexfluor 488. Histogram represents overall distribution of fluorescence intensity in each parasite group. Number indicates mean fluorescence intensity of the corresponding histogram.

Supplementary Figure 2.2

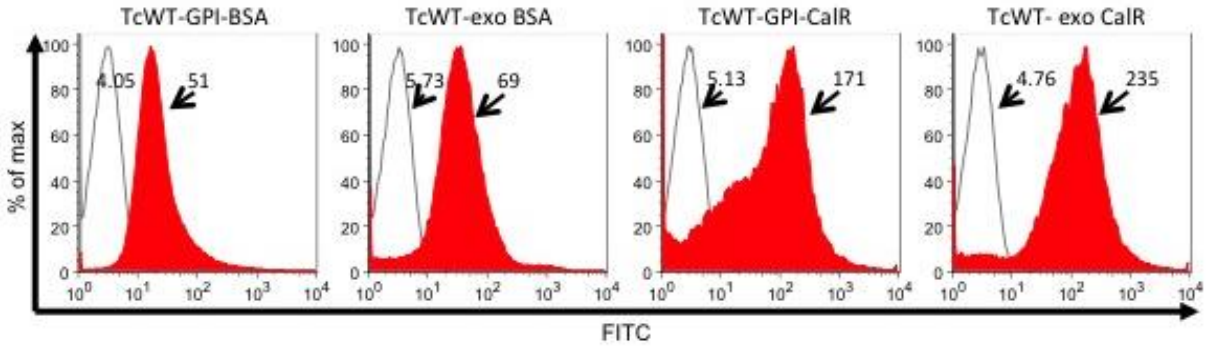

Supplementary Figure 2.3. *CalR overexpression phenotype is stably maintained in transgenic T. cruzi.* (A) TcCalR trypomastigotes recovered from chronically infected mice were stained with anti-*T. cruzi* CalR mouse serum (red) or control serum collected from naïve mice (shaded grey) while TcCalR and TcWT trypomastigotes freshly cultivated and passaged from Neomycin-supplemented Vero culture were stained with anti-*T. cruzi* CalR mouse serum (blue) or control serum (shaded green). Samples were subsequently stained with goat-anti mouse antibody conjugated with Alexfluor 488. Histogram represents overall distribution of fluorescence intensity per sample. (B) 1,000 TcCalR recovered from chronically infected mice or TcWT trypomastigotes were *i.p.* injected into IFN$\gamma^{-/-}$ mice. The left panel shows parasitemia at 14 and 21 dpi. The right panel shows the survival rate in both groups as monitored daily until day 32. Data are representative of two separate experiments, with 4-6 mice per group. Mean ±SEM.

Supplementary Figure 2.3

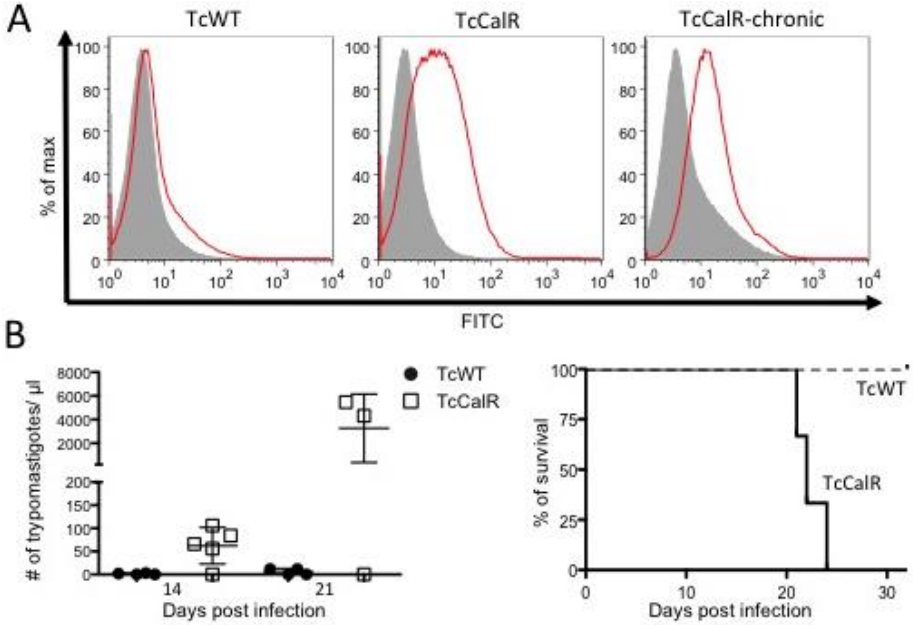

2.6 References

1. Hotez, P.J. *et al.* Control of neglected tropical diseases. *The New England journal of medicine* **357**, 1018-1027 (2007).

2. Padilla, A.M., Bustamante, J.M. & Tarleton, R.L. CD8+ T cells in *Trypanosoma cruzi* infection. *Curr Opin Immunol* **21**, 385-390 (2009).

3. Collins, M.H., Craft, J.M., Bustamante, J.M. & Tarleton, R.L. Oral exposure to *Trypanosoma cruzi* elicits a systemic CD8(+) T cell response and protection against heterotopic challenge. *Infection and immunity* **79**, 3397-3406 (2011).

4. Burger, E., Lay, W.H., Hypolito, L.V. & Fernandes, J.F. *Trypanosoma cruzi*: the fate of bloodstream trypomastigote, amastigote, metacyclic trypomastigote and epimastigote forms in the peritoneal macrophages of immune and non-immune mice in vivo. *Acta tropica* **39**, 111-122 (1982).

5. Tarleton, R.L., Koller, B.H., Latour, A. & Postan, M. Susceptibility of beta 2-microglobulin-deficient mice to *Trypanosoma cruzi* infection. *Nature* **356**, 338-340 (1992).

6. Tarleton, R.L. Depletion of CD8+ T cells increases susceptibility and reverses vaccine-induced immunity in mice infected with *Trypanosoma cruzi*. *J Immunol* **144**, 717-724 (1990).

7. Martin, D.L. *et al.* CD8+ T-Cell responses to *Trypanosoma cruzi* are highly focused on strain-variant trans-sialidase epitopes. *PLoS pathogens* **2**, e77 (2006).

8. Rosenberg, C.S., Martin, D.L. & Tarleton, R.L. CD8+ T cells specific for immunodominant trans-sialidase epitopes contribute to control of *Trypanosoma cruzi* infection but are not required for resistance. *J Immunol* **185**, 560-568 (2010).

9. Kuhn, R.E. Macrophages in experimental Chagas' disease. *Immunology series* **60**, 495-502 (1994).

10. Wirth, J.J., Kierszenbaum, F., Sonnenfeld, G. & Zlotnik, A. Enhancing effects of gamma interferon on phagocytic cell association with and killing of *Trypanosoma cruzi*. *Infection and immunity* **49**, 61-66 (1985).

11. Cummings, K.L. & Tarleton, R.L. Inducible nitric oxide synthase is not essential for control of *Trypanosoma cruzi* infection in mice. *Infection and immunity* **72**, 4081-4089 (2004).

12. Ferreira, V. *et al.* The classical activation pathway of the human complement system is specifically inhibited by calreticulin from *Trypanosoma cruzi*. *J Immunol* **172**, 3042-3050 (2004).

13. Johnson, C.A. *et al.* Thrombospondin-1 interacts with *Trypanosoma cruzi* surface calreticulin to enhance cellular infection. *PloS one* **7**, e40614 (2012).

14. Souto-Padron, T., Labriola, C.A. & de Souza, W. Immunocytochemical localisation of calreticulin in *Trypanosoma cruzi*. *Histochemistry and cell biology* **122**, 563-569 (2004).

15. Raghavan, M., Wijeyesakere, S.J., Peters, L.R. & Del Cid, N. Calreticulin in the immune system: ins and outs. *Trends in immunology* **34**, 13-21 (2013).

16. Inoue, H. & Tani, K. Multimodal immunogenic cancer cell death as a consequence of anticancer cytotoxic treatments. *Cell death and differentiation* **21**, 39-49 (2014).

17. Chao, M.P. *et al.* Calreticulin is the dominant pro-phagocytic signal on multiple human cancers and is counterbalanced by CD47. *Science translational medicine* **2**, 63ra94 (2010).

18. Gardai, S.J. *et al.* Cell-surface calreticulin initiates clearance of viable or apoptotic cells through trans-activation of LRP on the phagocyte. *Cell* **123**, 321-334 (2005).

19. Hodge, J.W. *et al.* Chemotherapy-induced immunogenic modulation of tumor cells enhances killing by cytotoxic T lymphocytes and is distinct from immunogenic cell death. *International journal of cancer. Journal international du cancer* **133**, 624-636 (2013).

20. Senovilla, L. *et al.* An immunosurveillance mechanism controls cancer cell ploidy. *Science* **337**, 1678-1684 (2012).

21. Zitvogel, L. *et al.* Immunogenic tumor cell death for optimal anticancer therapy: the calreticulin exposure pathway. *Clinical cancer research : an official journal of the American Association for Cancer Research* **16**, 3100-3104 (2010).

22. Sosoniuk, E. *et al. Trypanosoma cruzi* calreticulin inhibits the complement lectin pathway activation by direct interaction with L-Ficolin. *Molecular immunology* **60**, 80-85 (2014).

23. Garg, N., Nunes, M.P. & Tarleton, R.L. Delivery by *Trypanosoma cruzi* of proteins into the MHC class I antigen processing and presentation pathway. *Journal of immunology* **158**, 3293-3302 (1997).

24. Lorenzi, H.A., Vazquez, M.P. & Levin, M.J. Integration of expression vectors into the ribosomal locus of *Trypanosoma cruzi*. *Gene* **310**, 91-99 (2003).

25. Agrawal, S., van Dooren, G.G., Beatty, W.L. & Striepen, B. Genetic evidence that an endosymbiont-derived endoplasmic reticulum-associated protein degradation (ERAD) system functions in import of apicoplast proteins. *The Journal of biological chemistry* **284**, 33683-33691 (2009).

26. Cummings, K.L. & Tarleton, R.L. Rapid quantitation of *Trypanosoma cruzi* in host tissue by real-time PCR. *Molecular and biochemical parasitology* **129**, 53-59 (2003).

27. Bustamante, J.M., Bixby, L.M. & Tarleton, R.L. Drug-induced cure drives conversion to a stable and protective CD8+ T central memory response in chronic Chagas disease. *Nature medicine* **14**, 542-550 (2008).

28. Cooley, G. *et al.* High throughput selection of effective serodiagnostics for *Trypanosoma cruzi* infection. *PLoS neglected tropical diseases* **2**, e316 (2008).

29. Kurup, S.P. & Tarleton, R.L. Perpetual expression of PAMPs necessary for optimal immune control and clearance of a persistent pathogen. *Nature communications* **4**, 2616 (2013).

30. Ramirez, G., Valck, C., Ferreira, V.P., Lopez, N. & Ferreira, A. Extracellular *Trypanosoma cruzi* calreticulin in the host-parasite interplay. *Trends in parasitology* **27**, 115-122 (2011).

31. Ramirez, G. *et al. Trypanosoma cruzi* calreticulin: a novel virulence factor that binds complement C1 on the parasite surface and promotes infectivity. *Immunobiology* **216**, 265-273 (2011).

32. Mesaeli, N. *et al.* Calreticulin is essential for cardiac development. *The Journal of cell biology* **144**, 857-868 (1999).

33. Aguila, S. *et al.* Specific and non-overlapping functions of testosterone and 11-ketotestosterone in the regulation of professional phagocyte responses in the teleost fish gilthead seabream. *Molecular immunology* **53**, 218-226 (2013).

34. Furuya, T., Okura, M., Ruiz, F.A., Scott, D.A. & Docampo, R. TcSCA complements yeast mutants defective in Ca2+ pumps and encodes a Ca2+-ATPase that localizes to the endoplasmic reticulum of *Trypanosoma cruzi*. *The Journal of biological chemistry* **276**, 32437-32445 (2001).

35. Labriola, C., Cazzulo, J.J. & Parodi, A.J. *Trypanosoma cruzi* calreticulin is a lectin that binds monoglucosylated oligosaccharides but not protein moieties of glycoproteins. *Molecular biology of the cell* **10**, 1381-1394 (1999).

36. Labriola, C.A., Conte, I.L., Lopez Medus, M., Parodi, A.J. & Caramelo, J.J. Endoplasmic reticulum calcium regulates the retrotranslocation of *Trypanosoma cruzi* calreticulin to the cytosol. *PloS one* **5** (2010).

37. Ferreira, V., Molina, M.C., Schwaeble, W., Lemus, D. & Ferreira, A. Does *Trypanosoma cruzi* calreticulin modulate the complement system and angiogenesis? *Trends in parasitology* **21**, 169-174 (2005).

38. Sosoniuk, E. *et al. Trypanosoma cruzi* calreticulin inhibits the complement lectin pathway activation by direct interaction with L-Ficolin. *Molecular immunology* **60**, 80-85 (2014).

39. Sanz, O.P. *et al. Trypanosoma cruzi*: induction of changes in the peripheral nervous system in different strains of mice. *Revista Argentina de microbiologia* **23**, 30-34 (1991).

40. Ogden, C.A. *et al.* C1q and mannose binding lectin engagement of cell surface calreticulin and CD91 initiates macropinocytosis and uptake of apoptotic cells. *The Journal of experimental medicine* **194**, 781-795 (2001).

41. Lillis, A.P. *et al.* Murine low-density lipoprotein receptor-related protein 1 (LRP) is required for phagocytosis of targets bearing LRP ligands but is not required for C1q-triggered enhancement of phagocytosis. *J Immunol* **181**, 364-373 (2008).

42. Orr, A.W. *et al.* Low density lipoprotein receptor-related protein is a calreticulin coreceptor that signals focal adhesion disassembly. *The Journal of cell biology* **161**, 1179-1189 (2003).

43. O'Grady, P., Liu, Q., Huang, S.S. & Huang, J.S. Transforming growth factor beta (TGF-beta) type V receptor has a TGF-beta-stimulated serine/threonine-specific autophosphorylation activity. *The Journal of biological chemistry* **267**, 21033-21037 (1992).

44. Huang, S.S. *et al.* Cellular growth inhibition by IGFBP-3 and TGF-beta1 requires LRP-1. *FASEB journal : official publication of the Federation of American Societies for Experimental Biology* **17**, 2068-2081 (2003).

45. Van Leuven, F. *et al.* Structure of the gene (LRP1) coding for the human alpha 2-macroglobulin receptor lipoprotein receptor-related protein. *Genomics* **24**, 78-89 (1994).

46. Coutinho, C.M., Cavalcanti, G.H., van Leuven, F. & Araujo-Jorge, T.C. Alpha-2-macroglobulin binds to the surface of *Trypanosoma cruzi*. *Parasitology research* **83**, 144-150 (1997).

47. Waghabi, M.C. *et al.* Uptake of host cell transforming growth factor-beta by *Trypanosoma cruzi* amastigotes in cardiomyocytes: potential role in parasite cycle completion. *The American journal of pathology* **167**, 993-1003 (2005).

48. Golden, J.M. & Tarleton, R.L. *Trypanosoma cruzi*: cytokine effects on macrophage trypanocidal activity. *Experimental parasitology* **72**, 391-402 (1991).

49. Atwood, J.A., 3rd *et al.* The *Trypanosoma cruzi* proteome. *Science* **309**, 473-476 (2005).

CHAPTER 3

A FLAGELLAR MEMBRANE PROTEIN OF *TRYPANOSOMA CRUZI* IS ESSENTIAL FOR AMASTIGOTE-TO-TRYPOMASTIGOTE CONVERSION [2]

[2] Zhang, W. and Tarleton, R.L. To be submitted to *PLoS Pathogens*.

3.1 Abstract

Trypanosoma cruzi is the etiological agent for Chagas disease, a neglected tropical disease endemic to Latin America, and affects at least 8-11 million people. In mammalian hosts, *T. cruzi* cycles between the proliferative intracellular amastigote and the non-proliferative extracellular trypomastigote stages. Although the process and triggers for conversion of invading trypomastigotes into amastigotes have been extensively investigated, little attention has been paid to the important amastigote to trypomastigote conversion that is required before parasites can leave the infected cell. Here we report on a *T. cruzi* hypothetical protein (Hyp1) essential for amastigote–to-trypomastigote differentiation. *T. cruzi* Hyp1 is shown to be a kinetoplastid-specific, flagellar protein expressed in amastigotes and trypomastigotes, but not in epimastigotes. *T. cruzi* lacking Hyp1 displayed decreased amastigote proliferation and arrest in the amastigote stage, unable to differentiate into trypomastigotes. C57Bl/6 mice infected with *T. cruzi* lacking Hyp1 rapidly and completely cleared the infection. Overexpression of Hyp1 protein in *T. cruzi* also resulted in a compromised invasion *in vitro* and a high frequency of cure in chronic infection *in vivo*. This study identifies a previously uncharacterized protein critical for trypomastigogenesis (amastigote-to-trypomastigote differentiation) and implicates strict control of its expression for optimal *T. cruzi* infection.

3.2 Introduction

The protozoan parasite *Trypanosoma cruzi*, the etiologic agent of Chagas disease, infects an estimated 8-11 million people mostly in Latin America. In mammalian hosts, insect-stage-infective metacyclic trypomastigotes and mammalian-stage-infective trypomastigotes invade host cells and differentiate into amastigotes, which proliferate rapidly, filling the host cell in 4-5 days. An unknown trigger then prompts the conversion of these intracellular amastigotes back

into infective trypomastigotes, which mechanically disrupt the host cell, and are released into interstitial spaces and ultimately the host bloodstream. Blocking any of the steps of the mammalian-stage life cycle - invasion [1-8], amastigogenesis (trypomastigote-to-amastigote differentiation) [9], proliferation [10-16] and trypomastigogenesis (amastigote-to-trypomastigote differentiation) [17-19] should reduce infection and may even achieve parasite clearance. Although the mechanism of amastigogenesis has been studied extensively [20-24], little has been known about trypomastigogenesis that is which is an indispensable process for the continuation of the infection through the subsequent invasion of another host cell or transmission to another host.

The trypanosome flagellum is essential for parasite motility [25]. In trypomastigotes the flagellum emerges from the flagellar pocket near the posterior end of the cell and runs the whole entire length of the cell. The oval shaped amastigote have a residual flagellum that does not protrude and thus is commonly considered 'unflagellated' and immotile. In addition to motility, lipid raft-enriched flagella membrane is a platform for organization of transmembrane signaling events that regulate metabolism, differentiation and social behavior [26-33]. If amastigote-to-trypomastigote differentiation in *T. cruzi* relies on external stimuli, it seems likely that the sensing of these stimuli may also reside in the flagellar membrane.

In this study, we undertook the investigation of a hypothetical protein (Hyp1) encoded by gene TcCLB.510099.110, and predicted to be expressed on the surface of amastigotes of *T. cruzi*. Our initial interest in Hyp1 was in its potential to serve as an invariant target of *T. cruzi*-specific $CD8^+$ T cells for vaccine use. Instead we discovered that Hyp1 played a role in amastigote proliferation and was essential for trypomastigogenesis. Not surprisingly, Hyp1-knockout *T. cruzi* initially established an infection in mice but failed to persist and were cleared

within 35 days. This study identifies a *T. cruzi* protein with an essential role in trypomastigogenesis but the process is mediated by an as yet unknown mechanism.

3.3 Materials and Methods

3.3.1 *Mice, parasites, and infections*

C57BL/6J (B6), BALB/cByJ background (National Cancer Institute at Frederick) and B7.129S7-*Ifng*^{tm1Ts}/J (abbreviated as IFN$\gamma^{-/-}$, Jackson Laboratory) were bred and maintained in Coverdell Center animal facility (University of Georgia, Athens, GA) under specific pathogen-free conditions. Mice of the same gender between 6-8 weeks were used for experiments. Metacyclic trypomastigotes were derived from log-phase epimastigotes after 14 days of incubation at 28 °C in Grace's insect media (G8142, Sigma-Aldrich) supplemented with 10% heat-inactivated FBS and antibiotics including Penicillin, Streptomycin and Gentamycin. Trypomastigotes were prepared by passage in Vero cell cultures at 37 °C. Mice were infected intraperitoneally (*i.p.*) with 1,000 trypomastigotes or 250,000 metacyclic trypomastigotes, or subcutaneously in the pinna of the ear with 320,000 metacyclic trypomastigotes. Infected mice were immunosuppressed with cyclophosphamide (200 mg/kg/day) *i.p.* at 2-3-day intervals for a total of 5 to 6 doses [34].

3.3.2 *Transgenic parasites*

To construct Hyp1-overexpressing *T. cruzi*, wild-type CL epimastigotes was transfected with pTREX plasmid [35] containing the coding sequence of *T. cruzi* hypothetical protein (TcCLB.510099.110) with fusion to a downstream influenza haemagglutinin (HA) tag and selected with 200 μg/ml G418 as described previously [36]. Transfection to construct Hyp1-knockout *T. cruzi* epimastigotes was performed using the Clustered Regularly Interspaced Short Palindromic Repeats (CRISPR) and CRISPR-associated 9 (Cas9) system as described [37].

Briefly, *T. cruzi* expressing enhanced GFP and Cas9 was used as the backbone strain for transfection. The single guide RNAs (sgRNAs) targeting *hyp1* and *cas9* genes (Cas9 expression results in reduced proliferation of *T. cruzi* so it is mutated along with the targeted gene in order to remove this growth limitation [37]) were designed using the Eukaryotic Pathogen CRISPR gRNA Design Tool (http://grna. ctegd.uga.edu). sgRNAs predicted with the highest targeting efficiency and no potential off-target sites were further examined for self-complementation and only non-self-complementary sgRNAs were qualified for transfection. The sgRNA targeting *cas9* (GGACAAGCTGTTCATCCAGCTGG) was transfected simultaneously with one of the sgRNAs targeting *hyp1* described below. sgRNAs targeting *hyp1* include Hyp1-42 (GAACAGAACAAGGTTGCGGGAGG) targeting from the 42nd nucleotide of *hyp1*, Hyp1-79 (CTATGTGCAACTGTGTGCGGCGG), Hyp1-127 (ATTCGCCTCATTGGCCCCAGCGG), Hyp1-142 (TACTCAGACTTGTGTCCGCTGGG) and Hyp1-238 (TATGTCGTCTGGCCTTCTAGCGG). After transfection, epimastigotes were cultured in Liver digest-neutralized tryptose (LDNT) media for 1-2 days before being seeded at ~ 1 cell per well in 96-well clear-flat-bottom plates (Corning). Single cell event was identified and distributed using MoFlo XDP (Beckman Coulter).

Metacyclic parasites derived from stationary-phase epimastigotes were incubated with Vero cells. Complete inhibition of trypomastigogenesis and impaired amastigote proliferation was observed in 8% to 15% of the clones resulting from each transfection targeting the individual *hyp1* sequences. Less than 1.5% of infections with clones transfected with an sgRNA targeting a control *trans*-sialidase sequence showed such a phenotype. The TcHyp1KO clone was complemented by transfection with the pTREX plasmid containing Hyp1 and a C-terminal HA

tag with phleomycin^{R} gene. Complemented epimastigotes were selected with 60 μg/ml phleomycin.

3.3.3 *Anti-T. cruzi Hyp1 antibody production*

Recombinant Hyp1 protein was produced in *E. coli* BL21(DE3)pLysS strain by transformation of pDEST-PTD4 plasmid containing the coding sequence of *T. cruzi* Hyp1 and a N-terminal 6× His tag. Bacteria were cultured overnight at 37 °C, 280 rpm in the auto-induction media (ZYP-5052). His-tagged Hyp1 was harvested as previously described [38] and attached to Dynabeads TALON magnetic beads (Invitrogen) by incubating 300 μg Hyp1 protein with pre-equilibrated beads (30 mg) at RT for 10 min followed by washing the beads via magnetic separation for 5 times in Binding and Washing buffer (recipe in the product's instruction manual). The washed beads were resuspended in 700 μl PBS and kept at 4˚C. BALB/cByJ mice were subcutaneously injected with 70-100 μl protein-bound beads and boosted twice using the same regime at two-week intervals. Blood was collected into serum separator tubes (BD Microtainer) and mouse sera were isolated and kept at -20 ˚C until use. Antibody specificity and sensitivity was confirmed by ELISA using the recombinant protein as the bait, BSA and ddH_2O as negative control.

3.3.4 *Immunoblotting*

Extracellular amastigotes of trypomastigogenesis-competent transfectants were axenically derived from trypomastigotes as previously described [39]. Extracellular amastigotes of trypomastigogenesis-arrested transfectants were from the supernatant of the heavily infected Vero culture via centrifugation at 300 × g, 5 min to eliminate cell debris and aggregated amastigotes. Cell pellets of 10^8 parasites were washed in PBS and subjected to three or more rounds of freeze-thawing supplemented with protease inhibitor cocktail (Sigma) followed by

sonication and centrifugation at 13,500 × g, 20 min at 4 ˚C. Pellets were washed twice in PBS to be used as a crude membrane fraction, while the supernatant was passed through a 0.22 μm pore size, PVDF membrane filter (Millipore) used as the soluble cytosolic fraction. Protein concentration in cytosolic and membrane fractions was determined in Bradford assay (Bio-Rad). Membrane and cytosolic fractions of parasite lysates were probed with rat monoclonal anti-HA antibody (1:20,000; Roche) or anti-Hyp1 mouse serum (1:500), and mouse monoclonal anti-α-tubulin antibody (1:15,000; Sigma) were used as control.

3.3.5 *Immunofluorescence assay and time-lapse imaging*

The protocol for immunofluorescence analysis was modified from that previously described [40]. Briefly, amastigotes and trypomastigotes adhered to poly-L-lysine coverslips (BD Biosciences) were fixed in 3.7% paraformaldehyde in PBS. Parasites without permealization were first stained with rat monoclonal anti-HA antibody (1:500; Roche) followed by goat-anti-rat IgG Alex fluor488 (1:200; Life Technologies), stained with propidium iodide (5μg/ml) as an exclusion marker, and washed with DAPI (4 μg/ml). Coverslips were mounted with Fluoro-Gel, with TES buffer (Electron Microscopy Sciences) before microscopy analysis. For time-lapse imaging, infected Vero cells were seeded in 35 mm glass-bottom culture dishes with glass thickness of 1.5 mm (MatTek) in complete RPMI, and differential interference contrast microscopy (DIC) images of the same field were collected at a 15-min interval for a total of 19 to 21 hrs for cells. Deconvolution of the images was performed with a Delta Vision (Applied Precision) microscope and adjusted for contrast using Softworx software (Applied Precision).

3.3.6 *In vitro infection assay*

Vero cells (5×10^4) pre-seeded in chamber slides (Thermo Scientific) in complete RPMI supplemented with 10% FBS were infected with 5×10^5 trypomastigotes for 6 hrs for

TcHyp1/TcWT infection or 1×10^6 metacyclic trypomastigotes overnight for TcHyp1KO/TcWT infection at 37 ˚C. Trypomastigotes were harvested from the supernatant of 5 day-infected Vero culture. Metacyclic trypomastigotes were derived from log-phase epimastigotes grown in Grace's insect media for 14 days and purified after overnight incubation in non-heat-inactivated FBS at 37 ˚C to achieve high purity. Post infection, vero cells were washed at least six times to eliminate extracellular parasites. For invasion assays, medium was removed and the adherent cells were stained with Hema 3 fixative and solutions (Fisher Diagnostics). For proliferation assays, slides were washed, dried and stained in the same manner at day 3 post infection. For TcHyp1/TcWT infection assay, numbers of infected cells per 100 cells and the number of parasites in at least 50 infected cells were counted per well. For TcHyp1KO/TcWT infection assay, to measure invasion efficiency, the number of intracellular parasites and parasites attached to the cell surface in 100 cells per well was measured. To measure proliferation efficiency, the number of intracellular parasites per infected cell was measured in at least 30 infected cells per well. Counting of parasites and Vero cells was performed under a compound light microscope (100×).

3.3.7 *T cell phenotyping by flow cytometry*

Peripheral blood was collected from the tail vein and lysis of red blood cells was performed prior to staining in PAB (2% BSA, 0.02% azide in PBS). T cell phenotyping was performed with tetramer-phycoerythrin (TSKB20-PE; ANYKFTLV peptide on H2Kb; NIH Tetramer Core Facility, Emory University; 1:800) and the following: anti-CD8 eFluor 450 (1:800), anti-CD127 APC (1:100), anti-CD44 FITC (1:400), anti-B220 PE- Cy5 (1:200), anti-CD11b PE-Cy5 (1:200), anti-CD4 PE-Cy5 (1:200). Staining with PE-Cy5-conjugated antibodies was used for a dump channel. T cell phenotyping was performed with tetramer-APC (TSKB20-APC; ANYKFTLV

peptide on H2Kb; NIH Tetramer Core Facility, Emory University; 1:200) and the followings: anti-CD8 FITC (1:800), anti-CD4 APC eFluor780 (1:400), anti-CD44 PerCP-Cy5.5 (1:400), anti-CD127 PE (1:100), anti-KLRG1 PE-Cy7 (1:100). The fluorophore-conjugated anti-mouse antibodies were purchased from eBioscience except anti-CD8 FITC (Accurate Chemical & Scientific).

3.3.7 *Quantitative real-time PCR*

Parasite load in the skeletal muscle, adipose, cardiac muscle and the pinna of the ears was analyzed by quantitative real-time PCR as previously described [41].

3.3.8 *Parasitemia and mortality assessment*

Five microliter of the blood was collected from the tail vein of the mice and the number of parasites was quantified in 100 microscopic fields (40×) using a compound light microscope and expressed as the number of live trypomastigotes per μl. Survival was monitored daily.

3.3.9 *Rescue efficiency of complemented TcHyp1KO parasites*

Metacyclic trypomastigotes of TcHyp1KO (6×10^6) transfected or not with pTREX_Hyp1plasmid were incubated with 2×10^5 Vero cells in 3 ml of complete RPMI supplemented with 10% FBS in $25cm^2$ BioLite flask (Thermo) overnight. Extracellular parasites were washed extensively the next day and replenished with 3 ml complete RPMI. The number of extracellular trypomastigotes and infected cells at day 10 were counted in 20 fields under compound light microscopy (40×) and the number of released trypomastigotes per 50 infected cells was calculated.

3.3.10 *Statistical analysis*

Data are presented as the mean ±SEM. Comparison of the means was performed using two-tailed Student's *t* test. P-values of $p<0.05$ were considered significant.

3.4 Results

3.4.1 *T. cruzi Hyp1 is a flagellum membrane protein expressed by trypomastigotes and amastigotes*

Hyp1 (encoded by gene TcCLB.510099.110, gI: 71420049) undergoes stage-specific transcription and expression, with expression highest in amastigotes and trypomastigotes and down-regulated in epimastigotes and metacyclic trypomastigotes (Fig. 3.1A) [42]. Consistent with the stage-specific transcription profile, Hyp1 protein is detected in the amastigote and trypomastigote stages but not in the epimastigote stage, as determined by whole organism proteome analysis [43]. Hyp1 in *T. cruzi* possesses an additional 40 amino acid-long sequence at the N-terminus. The additional sequence is predicted to include a signal peptide (amino acids 1^{st} – 22^{nd}). Since Blastp failed to find any related motif or domain in Hyp1, the tertiary structure of Hyp1 was predicted and the motifs or domains that may share a similar tertiary structure were searched (pDomTHREADER). The motif predicted with the highest value of confidence and broadest coverage (amino acids 77^{th} – 149^{th} of Hyp1) is the zinc-finger ssDNA-binding motif of ADP-ribose polymerase 1 (pADPRT) which catalyzes poly ADP-ribose (pADPR) synthesis.

Parasites overexpressing Hyp1 were constructed by transfection of a HA-tagged Hyp1-containing plasmid. HA-tagged Hyp1 is located to the flagellar surface of amastigotes and trypomastigotes (Fig. 3.1B). We infer from this result that native Hyp1 also localizes to the flagellar surface membrane due to the potential signal presence at the N-terminus, however the apparent low level of expression in WT parasite prevented its detection using a polyclonal antibody. Likewise, the expression level of this homologue is also low compared to other flagellar proteins (ranking 542 out of the 666 proteins detected [44]).

3.4.2 *T. cruzi amastigotes lacking Hyp1 fail to differentiate into trypomastigotes*

To address the function of Hyp1 we used CRISPR-Cas9 to knockout Hyp1. Clonal lines from Hyp1 gRNA-transfected epimatigotes were converted to metacyclic trypomastigoes and then tested for the ability to infect and replicate in Vero cells. Approximately 12% of all clonal lines failed to produce trypomastigotes but instead ultimately released amastigotes into the culture medium (Fig. 3.2A). The absence of Hyp1 expression in lines defective in trypomastigote production was confirmed by western blot (Fig. 3.2B).

Complementation of the trypomastigogenesis-defective lines with a HA-tagged version of Hyp1 partially rescued trypomastigote generation in the KO lines, as demonstrated by intracellular conversion of amastigotes to trypomastigotes (Fig 3.2C) and the release of trypomastigotes from infected cells (Fig. 3.2D). Hyp1 expression in the rescued trypomastigotes was confirmed by detecting HA at the flagellar surface (Fig. 3.2E).

3.4.3 *TcHyp1KO metacyclic trypomastigotes infect host cells normally but have impaired intracellular proliferation*

TcHyp1KO parasites were assessed for potential defects in other aspects of host cell invasion and replication. The number of membrane-bound and intracellular parasites in host cells after overnight exposure to metacyclic trypomastigotes was comparable between TcHyp1KO and WT parasites (Fig. 3.3A), indicating that Hyp1 is not required for invasion. However, 3 days after initial infection, the number of intracellular amastigotes was significantly decreased in TcHyp1KO-infected Vero cells compared to TcWT-infected cells (Fig. 3.3B).

3.4.4 *TcHyp1KO parasites fail to maintain a persistent infection in mice*

We next examined the *in vivo* behavior of TcHyp1KO parasites by infection in mice. As in the case of in vitro infection, TcHyp1KO metacyclic trypomastigotes are able to establish

infection *in vivo* as evidenced by the detection of increasing *T. cruzi* DNA at the site of inoculation between 4 and 7 dpi (Fig. 3.3C). However it is clear that particularly in the first round of host cell invasion *in vivo*, the TcHyp1KO parasites have much reduced amastigote replication relative to WT parasites (Fig. 3.3C day 4). As a further indication of established infection, we observed the generation of $CD8^+$ T cells specific for the *T. cruzi trans*-sialidase-derived epitope TSKB20, a dominant MHC class I-restricted antigen in C57BL/6 mice, at 14 days post infection (Fig. 3.3D, E). It is noteworthy that in previous studies, mice in which WT infection is aborted by treatment with curative drugs within 1-2 days of infection generated no detectable TSKb20-specific T cell response (Juan Bustamante, unpublished).

As expected, TSKB20-specific $CD8^+$ T cell responses in TcHyp1KO infection were lower compared to that in TcWT infection at 14 days post infection (Fig. 3.3D, E), reflecting a decreased parasite load in the TcHyp1KO infected mice [45]. The persistence of TcHyp1KO parasites was assessed by submitting the mice to an immunosuppression regiment at 30 days post-infection [34]. Real-time PCR analysis of *T. cruzi* DNA in skeletal muscle, fat and heart showed no *T. cruzi* DNA in mice infected with TcHyp1KO metacyclic trypomastigotes, indicating that parasites were cleared between 7 and 30 days post-infection (Fig. 3.4A).
To further investigate the potential of TcHyp1KO parasites to maintain infection *in vivo*, we infected highly susceptible $IFN\gamma^{-/-}$ mice. Again, infection with TcHyp1KO parasites elicited TSKB20-specific $CD8^+$ T cell response, indicating an established infection (Fig. 3.4B), but parasites in the blood (Fig. 3.4C) or in tissues (Fig. 3.4D) were undetectable at 21 days post-infection. The collective results from both immune competent and immune deficient mice suggest that in the absence of Hyp1, *T. cruzi* is highly attenuated and cannot maintain an infection *in vivo*.

3.4.5 *Overexpression of Hyp1 impairs invasion of host cells in vitro and attenuates infection in vivo*

We next asked if the low level of expression of Hyp1 was important to its function by assessing the *in vitro* and *in vivo* growth characteristics of parasites over-expressing Hyp1 (TcHyp1; Figure 1). Hyp1 over-expressers showed reduced invasion of host cells (Fig. 3.5A) but comparable replication of amastigotes within infected cells, relative to TcWT (Fig. 3.5B). As expected, IFN$\gamma^{-/-}$ mice infected with TcHyp1 parasites displayed reduced parasitemia (Fig. 3.6A) and no mortality (Fig. 3.6B) during 85 days of the experiment. Real-time PCR analysis in tissues of mice immunosuppressed after 15 months of infection showed that, in contrast to parasite persistence in all of the TcWT-infected mice, only 1 out of 8 of TcHyp1-infected mice showed parasites in skeletal muscle and fat (Fig. 3.6C, D), demonstrating that Hyp1 overexpression attenuates infection or leads to abortion of the infection in immune competent mice.

3.5 Discussion

Although a critical step in maintenance of *T. cruzi* infection in mammals, the initiation of trypomastigogenesis is yet poorly understood. So far only a few *T. cruzi* surface molecules have been implicated to be involved in this process. Certain proteins anchored to *T. cruzi* surface may be involved as reduction in GPI expression resulted in greatly reduced amastigote proliferation and subsequent failure of trypomastigogenesis [17]. One of these *T. cruzi* surface proteins could be glycoprotein δ-amastin, since overexpression of *T. cruzi* δ-amastin increased trypomastigogenesis without affecting amastigote proliferation [46].

The protrusion of the flagella from the cell bodies of various organisms make them ideal sensory structures for controlling motility, metabolism, and differentiation [47-49]. In bacteria,

flagella of *Salmonella typhimurium* acts as a wetness sensor to initiate swarmer cell differentiation [49]. Trypanosomal flagella are enriched in lipid rafts that organize transmembrane signaling events [26-28]. In *Trypanosoma brucei*, two flagellar proteins, cyclic nucleotide phosphodiesterase B1 (TbrPDEB1) and adenylate cyclase AC6, control intracellular cyclic AMP levels to regulate the social motility of procyclic trypomastigotes in response to an unknown extracellular signal [31-33]. LmXGT1, a glucose transporter protein and potential glucose sensor in *Leishmania mexicana*, and flagellar calcium-binding protein (FCABP), which senses calcium are additional sensors located in the flagellum of trypanosomitids [29, 30]. If *T. cruzi* trypomastigogenesis is initiated by sensing external stimuli, it seems likely that the sensors would be located in the flagellar membrane. In this study, we identified one such protein that localizes to the flagellar membrane and is essential for amastigote-to-trypomastigote conversion in *T. cruzi*.

Hyp1 was originally of interest to us for its potential to be an invariant target of CD8+ T cells. Encode by a single diploid gene, Hyp1 expression is produced by amastigotes and the presence of a putative signal peptide indicated access to the extracellular milieu. However, we did not detect secretion of Hyp1 to culture medium in Hyp1 over-expressing parasites (data not shown). Instead, HA-tagged Hyp1 in Hyp1 over-expressers is localized to flagellar membrane in amastigotes and trypomastigotes (Fig. 1B), implying that native Hyp1 protein is a flagellar constituent. Compared to the homologues in *T. brucei*, *T. vivax*, *T. congolense* and *L. major*, Hyp1 in *T. cruzi* possesses a 40 amino acid-long sequence at the N-terminus predicted to include a signal peptide (amino acids 1^{st} -22^{nd}). We propose that this signal peptide contributes to the surface translocation of Hyp1 in amastigotes and trypomastigotes of *T. cruzi*. In contrast, the *T. brucei* homologue is exclusively detected in the flagellar skeleton and flagellar matrix but not

flagellar surface membrane[44]. Emergence of the signal peptide in *T. cruzi* Hyp1 may be an evolutionary consequence of the unique environmental needs to *T. cruzi* as it has a distinct life cycle in mammalian hosts compared to *T. brucei, T. vivax, T. congolense* and *L. major*. Compared to *T. cruzi* with both extracellular and intracellular stages, infections with *T. brucei, T. vivax* and *T. congolense* in mammalian hosts occur extracellularly. In contrast to *T. cruzi* that undergoes trypomastigogenesis before mechanical rupture of an infected cell, *L. major* in the macrophage undergoes proliferation as amastigotes followed by no differentiation before lysis of the infected cell. Due to its distinct life cycle compared to other trypanosomatids, *T. cruzi* may initiate trypomastigogenesis in response to signals in the host cell that requires detection by a unique flagellar surface membrane protein.

In this study, the flagellar surface protein Hyp1 is shown to be required for trypomastigogenesis (Fig. 3.2). Furthermore, the fact that *T. cruzi* Hyp1 expression is not detected in epimastigote stage which also features with a protruding flagellum [42, 43], and that lacking Hyp1 expression in TcHyp1KO epimastigotes does not interfere epimastigote growth (data not shown) both suggests that Hyp1 may not be an essential constitutive element for flagellum assembly. Instead, Hyp1 may play a regulatory role in amastigote-to-trypomastigote conversion.

To address the potential function of this trypanosomatid-specific hypothetical protein, the tertiary structure was predicted (pDomTHREADER), and prediction with the highest value lies in the sequence between amino acid 77th and 149th that shares similarity with the zinc-finger ssDNA-binding motif of ADP-ribose polymerase 1 (pADPRT), an enzyme catalyzing poly ADP-ribose (pADPR) synthesis. Interestingly, a few studies suggest that pADPRT, either produced by the host cell or *T. cruzi*, may be involved in differentiation from amastigotes to trypomastigotes.

Earlier studies conducted by Williams found that two pADPRT inhibitors, 3-methoxybenzamide and 5-methylnicotinamide, both targeting the catalytic domain of the protein, inhibited trypomastigogenesis in infected cells and in the cell-free medium, possibly due to inhibition of *T. cruzi* pADPRT [19]. However, later work by Larrea *et al.* suggests that host pADPRT may be important for trypomastigogenesis, since siRNA knockdown of host pADPRT reduced the number of released trypomastigotes from infected cells [18]. In addition, infected cells treated with Olaparib, another pADPRT inhibitor selectively binding to the catalytic domain of pADPRT, displayed inhibited intracellular amastigote proliferation with no loss of released trypomastigotes or initial invasion [18]. Synthesis of pADPR in the catalytic domain of pADPRT requires detection of DNA single strand breaks in the DNA-binding domain. Given that Olaparib impacts the catalytic domain but not DNA-binding domain of pADPRT, while siRNA knockdown impacts expression of all the domains, it is possible that conversion from amastigotes to trypomastigotes involves detection of ssDNAs in the host cell while the catalytic activity of pADPRT may be required for amastigote proliferation.

Upon DNA damage, truncated DNAs, either single-stranded or double-stranded, are released from the nucleus and accumulate in the cytoplasm [50]. If Hyp1 possesses a DNA-binding zinc-finger motif of pADPRT as predicted, with potential localization in the flagellum surface membrane, Hyp1 may bind to ssDNAs accumulated in the cytoplasm of an infected and damaged cell, which triggers amastigote-to-trypomastigote conversion. However, no data yet indicates DNA-binding ability in Hyp1, which is worthy of further investigation.

Hyp1 expression is also linked to amastigote proliferation *in vitro* (Fig. 3.3A, B), raising the concern that the defect in trypomastigogenesis may be attributable to a deficiency in amastigote proliferation. However, a number of previous studies demonstrated that attenuated

amastigote proliferation does not necessarily lead to the complete failure of trypomastigogenesis as shown here in the case of TcHyp1KO parasites. For example, monoallelic mutant parasites for the *dhfr-ts* gene in *T. cruzi* showed attenuated epimastigote growth and impaired virulence during *in vivo* infection in multiple mice strains. However, *in vivo* infection with *dhfr-ts*$^{+/-}$ metacyclic trypomastigotes maintained at least for 120 days in most nude mice and BALB/c mice [51]. Disruption of fatty acid metabolism, such as single knock down of fatty acid transporter protein (*fatp*), resulted in delayed amastigote proliferation while the release of trypomastigotes was not affected (Hartley, unpublished data). In addition, GPI-deficient *T. cruzi* displaying severely attenuated amastigote proliferation still underwent trypomastigogenesis, although less efficiently, in infected cells *in vitro*, and *in vivo* infection with GPI-deficient *T. cruzi* still resulted in parasitemia detected during acute phase and mortality in SCID mice and C3H/HeSnJ mice [17]. Therefore, the complete blocking of amastigote-to-trypomastigote conversion in TcHyp1KO parasites appears to be independent from impaired amastigote proliferation. Consistent with the uncompromised ability to invade host cells *in vitro*, parasites lacking Hyp1 were also able to establish infection in mice. However, likely due to the compromised amastigote proliferation and complete failure of trypomastigogenesis, TcHyp1KO parasites were rapidly cleared at least within 35 days of infection regardless of IFNγ-dependent immune control.

Similar to the relatively low expression of Hyp1 homologue in *T. brucei* [44], Hyp1expression in *T. cruzi* also appears to be relatively low, as suggested by failure to detect this protein on the surface of WT parasites using a polyclonal antibody. Although Hyp1 is required for completion of *T. cruzi* life cycle, over-presentation of Hyp1 is also disfavored, as shown by the weakened infection with *T. cruzi* overexpressing Hyp1 *in vitro* and *in vivo*, suggesting that low but necessary expression of Hyp1 may be optimal for efficient *T. cruzi* infection.

Our work identifies a previously uncharacterized *T. cruzi* flagellar membrane protein that is essential for amastigote-to-trypomastigote conversion and sheds light on future exploration of the mechanism underlying this life-stage conversion process. Because Hyp1 protein is trypanosomatid-specific, Hyp1 protein may be a promising chemotherapeutic target for rapid cure in an infected host.

Figure 3.1. *T. cruzi Hyp1 is a mammalian stage-specific flagellum membrane protein*. (A) Level of hyp1 transcript expression as a log2 ratio over a cDNA reference sample in each life stage, as previously determined [23]. (B) Flagellar localization of HA-tagged Hyp1 in TcHyp1 trypomastigotes and amastigotes were determined by indirect immuno-fluorescence microscopy upon staining with rat anti-HA monoclonal antibody without permeablization. Differential interference contrast (DIC) and fluorescent images were acquired (100 ×), deconvolved with a Delta Vision (Applied Precision) and adjusted for contrast using Softworx software (Applied Precision). Scale bar represents 5 μm.

Figure 3.1

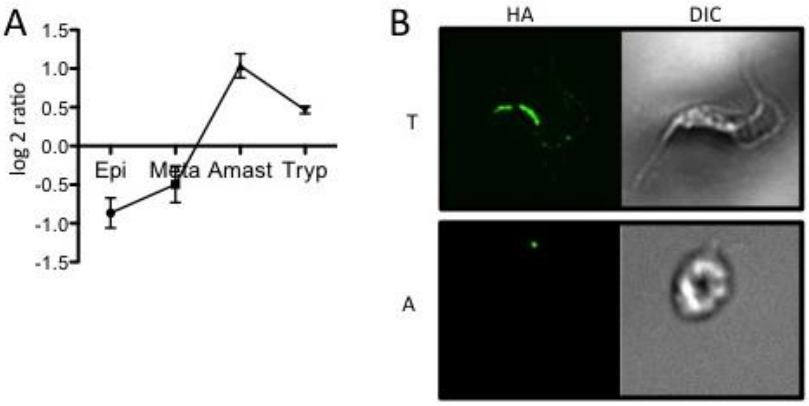

Figure 3.2. *Disruption of Hyp1 expression abolishes trypomastigogenesis and is partially rescued by complementation via transfection of pTREX_Hyp1*. (A) Time-lapse snapshots of Vero cells infected with metacyclic trypomastigotes of *T. cruzi* either wild type or transfected with the sgRNAs targeting *cas9* and *hyp1* as described in Materials and Methods. Videos were taken from day 3 for TcWT infection and day 6 for TcHyp1KO infection, when cells in focus were heavily infected with amastigotes. Scale bar represents 15 μm. (B) Disruption of Hyp1 expression correlates with complete arrest of trypomastigogenesis *in vitro*. Two clones from *T. cruzi* transfected with sgRNA_Hyp1_79 and sgRNA_Cas9 were either capable (middle) or incapable of trypomastigotegenesis (right). The membrane fraction of the amastigote lysates of WT *T. cruzi* (left) and the two clones was immune-blotted with anti-Hyp1 mouse serum and mouse anti-α-tubulin monoclonal antibody. (C) Fluorescence and DIC microscopy of live complemented TcHyp1KO parasites expressing GFP in an infected cell. Arrow indicates one parasite with a protruding flagellum while the other parasites are amastigote-like. Scale bar represents 5 μm. (D) Metacyclic trypomastigotes of TcHyp1KO transfected with or without pTREX_Hyp1 were incubated with Vero cells (parasite: Vero = 30:1) overnight and extracellular parasites were removed the next day. At day 10 post infection, the number of released trypomastigotes per 50 infected cells was determined as described in Materials and Methods. Data are representative of two experiments. Mean ±SEM. (E) HA-tagged Hyp1 expression in the trypomastigote stage of complemented TcHyp1KO was determined by indirect immuno-fluorescence microscopy using modified non-permeablizing staining protocol [95]. Rat monoclonal anti-HA antibody was used to mark the target protein. PI and DAPI were applied sequentially to label DNA in non-permeablized parasites (PI labeling served as exclusion marker was negative and not shown). Scale bar represents 5 μm. DIC and fluorescence images were

acquired with 100 × magnification and deconvolved with a Delta Vision (Applied Precision) and adjusted for contrast using Softworx software (Applied Precision).

Figure. 3.2

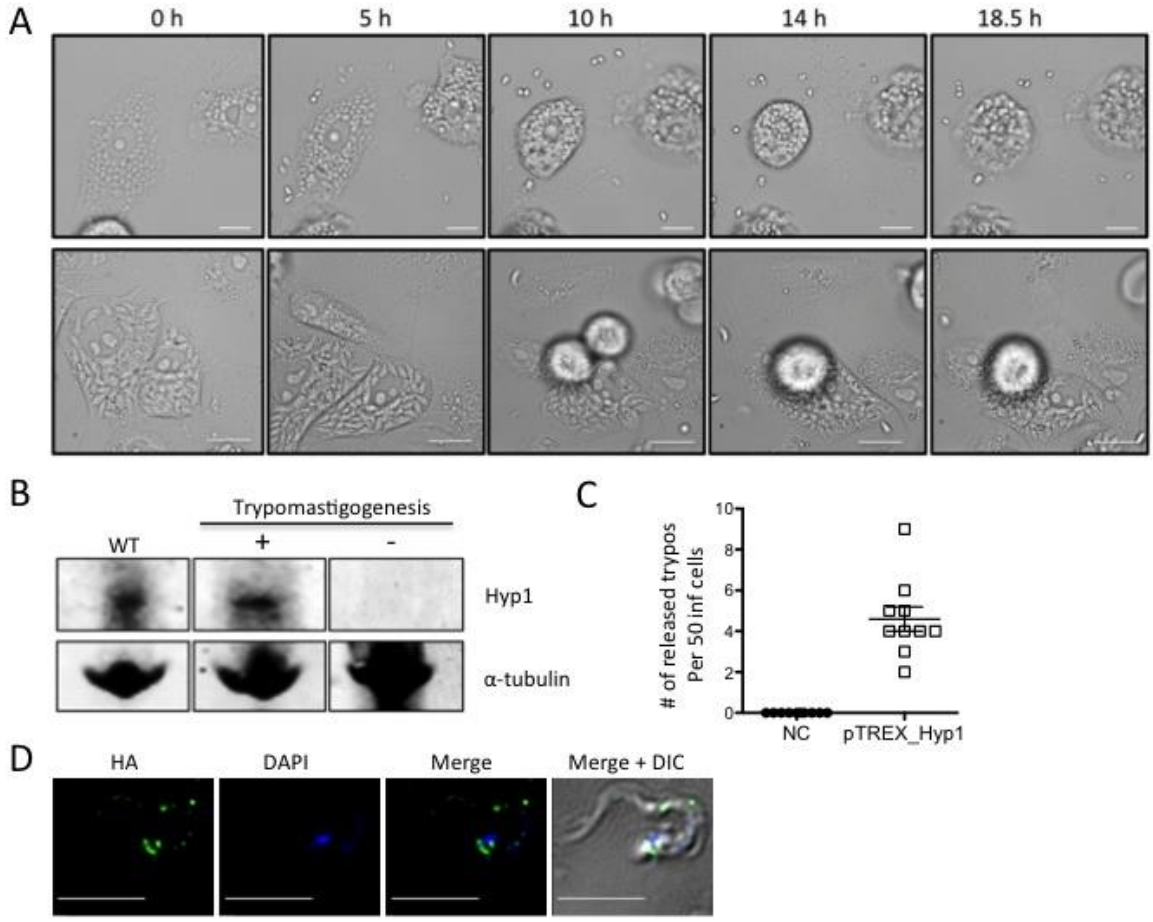
A
0 h
5 h
10 h
14 h
18.5 h
B
Trypomastigogenesis
WT
+
-
Hyp1
α-tubulin
C
# of released trypos
Per 50 inf cells
10
8
6
4
2
0
NC
pTREX_Hyp1
D
HA
DAPI
Merge
Merge + DIC

Figure 3.3. *Disruption of Hyp1 expression impairs amastigote proliferation but not invasion of metacyclic trypomastigotes in vitro and reduces severity of infection in immune competent mice in vivo.* (A-B) TcHyp1KO and TcWT metacyclic trypomastigotes were incubated overnight with Vero cells at 20:1 ratio followed by washes to eliminate extracellular parasites unbound or loosely bound to Vero cells. (A) Invasion was assessed as the number of membrane-bound and intracellular parasites per 100 cells after overnight infection. (B) Proliferation was measured by the number of intracellular parasites per infected cell at day 3 post incubation. At least 30 cells were counted in triplicate wells per condition. Data are representative of three separate experiments. (C) *T. cruzi* DNA in ears of C57BL/6 mice *s.c.* inoculated with 3.2×10^5 TcWT or TcHyp1KO metacyclic trypomastigotes at 4 and 7 dpi as determined by quantitative real-time PCR. Data are representative of two separate experiments with 4 ears per group. (D) The number represents the frequency of $TSKB20^{+}CD44^{hi}$ cells (the gated population) in $CD8^{+}$ T cells from peripheral blood of mice *i.p.* inoculated of 2.5×10^5 TcWT or TcHyp1KO metacyclic trypomastigotes at 14 dpi. Each flow plot displays one representative from each group. Experiments were done three times with similar number of mice in each group. Results in D are summarized in E. Mean ±SEM. ** $p\leq0.01$ or *** $p\leq0.001$, as determined by Student's *t*-test.

Figure 3.3

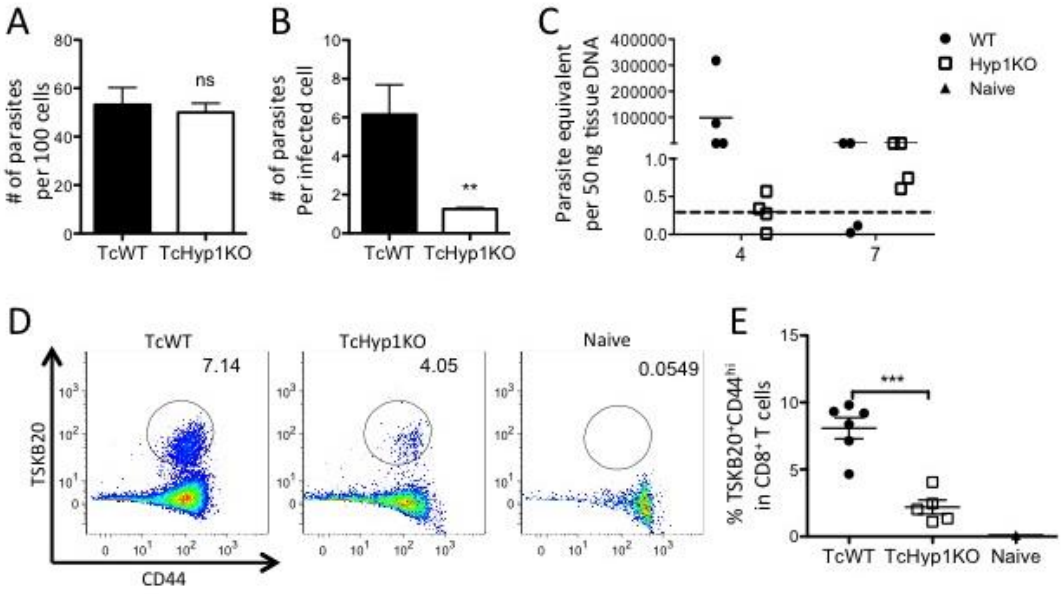
A
# of parasites per 100 cells
ns
TcWT TcHyp1KO
B
# of parasites Per infected cell
**
TcWT TcHyp1KO
C
Parasite equivalent per 50 ng tissue DNA
WT
Hyp1KO
Naive
D
TcWT
7.14
TcHyp1KO
4.05
Naive
0.0549
TSKB20
CD44
E
% TSKB20+CD44hi in CD8+ T cells
***
TcWT TcHyp1KO Naive

Figure 3.4. *Parasites lacking Hyp1 expression are unable to persist through acute phase in vivo regardless of IFNγ-dependent immune control.* (A) *T. cruzi* in skeletal muscle (left), fat (middle) and heart (right) of C57BL/6 mice *i.p.* inoculated with 2.5×10^5 TcHyp1KO or TcWT metacyclic trypomastigotes for 35 days followed by immunosuppression, as determined by quantitative real-time PCR. Experiments were done twice with similar number of mice in each group. (B) The frequency of $TSKB20^+CD44^{hi}$ cells in $CD8^+$ T cells from peripheral blood in $IFN\gamma^{-/-}$ C57BL/6 mice at day 21 of *i.p.* infection with 2.5×10^5 TcWT or TcHyp1KO metacyclic trypomastigotes. Data are representative of three experiments with 3-6 mice per group in each experiment. (C) The parasitemia in $IFN\gamma^{-/-}$ C57BL/6 mice at day 21 of infection as in B. Data represent two separate experiments with five mice per group. (D) *T. cruzi* in skeletal muscle of C57BL/6 mice that are either IFNγ-expressing or IFNγ-deficient and *i.p.* inoculated with 2.5×10^5 TcHyp1KO or TcWT metacyclic trypomastigotes for 35 days followed by immunosuppression, as determined by quantitative real-time PCR. Experiments were done twice with 4-6 mice per group in each experiment. Mean ±SEM.

Figure 3.4

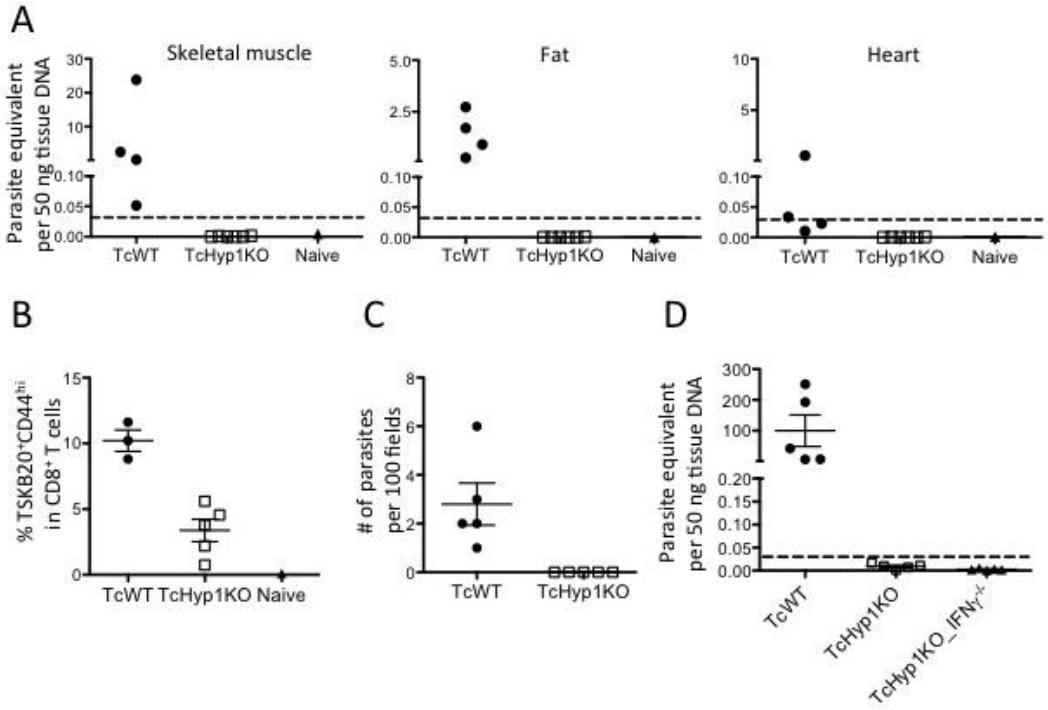
A
Skeletal muscle
Fat
Heart
Parasite equivalent per 50 ng tissue DNA
TcWT
TcHyp1KO
Naive
B
% TSKB20+CD44hi in CD8+ T cells
TcWT TcHyp1KO Naive
C
# of parasites per 100 fields
TcWT
TcHyp1KO
D
Parasite equivalent per 50 ng tissue DNA
TcWT
TcHyp1KO
TcHyp1KO_IFNγ-/-

Figure 3.5. *Hyp1 overexpression in T. cruzi impairs trypomastigote invasion but not amastigote proliferation in vitro.* (A) Vero cells infected with TcHyp1 or TcWT trypomastigotes (typs: Vero = 10:1) were examined 6 h post infection for the percentage of cells infected. Data represent three separate experiments with triplicates per group. (B) Vero cells infected for 6 h in Fig. A were incubated for another 3 days and the number of intracellular parasites were assessed in at least 30 infected cells in triplicates per group. Data represent three separate experiments. Mean ±SEM. ** $p \leq 0.01$ as determined by Student's *t*-test.

Figure 3.5

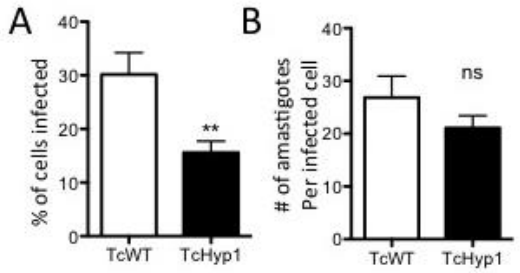
A
% of cells infected
40
30
20
10
0
**
TcWT
TcHyp1
B
# of amastigotes
Per infected cell
40
30
20
10
0
ns
TcWT
TcHyp1

Figure 3.6. *Hyp1overexpression attenuates infection with frequent chronic cure in vivo.* (A) The parasitemia and (B) the survival rate in IFN$\gamma^{-/-}$ C57BL/6 mice *i.p.* inoculated with 1,000 TcWT or TcHyp1 trypomastigotes. Data represents three separate experiments with 4-5 mice per group. (C-D) *T. cruzi* in skeletal muscle (C) and fat (D) of immunosuppressed C57BL/6 mice chronically infected with TcHyp1 or TcWT trypomastigotes, as determined by quantitative real-time PCR. Data are representative of two experiments with 5-8 mice per group. Mean ±SEM. * $p \leq 0.05$, as determined by Student's *t*-test.

Figure 3.6

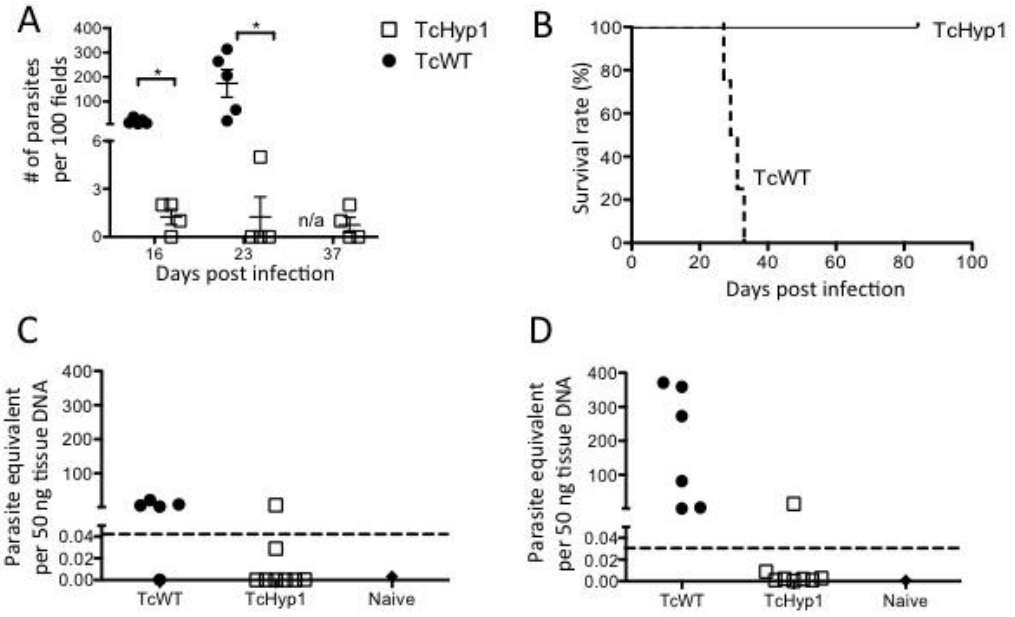
A
# of parasites per 100 fields
TcHyp1
TcWT
*
*
n/a
16
23
37
Days post infection
B
Survival rate (%)
TcHyp1
TcWT
Days post infection
C
Parasite equivalent per 50 ng tissue DNA
TcWT
TcHyp1
Naive
D
Parasite equivalent per 50 ng tissue DNA
TcWT
TcHyp1
Naive

3.6 References

1. Ulrich, H., Magdesian, M.H., Alves, M.J. & Colli, W. In vitro selection of RNA aptamers that bind to cell adhesion receptors of *Trypanosoma cruzi* and inhibit cell invasion. *The Journal of biological chemistry* **277**, 20756-20762 (2002).

2. Schenkman, S., Jiang, M.S., Hart, G.W. & Nussenzweig, V. A novel cell surface trans-sialidase of *Trypanosoma cruzi* generates a stage-specific epitope required for invasion of mammalian cells. *Cell* **65**, 1117-1125 (1991).

3. Schenkman, S., Kurosaki, T., Ravetch, J.V. & Nussenzweig, V. Evidence for the participation of the Ssp-3 antigen in the invasion of nonphagocytic mammalian cells by *Trypanosoma cruzi*. *The Journal of experimental medicine* **175**, 1635-1641 (1992).

4. Manque, P.M. *et al.* Characterization of the cell adhesion site of *Trypanosoma cruzi* metacyclic stage surface glycoprotein gp82. *Infection and immunity* **68**, 478-484 (2000).

5. Silber, A.M. *et al. Trypanosoma cruzi*: identification of a galactose-binding protein that binds to cell surface of human erythrocytes and is involved in cell invasion by the parasite. *Experimental parasitology* **100**, 217-225 (2002).

6. Johnson, C.A. *et al.* Thrombospondin-1 interacts with *Trypanosoma cruzi* surface calreticulin to enhance cellular infection. *PloS one* **7**, e40614 (2012).

7. Castillo, C. *et al.* The interaction of classical complement component C1 with parasite and host calreticulin mediates *Trypanosoma cruzi* infection of human placenta. *PLoS neglected tropical diseases* **7**, e2376 (2013).

8. Fernandes, M.C. & Andrews, N.W. Host cell invasion by *Trypanosoma cruzi*: a unique strategy that promotes persistence. *FEMS microbiology reviews* **36**, 734-747 (2012).

9. Salto, M.L. *et al.* Formation and remodeling of inositolphosphoceramide during differentiation of *Trypanosoma cruzi* from trypomastigote to amastigote. *Eukaryotic cell* **2**, 756-768 (2003).

10. Liendo, A., Lazardi, K. & Urbina, J.A. In-vitro antiproliferative effects and mechanism of action of the bis-triazole D0870 and its S(-) enantiomer against *Trypanosoma cruzi*. *The Journal of antimicrobial chemotherapy* **41**, 197-205 (1998).

11. Urbina, J.A. *et al.* Antiproliferative effects and mechanism of action of SCH 56592 against Trypanosoma (Schizotrypanum) cruzi: in vitro and in vivo studies. *Antimicrobial agents and chemotherapy* **42**, 1771-1777 (1998).

12. Alexander, A.D., Villalta, F. & Lima, M.F. Transforming growth factor alpha binds to *Trypanosoma cruzi* amastigotes to induce signaling and cellular proliferation. *Infection and immunity* **71**, 4201-4205 (2003).

13. Hudock, M.P. *et al.* Inhibition of *Trypanosoma cruzi* hexokinase by bisphosphonates. *Journal of medicinal chemistry* **49**, 215-223 (2006).

14. Santoro, G.F., Cardoso, M.G., Guimaraes, L.G., Freire, J.M. & Soares, M.J. Anti-proliferative effect of the essential oil of Cymbopogon citratus (DC) Stapf (lemongrass) on intracellular amastigotes, bloodstream trypomastigotes and culture epimastigotes of *Trypanosoma cruzi* (Protozoa: Kinetoplastida). *Parasitology* **134**, 1649-1656 (2007).

15. Damasceno, F.S., Barison, M.J., Pral, E.M., Paes, L.S. & Silber, A.M. Memantine, an antagonist of the NMDA glutamate receptor, affects cell proliferation, differentiation and the intracellular cycle and induces apoptosis in *Trypanosoma cruzi*. *PLoS neglected tropical diseases* **8**, e2717 (2014).

16. Yakubu, M.A., Basso, B. & Kierszenbaum, F. DL-alpha-difluoromethylarginine inhibits intracellular *Trypanosoma cruzi* multiplication by affecting cell division but not trypomastigote-amastigote transformation. *The Journal of parasitology* **78**, 414-419 (1992).

17. Garg, N., Postan, M., Mensa-Wilmot, K. & Tarleton, R.L. Glycosylphosphatidylinositols are required for the development of *Trypanosoma cruzi* amastigotes. *Infection and immunity* **65**, 4055-4060 (1997).

18. Vilchez Larrea, S.C. *et al.* Inhibition of poly(ADP-ribose) polymerase interferes with *Trypanosoma cruzi* infection and proliferation of the parasite. *PloS one* **7**, e46063 (2012).

19. Williams, G.T. *Trypanosoma cruzi*: inhibition of intracellular and extracellular differentiation by ADP-ribosyl transferase antagonists. *Experimental parasitology* **56**, 409-415 (1983).

20. Contreras, V.T. *et al.* Early and late molecular and morphologic changes that occur during the in vitro transformation of *Trypanosoma cruzi* metacyclic trypomastigotes to amastigotes. *Biological research* **35**, 47-58 (2002).

21. Queiroz, R.M. *et al.* Quantitative proteomic and phosphoproteomic analysis of *Trypanosoma cruzi* amastigogenesis. *Molecular & cellular proteomics : MCP* **13**, 3457-3472 (2014).

22. Gonzalez, J. *et al.* Proteasome activity is required for the stage-specific transformation of a protozoan parasite. *The Journal of experimental medicine* **184**, 1909-1918 (1996).

23. Tomlinson, S., Vandekerckhove, F., Frevert, U. & Nussenzweig, V. The induction of *Trypanosoma cruzi* trypomastigote to amastigote transformation by low pH. *Parasitology* **110 (Pt 5)**, 547-554 (1995).

24. Grellier, P. *et al.* Involvement of calyculin A-sensitive phosphatase(s) in the differentiation of *Trypanosoma cruzi* trypomastigotes to amastigotes. *Molecular and biochemical parasitology* **98**, 239-252 (1999).

25. Walker, P.J. Organization of function in trypanosome flagella. *Nature* **189**, 1017-1018 (1961).

26. Tyler, K.M. *et al.* Flagellar membrane localization via association with lipid rafts. *Journal of cell science* **122**, 859-866 (2009).

27. Maric, D., Epting, C.L. & Engman, D.M. Composition and sensory function of the trypanosome flagellar membrane. *Current opinion in microbiology* **13**, 466-472 (2010).

28. Langousis, G. & Hill, K.L. Motility and more: the flagellum of *Trypanosoma brucei*. *Nature reviews. Microbiology* **12**, 505-518 (2014).

29. Buchanan, K.T. *et al.* A flagellum-specific calcium sensor. *The Journal of biological chemistry* **280**, 40104-40111 (2005).

30. Rodriguez-Contreras, D. *et al.* Regulation and biological function of a flagellar glucose transporter in *Leishmania mexicana*: a potential glucose sensor. *FASEB journal : official publication of the Federation of American Societies for Experimental Biology* **29**, 11-24 (2015).

31. Oberholzer, M., Lopez, M.A., McLelland, B.T. & Hill, K.L. Social motility in african trypanosomes. *PLoS pathogens* **6**, e1000739 (2010).

32. Oberholzer, M., Saada, E.A. & Hill, K.L. Cyclic AMP Regulates Social Behavior in African Trypanosomes. *mBio* **6**, e01954-01914 (2015).

33. Luginbuehl, E. *et al.* The N terminus of phosphodiesterase TbrPDEB1 of *Trypanosoma brucei* contains the signal for integration into the flagellar skeleton. *Eukaryotic cell* **9**, 1466-1475 (2010).

34. Bustamante, J.M., Bixby, L.M. & Tarleton, R.L. Drug-induced cure drives conversion to a stable and protective CD8+ T central memory response in chronic Chagas disease. *Nature medicine* **14**, 542-550 (2008).

35. Lorenzi, H.A., Vazquez, M.P. & Levin, M.J. Integration of expression vectors into the ribosomal locus of *Trypanosoma cruzi*. *Gene* **310**, 91-99 (2003).

36. Garg, N., Nunes, M.P. & Tarleton, R.L. Delivery by *Trypanosoma cruzi* of proteins into the MHC class I antigen processing and presentation pathway. *J Immunol* **158**, 3293-3302 (1997).

37. Peng, D., Kurup, S.P., Yao, P.Y., Minning, T.A. & Tarleton, R.L. CRISPR-Cas9-mediated single-gene and gene family disruption in *Trypanosoma cruzi*. *mBio* **6**, e02097-02014 (2015).

38. Cooley, G. *et al.* High throughput selection of effective serodiagnostics for *Trypanosoma cruzi* infection. *PLoS neglected tropical diseases* **2**, e316 (2008).

39. Laucella, S.A. *et al.* Frequency of interferon- gamma -producing T cells specific for *Trypanosoma cruzi* inversely correlates with disease severity in chronic human Chagas disease. *The Journal of infectious diseases* **189**, 909-918 (2004).

40. Agrawal, S., van Dooren, G.G., Beatty, W.L. & Striepen, B. Genetic evidence that an endosymbiont-derived endoplasmic reticulum-associated protein degradation (ERAD) system functions in import of apicoplast proteins. *The Journal of biological chemistry* **284**, 33683-33691 (2009).

41. Cummings, K.L. & Tarleton, R.L. Rapid quantitation of *Trypanosoma cruzi* in host tissue by real-time PCR. *Molecular and biochemical parasitology* **129**, 53-59 (2003).

42. Minning, T.A., Weatherly, D.B., Atwood, J., 3rd, Orlando, R. & Tarleton, R.L. The steady-state transcriptome of the four major life-cycle stages of *Trypanosoma cruzi*. *BMC genomics* **10**, 370 (2009).

43. Atwood, J.A., 3rd *et al.* The *Trypanosoma cruzi* proteome. *Science* **309**, 473-476 (2005).

44. Oberholzer, M. *et al.* Independent analysis of the flagellum surface and matrix proteomes provides insight into flagellum signaling in mammalian-infectious *Trypanosoma brucei*. *Molecular & cellular proteomics : MCP* **10**, M111 010538 (2011).

45. Martin, D.L. *et al.* CD8+ T-Cell responses to *Trypanosoma cruzi* are highly focused on strain-variant trans-sialidase epitopes. *PLoS pathogens* **2**, e77 (2006).

46. Cruz, M.C. *et al. Trypanosoma cruzi*: role of delta-amastin on extracellular amastigote cell invasion and differentiation. *PloS one* **7**, e51804 (2012).

47. Wang, Q., Pan, J. & Snell, W.J. Intraflagellar transport particles participate directly in cilium-generated signaling in Chlamydomonas. *Cell* **125**, 549-562 (2006).

48. Berbari, N.F., O'Connor, A.K., Haycraft, C.J. & Yoder, B.K. The primary cilium as a complex signaling center. *Current biology : CB* **19**, R526-535 (2009).

49. Wang, Q., Suzuki, A., Mariconda, S., Porwollik, S. & Harshey, R.M. Sensing wetness: a new role for the bacterial flagellum. *The EMBO journal* **24**, 2034-2042 (2005).

50. Hartlova, A. *et al.* DNA damage primes the type I interferon system via the cytosolic DNA sensor STING to promote anti-microbial innate immunity. *Immunity* **42**, 332-343 (2015).

51. Perez Brandan, C., Padilla, A.M., Xu, D., Tarleton, R.L. & Basombrio, M.A. Knockout of the dhfr-ts gene in *Trypanosoma cruzi* generates attenuated parasites able to confer protection against a virulent challenge. *PLoS neglected tropical diseases* **5**, e1418 (2011).

CHAPTER 4

CONCLUSIONS AND FUTURE DIRECTIONS

4.1 Conclusion

T. cruzi is the etiologic agent for Chagas disease in the Americas, with 8-11 million people estimated to be infected in the Americas. Currently no reliable chemotherapeutic strategies or vaccines are available against *T. cruzi* infection. During infection in mammalian host cells, following initial invasion, (metacyclic) trypomastigotes convert to amastigotes to multiply until converting back to trypomastigotes before being released from the ruptured cell for subsequent infection. Understanding the mechanism of each of these steps is critical for elucidating how *T. cruzi* establishes and develops infection in the mammalian hosts and manipulation of any of these steps may profoundly impact establishment, progression and control of *T. cruzi* infection and shed light on new strategies to improve infection control.

In the first part of this project, I attempted to evaluate the potential of *T. cruzi* CalR to influence the interaction of *T. cruzi* and the host cells, in particular macrophages, which can serve as both host cells for parasite replication and effectors for parasite destruction. I hypothesized that *T. cruzi* extracellular CalR sends the 'eat-me' signal to phagocytes via recognition by LRP1, a function recently identified in mammalian CalR upon surface exposure on stressed, cancer and neoplastic cells [1-4]. By using a transgenic parasite line overexpressing CalR, I determined that overexpression of *T. cruzi* CalR markedly increased infection of Vero cells and mouse macrophages *in vitro* and infection efficiency and parasite proliferation in mice *in vivo*. However, compared to TcWT infection, the initial expansion of CalR over-expressers was increased *in vivo,* yet followed by a more rapid parasite control. The distinct progression of

the overall infection with CalR over-expressers is largely attributed to the enhanced infection in phagocytes, since CalR overexpression directed increased invasion primarily in infiltrating monocytes, tissue-resident macrophages and neutrophils *in vivo*, largely via recognition of surface and secreted *T. cruzi* CalR by LRP1 on the these host cells and dependent on IFNγ production. Macrophages can both support *T. cruzi* proliferation as host cells and eliminate parasites as immune effectors [5-8]. My work identifies interaction of *T. cruzi* CalR and LRP1 in enhancing infection in phagocytes and confirms the two equally important roles that macrophages play at different stages of infection.

In the second part of this project, I identified a previously uncharacterized protein of *T. cruzi* that is essential for amastigote-to-trypomastigote conversion. The trypanosomatid-specific protein is localized to flagellar membrane and is expressed in amastigotes and trypomastigotes, but not in epimastigotes. Using the CRISPR-Cas9 system recently shown to be useful in *T. cruzi* gene editing [9], I constructed *T. cruzi* lacking Hyp1 expression which displayed attenuated amastigote proliferation and full arrest in the amastigote stage, unable to differentiate to trypomastigote stage. *In vivo*, *T. cruzi* lacking Hyp1 expression failed to maintain a persistent infection regardless of IFNγ-dependent immune control. Meanwhile, overexpression of Hyp1 also showed compromised invasion *in vitro* and high frequency of cure in chronic infection *in vivo*. These findings indicate not only an essential role of Hyp1 expression in amastigote-to-trypomastigote conversion, but also the importance of keeping a low Hyp1expression profile for optimal infection. By identifying a critical flagellum protein in regulating differentiation, this study also supports the trypanosomal flagellum as a potential platform for harboring regulatory proteins involved in critical biological processes [10-12].

This work attempts to shed light on some critical aspects and contributing factors of the *in vivo* success of *T. cruzi* in mammalian hosts. However, many important questions are still elusive. In the first part of the project, although LRP1 expression in professional phagocytes is important for CalR-induced infection and subsequent IFNγ-dependent infection control, further investigation is required to understand whether interaction of CalR and LRP1 requires additional molecules and if so, what those additional molecules are. Moreover, it may be interesting to further elucidate whether the accelerated parasite control is achieved mainly by killing of internalized parasites in infected macrophages or digestion of engulfed and infected cells by newly recruited macrophages upon IFNγ-dependent activation. In the second part of the project, further research is required to find genetic link of disruption of *hyp1* gene in the parasites lacking Hyp1 expression. It is also important to understand the biochemical function of this uncharacterized protein. Future work to identify the molecules that interact with Hyp1 may also help understand the function of Hyp1 in triggering amastigote-to-trypomastigote differentiation.

This work demonstrates how *T. cruzi* invasion can be directed towards a particular cell population for accelerated infection control by manipulation of a single *T. cruzi* 'eat-me' signal calreticulin, and how *T. cruzi* amastigote-to-trypomastigote conversion can be arrested by disrupting expression of a flagellum protein, resulting in rapid and complete clearance in an *in vivo* infection. The strategies utilized in this study may give insight on not only enhancement of immunogeneicity and infection control of live attenuated anti-*T. cruzi* vaccines, but also rapid parasite clearance in an infected host.

4.2 References

1. Chao, M.P. *et al.* Calreticulin is the dominant pro-phagocytic signal on multiple human cancers and is counterbalanced by CD47. *Science translational medicine* **2**, 63ra94 (2010).

2. Gardai, S.J. *et al.* Cell-surface calreticulin initiates clearance of viable or apoptotic cells through trans-activation of LRP on the phagocyte. *Cell* **123**, 321-334 (2005).

3. Inoue, H. & Tani, K. Multimodal immunogenic cancer cell death as a consequence of anticancer cytotoxic treatments. *Cell death and differentiation* **21**, 39-49 (2014).

4. Senovilla, L. *et al.* An immunosurveillance mechanism controls cancer cell ploidy. *Science* **337**, 1678-1684 (2012).

5. Burger, E., Lay, W.H., Hypolito, L.V. & Fernandes, J.F. *Trypanosoma cruzi*: the fate of bloodstream trypomastigote, amastigote, metacyclic trypomastigote and epimastigote forms in the peritoneal macrophages of immune and non-immune mice in vivo. *Acta tropica* **39**, 111-122 (1982).

6. Kuhn, R.E. Macrophages in experimental Chagas' disease. *Immunology series* **60**, 495-502 (1994).

7. Cummings, K.L. & Tarleton, R.L. Inducible nitric oxide synthase is not essential for control of *Trypanosoma cruzi* infection in mice. *Infection and immunity* **72**, 4081-4089 (2004).

8. Wirth, J.J., Kierszenbaum, F., Sonnenfeld, G. & Zlotnik, A. Enhancing effects of gamma interferon on phagocytic cell association with and killing of *Trypanosoma cruzi*. *Infection and immunity* **49**, 61-66 (1985).

9. Peng, D., Kurup, S.P., Yao, P.Y., Minning, T.A. & Tarleton, R.L. CRISPR-Cas9-mediated single-gene and gene family disruption in *Trypanosoma cruzi*. *mBio* **6**, e02097-02014 (2015).

10. Tyler, K.M. *et al.* Flagellar membrane localization via association with lipid rafts. *Journal of cell science* **122**, 859-866 (2009).

11. Maric, D., Epting, C.L. & Engman, D.M. Composition and sensory function of the trypanosome flagellar membrane. *Current opinion in microbiology* **13**, 466-472 (2010).

12. Langousis, G. & Hill, K.L. Motility and more: the flagellum of *Trypanosoma brucei*. *Nature reviews. Microbiology* **12**, 505-518 (2014).

APPENDIX A

CALRETICULIN OVEREXPRESSION IN AN ATTENUATED *TRYPANOSOMA CRUZI* LINE RESULTS IN COMPLETE PARASITE CLEARANCE BUT CONFERS NO PROTECTION AGAINST THE SECONDARY INFECTION

Calreticulin (CalR) overexpression in *T. cruzi* results in more rapidly controlled yet persistent infection in mice. To determine if CalR overexpression could act in concert with other attenuating mutations, we hypothesize that parasite persistence during TcCalR chronic infection may be due to the full proliferative capacity of the transgenic parasites and thus the fast growth may compensate increased killing of parasites. Therefore we propose that infection by our lab-made attenuated *T. cruzi* line ECH3 (single allele knockout in the enoyl-CoA hydratase1, enoyl-CoA hydratase2, membrane-bound acid phosphatase genes) with occasional clearance, may achieve clearance in higher frequency in chronic phase upon CalR overexpression. Similar to CalR overexpression in WT parasites, CalR overexpression in ECH3 line exhibited reduced TSKB20-specific $CD8^+$ T cell response compared to ECH3 line itself at around day 30 (Fig. A), which mirrored decreased parasite burden upon CalR overexpression during post acute phase [1]. CalR overexpression in ECH3 infection achieved complete parasitic clearance as indicated by tissue-qPCR, parasitemia and hemoculture after immunosuppression at 1 year post infection (Fig. B, C), suggesting that while parasites with attenuating mutations may not be complete cleared, combining CalR overexpression with such mutations may be able to gain complete cure in infected mice.

It remains unclear whether vaccination with attenuated parasites that are slowly eliminated during chronic phase can confer protection against the secondary challenge after

vaccinated strains are cleared. To address this question, mice vaccinated by ECH3CalR for 500 days and showed immunological signs of parasite clearance [2] (data not shown) were challenged with *T. cruzi* expressing Tdtomato fluorescent protein (CL strain) [3] in each footpad, and parasite expansion was monitored by *in vivo* imaging during the initial stage (day 1 to 10) [4]. Compared to parasite expansion in unvaccinated mice, mice vaccinated with ECH3CalR did not show improved control of the secondary infection, which was in contrast to the mice pre-infected with persistent WT parasites that displayed suppressed parasite expansion against the secondary infection. These findings indicate that chronic exposure in this manner does not confer protection against the secondary challenge once live attenuated parasites are cleared during the chronic stage.

Appendix Figure A. *CalR overexpression in ECH3 attenuated strain resulted in complete parasite clearance but had no protection against the secondary challenge in vivo*. (A) The kinetics of TSKb20^{+} CD44^{hi} CD8^{+} T cell response in circulation in C57BL/6 mice *i.p.* inoculated with 10,000 metacyclic trypomastigotes of ECH3CalR compared with mice inoculated with the same number of ECH3 or TcWT. 10-20 mice per group. (B) *T. cruzi* in skeletal muscle of immunosuppressed mice from A, 350 dpi, as determined by quantitative real-time PCR (n=6/group). Data represent one experiment. (C) Blood parasitemia and hemoculture from the immunosuppressed mice used in B. Data represent one experiment. Mean ±SEM. (D) Mice from A and B that had been infected with ECH3CalR and TcWT for over 500 days were subcutaneously inoculated with 250,000 Tdtomato fluorescent protein-expressing *T. cruzi* (CL strain) in each footpad. Footpad imaging was acquired using Maestro 2 *in vivo* imaging system (Caliper Life Sciences) as previously described [5]. n= 8 per group. Data represent one experiment.

Appendix Figure A

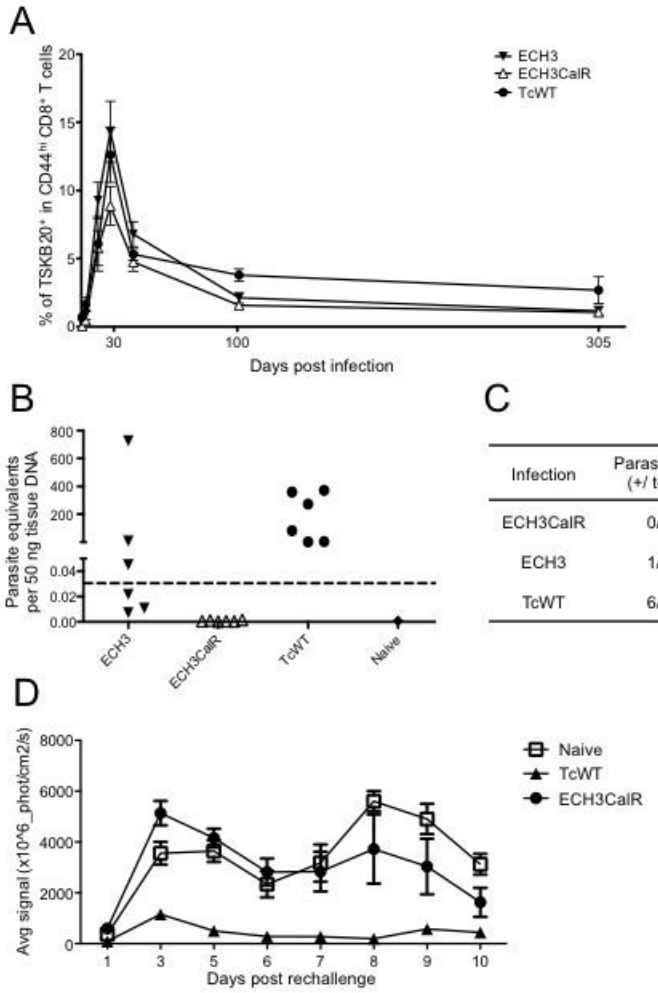

Infection	Parasitemia (+/ total)	Hemoculture (+/ total)
ECH3CalR	0/6	0/6
ECH3	1/6	2/6
TcWT	6/6	6/6

Appendix A References

1. Martin, D.L. *et al.* CD8+ T-Cell responses to *Trypanosoma cruzi* are highly focused on strain-variant trans-sialidase epitopes. *PLoS pathogens* **2**, e77 (2006).

2. Bustamante, J.M., Bixby, L.M. & Tarleton, R.L. Drug-induced cure drives conversion to a stable and protective CD8+ T central memory response in chronic Chagas disease. *Nature medicine* **14**, 542-550 (2008).

3. Canavaci, A.M. *et al.* In vitro and in vivo high-throughput assays for the testing of anti-*Trypanosoma cruzi* compounds. *PLoS neglected tropical diseases* **4**, e740 (2010).

4. Collins, M.H., Craft, J.M., Bustamante, J.M. & Tarleton, R.L. Oral exposure to *Trypanosoma cruzi* elicits a systemic CD8(+) T cell response and protection against heterotopic challenge. *Infection and immunity* **79**, 3397-3406 (2011).

5. Kurup, S.P. & Tarleton, R.L. The *Trypanosoma cruzi* flagellum is discarded via asymmetric cell division following invasion and provides early targets for protective CD8(+) T cells. *Cell host & microbe* **16**, 439-449 (2014).